Utrecht University
Graduate school of natural sciences
Institute for theoretical physics

Stability of Higher Dimensional Black Holes in Warped Spacetimes

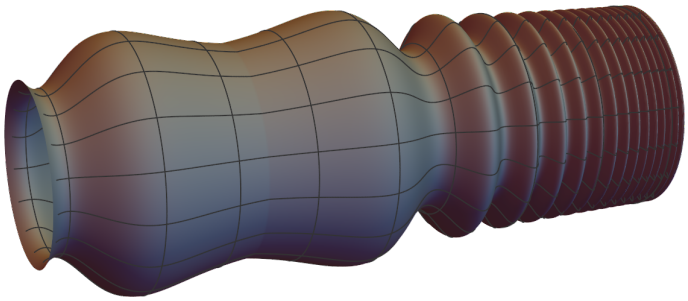

Marien Hofstee

June 28, 2024

Master's thesis

under the supervision of

Dr. Tanja Hinderer
Dr. Alvaro del Pino Gomez

Utrecht University

Abstract

Recent developments in string theory, such as the AdS/CFT correspondence, have increased the interest in higher dimensional curved spaces. The Randall-Sundrum model, a five-dimensional spacetime with strongly warped extra dimension, is a promising model that offers potential solutions to some of the major theoretical physics problems. However, some of the black holes in this model appear to be unstable. We study the mode stability of Randall-Sundrum black holes, focusing on linear perturbations of a specific complex frequency. The instability is a generalization of the Gregory-Laflamme instability, which affects torus shaped black holes in five-dimensional flat space. While previous studies have been numerical, this thesis analytically proves the Gregory-Laflamme instability using spectral theory. We extend this instability to warped spaces to determine the mass range for unstable black holes. We conclude that black holes with a mass below that of the Earth are unstable in the Randall-Sundrum model, suggesting that solar-mass black holes could still exist in this model.

Keywords: Randall-Sundrum model; Mode stability; Black string

Acknowledgements

This work would not have been possible without the guidance of Dr. Tanja Hinderer and Dr. Alvaro del Pino Gomez.

I would like to thank Tanja for all the hours she invested in the supervision. Thanks to her postivity and ideas there were always new directions that we could explore during the project. Moreover, her detailed comments highly improved the quality of the thesis.

My sincere thanks also goes to Alvaro for all the time and energy he invested in the project. His sharp questions during our discussions challenged me to understand every part of the material and improved the level of rigor in the thesis. During future research I will always ask the question "are we happy?" at each step of a proof.

Finally, I am appreciative of the discussions I had with Dr. Michal Wrochna and Dr. Pablo Bosch. They both pointed me to useful literature that accelerated the progression of the project.

Contents

Chapter 1

Introduction

Almost a hundred years after Einstein published his theory of general relativity, gravitational waves were finally detected by the LIGO and Virgo detectors in September 2015 [1]. The existence of gravitational waves is one among the profound features of Einstein's theory. Nevertheless, this detection might also be foreshadowing the downfall of general relativity, because gravitational waves opened the door for new tests of gravity. Dozens of modified gravity theories are ready to compete with general relativity [2, 3]. Additionally, opportunities arise to improve bounds of fundamental parameters and to test other theories.

An example of another theory which many physicists believe, but for which no observational evidence has been found yet, is string theory. In string theory it is assumed that particles are one-dimensional strings instead of the usual point-like objects [4]. One of the remarkable aspects of string theory is that it predicts that the universe consists of ten dimensions rather than the four dimensions that we experience in our daily life. If these extra dimensions would exist, how would it be possible that we do not notice them?

There are several possible explanations for this. One possibility is that these extra dimensions are too small to influence us. This process is called compactification [5]. In this process, extra dimensions of finite volume are combined with the original four-dimensional space, for example by taking the product space with a torus. Experiments done at CERN have put restrictions on the possible size of these extra dimensions [6]. They have shown that these extra dimensions cannot be larger than ~ 1 mm. At first glance, this bound does not seem so troubling. However, when considering higher dimensional theories it is important that the effective 4-dimensional theory still agrees with our current theories, like the standard model of particle physics and general relativity. It can be difficult to adhere both requirements

A way to avoid this problem, is to consider higher dimensional models where the standard model is restricted to a 3-brane. The word brane originates from string theory, an n-brane is a $n+1$-dimensional subspace of the higher dimensional space that includes the time-direction. Since the standard model is restricted to a 3-brane, it is automatically included in the higher dimensional model. An example of such a space is the Randall-Sundrum model [7, 8]. The Randall-Sundrum model is a five-dimensional model that includes two 3-branes. The visible brane, which is also called the TeV-brane, is where the standard model is located. The other brane is called the hidden or Planck brane. A schematic picture of this scenario is shown in figure 1.1. The space between the branes is strongly warped. This has the consequence that gravity is much stronger on one of the branes compared to the other.

In summary, there are two types of physically feasible higher dimensional models. These

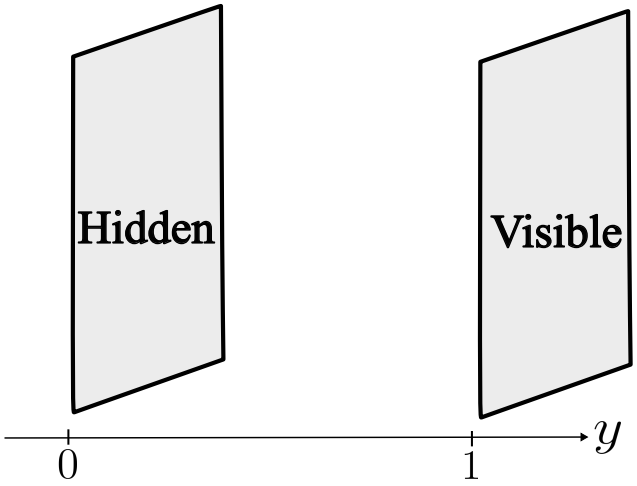

Figure 1.1: A schematic picture of the Randall-Sundrum model. The grey surfaces represent the hidden and visible brane. The two branes are parallel to each other. The directions parallel to the branes represent the usual four dimensions, the extra dimension is in the y-direction.

models either include very small extra dimensions or dimensions that are inaccessible for the standard model particles. So how can we ever detect these extra dimensions? According to Einstein's theory, gravity is a consequence of the geometry of spacetime. Consequently, gravity cannot be restricted to a brane and must be influenced by these extra dimensions. Therefore, gravitational waves make it possible to find evidence for extra dimensions [9, 10]. If this is successful, then this would be a hint towards the validity of extra dimensional theories.

A possible test can be done by using standard sirens [10]. A standard siren is a cosmological event that emits both gravitational waves and electromagnetic waves. An example of a standard siren is the coalescence of binary neutron stars. Through theory, the strength of the electromagnetic wave that is emitted during the coalescence is known. With this we can estimate the distance to the source by observing the electromagnetic wave [11]. Additionally, the gravitational wave measurements also predicts a distance, and we can see whether the two values agree. For example, if the electromagnetic wave is restricted to some 3-brane, then the gravitational wave could 'leak out' into the extra dimensions, resulting in a weaker signal and thus a different estimate for the distance to the source. So far we have only once detected such multimessenger signal from coalescing binary neutron stars [12, 13], but with the next generation of detectors we predict that such events will be detected more frequently. It is predicted that the next generation of ground based detectors, such as the Einstein Telescope, will observe around 7×10^4 binary neutron stars in one year [14].

To enable these standard siren tests we will need models for the gravitational waves in extra dimensions that can be cross-correlated with the data. Models have already been constructed for flat compact extra dimensions [9]. For flat spaces, the conclusion is that a gravitational wave signal from a binary in the five-dimensional theory has 20.8% less luminosity and a phase difference of 26% compared to a four-dimensional binary with the same characteristics. These numbers disagree with the current observations of gravitational waves, so these models are unrealistic. Nevertheless, constructing more gravitational waveforms for other higher dimensional models, might improve our understanding of these spaces and may lead to a waveform which matches better with our observations. Furthermore, if waveforms only fit for certain values of parameters, it can lead to new restrictions on higher dimensional models.

In this thesis we study the Randall-Sundrum model. This is a five-dimensional model where

the extra dimension is warped and negatively curved. This means that the four-dimensional metric also depends on the extra-dimension. Consequently, the size of the extra dimension does not need to be small to retrieve four-dimensional gravity on the brane. Furthermore, warped spaces are a generalization of flat spaces, so by studying them we are studying a wider range of models.

Before studying gravitational wave signals in the Randall-Sundrum model, we need to make sure that the generation of gravitational waves is possible in this model. So far, the vast majority of detected gravitational wave sources are binary black holes with masses between $3-100M_\odot$ [15, 16]. Therefore, we need to check if solar mass black holes exist in the Randall-Sundrum model. It turns out that the Schwarzschild solution can be extended in the extra dimension to form a black hole solution in the Randall-Sundrum model, such a solution is called a black string [17]. However, for this solution to be physical, it needs to be stable under small perturbations.

It is known that the Randall-Sundrum black string is modally unstable [17, 18]. If Randall-Sundrum could be a model to describe our universe, we require the existence of stable solar mass black holes in this model. A natural question to ask is then: Does this instability also apply to solar mass black holes? To answer this question we study the stability of the Randall-Sundrum black strings. This mode instability has so far mostly been studied numerically. In this thesis we analytically study the instability and find unstable modes of the RS black string.

To prove this analytically we combine results from general relativity and spectral theory and apply these to the black string in the Randall-Sundrum model. The necessary background is explained in chapters 2 and 3. The stability is proven in chapter 4. In the following sections we discuss the content and most important results from each chapter. The following theorem describes our main result. It is more rigorously stated and proven in Section 4.3.

Theorem 1.0.1. *In RS1 there exists a $M_0 > 0$ such that the Randall-Sundrum black string of mass M is modally unstable if $M < M_0$.*

1.1 Stability theory in general relativity

The goal of chapter 2 is to introduce the notion of stability in general relativity and gather tools from spectral theory with which we can prove stability of spacetimes.

In Section 2.1 we define the most important concepts in general relativity. General relativity is a theory on semi-Riemannian manifolds (M, g), where the dynamics of the metric are governed by the Einstein equations. There exists an action of the group of diffeomorphisms on the set of Einstein metrics. The Einstein equations are invariant under this action. This introduces the important concept of gauge fixing. By gauge fixing the metric we choose a representation of the metric by picking an element in the orbit of g.

In Section 2.2 we define different notions of stability. A metric is stable if small changes in the metric do not have big consequences. To study the stability of a metric we can define a new metric on a suitable initial surface, and use the Einstein equations to determine the evolution of the other metric. It is not a given that a metric which is initially close to the original metric, stays close at any time. A slight change in the metric might drastically change the resulting metric. If a metric is almost unaffected by perturbations we call it stable. However, if there exists a certain perturbation under which the metric diverges from its original state, it is unstable.

We define different levels of stability. For stability we perturb the metric g with a 2-tensor h.

There are three different levels of stability that we define.

- (Non-linear) stability: the evolution of the metric $g+h$ is determined by the full Einstein equation.
- Linear stability: the evolution is determined by the linearized Einstein equations.
- Mode stability: only considers the linear evolution of modes h of a particular complex frequency $\omega \in \mathbb{C}$.

It is important to note that these are really different types of stability, and one type does not imply the other. However, due to the increasing complexity it is common to first study mode stability, then linear stability and finally full stability. Even though mode stability does not imply linear stability, it can improve the understanding of the problem. The stability analyses in Chapter 4 only focuses on mode stability of spacetimes. The most important result for mode stability problems is that most problems are described by a master equation of the form

$$-\frac{d^2\psi}{dx^2} + V(x)\psi = \omega^2\psi. \tag{1.1}$$

Here $V : \mathbb{R} \to \mathbb{R}$ is some potential and $\psi \in L^2(\mathbb{R})$ is some function related to the perturbation. This type of master equation is useful, because it turns the stability problem into an eigenvalue problem. In particular, if there exist negative eigenvalues, then there exist unstable modes.

The eigenvalues can be studied with spectral theory, which is introduced in Section 2.3. For a well behaved potential, the left hand side of Eq. 1.1 can viewed as a self-adjoint operator. For a self-adjoint operator A we can define the spectrum $\sigma(A)$, which intuitively describes the set of eigenvalues of A. In this section we derive that, if V is non-negative, then $\sigma(A) \subset [0, \infty)$. Additionally, we state a result that is crucial for the proof of Theorem 1.0.1.

Lemma 1.1.1. *Let $A : D(A) \to \mathcal{H}$ be self-adjoint. If there exists a $f \in D(A)$ such that $\langle f, Af\rangle < 0$, then there exists a $E \in \sigma(A)$ with $E < 0$.*

This is especially useful in proving the existence of unstable modes, because now there only needs to exist one function in the domain such that the inner product becomes negative. Finding such a function for an operator such as in Eq. 1.1, implies the existence of unstable modes.

1.2 The Randall-Sundrum model

After defining stability theory in Chapter 2, we want to apply it to spacetimes. Chapter 3 is dedicated to illustrating the motivation behind the Randall-Sundrum model, to derive different examples of the model, and to prove important properties of the model.

In Section 3.1 we give some arguments why one should consider the Randall-Sundrum model. The most important reason is that it offers a solution to the hierarchy problem. The hierarchy problem is the lack of explanation for the huge difference between the electroweak and Planck scale. It is explained in detail in Section 3.1.1. Another reason to consider the Randall-Sundrum model are the recent developments in the AdS/CFT correspondence.

In Section 3.2 the model is defined and we derive an easy way to construct RS models. A RS1 model has a topology of $\mathbb{R}^4 \times [0, 1]$ and can be constructed from two parameters and a Ricci

flat four-dimensional metric $g^{(4)}$. The parameters are the curvature scale κ and the distance between the branes y_c. A RS1 metric has the following form in standard coordinates

$$g = e^{-2\kappa|y|} g^{(4)}(x) + y_c^2 dy^2, \tag{1.2}$$

where x are the coordinates parallel to the brane and y is the extra dimensional direction. A RS2 model has a topology of $\mathbb{R}^4 \times [0, \infty)$ and only needs the curvature scale κ and a Ricci flat four-dimensional metric.

The RS models have nice properties, some of which we derive in Section 3.3. First of all, due to the exponent in Eq. 1.2, lengths seem smaller and energies seem lower on the visible brane at $y = 1$. Therefore, RS1 models offer a solution to the hierarchy problem if $\kappa y_c \sim 35$. For this value, the global electroweak scale is of the order of the Planck scale, but the effective electroweak scale is of the order that we observe. Additionally, we show that models with these values can be constructed in a natural way. Finally, we see that the same exponential causes gravity to be much stronger on one of the branes compared to the other. It turns out that as a consequence, one experiences four-dimensional gravity even though the RS model is five-dimensional.

With the construction in Eq. 1.2, a way to obtain black hole solutions is by substituting the Schwarzschild metric for the four-dimensional metric $g^{(4)}$. The resulting space is called the RS black string. A point of infinite curvature, also called a singularity, appears at $y = \infty$ in the RS2 black string. Therefore, Hawking postulates that the black string pinches off away from the brane, instead of reaching all the way to infinity [17]. The resulting black hole has a cigar shape and is therefore called a black cigar. This hints to the existence of an instability. If there exists an instability in RS2, then there might also exist unstable black holes in RS1.

In summary, the RS1 model can be constructed naturally and has the potential to solve the hierarchy problem. Therefore, it could be a representation of our universe. However, it seems that some black holes are unstable in this model. From Earth, we observe black holes that have a mass of at least one solar mass [19]. Therefore, for RS1 to be a good representation of our universe, we want solar mass black holes to be stable. Consequently, this requires a study of the stability of the RS black string. This is the motivation behind the main Theorem 1.0.1.

1.3 Mode stability of black holes

In Chapter 4, Theorem 1.0.1 is proven. To prove this, we first study the mode stability of the Schwarzschild metric and the five-dimensional flat black string in Sections 4.1 and 4.2, respectively. The techniques and results from these studies can then be generalized to the stability of the RS black string in Section 4.3.

The Schwarzschild solution in four-dimensions has proven to be modally stable. This has first been done by Regge and Wheeler [20], and later more rigorously by Vishveshwara [21] and Zerilli [22]. We follow these derivations in Section 4.1. The perturbations of the metric can be decomposed into scalar, vector and tensor spherical harmonics of different parity and angular momentum. The linearized Einstein equations decouple for components of different parity and angular momentum, so these components can be studied separately. In this section, we conclude that both types of parity have similar behaviour and only contain stable modes.

Section 4.2 focuses on the stability analyses of the flat black string. In five-dimensional flat space with compact extra dimension, there are two types of black holes: hyperspherical black holes and black strings. If the size of the extra dimension is large compared to the mass of the black hole, the hyperspherical black hole state is entropically favourable over the black

string state. Therefore, an instability of the black string is expected. This is known as the Gregory-Laflamme instability [23] and was first studied numerically.

In this thesis we analytically analyse the instability. We derive a master equation of the form as in Eq. 1.1. The potential of this master equation will be well-behaved such that the left hand side of Eq. 1.1 can be viewed as a self-adjoint operator $A : D(A) \subset L^2(\mathbb{R}) \to L^2(\mathbb{R})$. As discussed in Section 1.1, in order to prove the existence of unstable modes, we need to prove the existence of negative eigenvalues. To do this we make use of Lem. 1.1.1. For this lemma we need to construct suitable test functions f, such that $\langle f, Af \rangle < 0$. We use an intuitive way to construct the test functions. Namely, we approximate the potential by the asymmetric finite well potential. This is a step function that is a generalization of the finite well operator that might be known from basic quantum mechanics books [24, Section 2.6]. This potential has very similar behaviour as the potential we obtain. By constructing eigenfunctions of the asymmetric finite well operator, we obtain a big set of test functions that can be used to find negative eigenvalues. With this technique we are able to prove the existence of unstable modes if the mass of the black string M is in the range $M \in \left[\frac{0.1L}{4\pi}, \frac{0.85L}{4\pi}\right]$, where L is the size of the extra dimension.

Now Theorem 1.0.1 can be proven by generalizing the unstable modes of the flat black string to the warped RS black string. In Section 4.3 we finalize the proof by constructing modes of the RS black string that reduce the master equation to the same master equation as the flat black string. This can be done with the aid of Bessel functions. In RS1, due to boundary conditions caused by the branes, we can derive for which black holes there exist unstable modes. Consequently, the M_0 in Theorem 1.0.1 depends on the two parameters κ and y_c. In particular, for the value $\kappa y_c \sim 35$, the value which solves the hierarchy problem, it holds that $M_0 \ll M_\odot$, where $M_\odot$ denotes one solar mass. In RS2, there exist unstable modes for any mass black string.

Remark. *A full analytical proof of the Gregory-Laflamme instability has been constructed in 2021 by S. Collingbourne [25]. Although many of the ideas in his article are similar to the ones used here, it is important to note that this analyses has been done completely independently from [25]. Only when finalizing the thesis I discovered the article. There are also some differences with Collingbourne's proof. His proof is completely analytical, whereas our approach uses some numerics to compute integrals. Additionally, we both make use of Lem. 1.1.1 to prove the existence of negative eigenvalues, but use different techniques to construct the test functions. Collingbourne constructs these functions by hand [25, Prop. 4.5], whereas in this thesis the eigenfunction of the asymmetric finite well form a set of test functions. Consequently, successfully using the simplified model to find negative eigenvalues helps gaining insights into the origin of the instability problem. Moreover, in this thesis the instability is proven in the range $M \in \left[\frac{0.1L}{4\pi}, \frac{0.85L}{4\pi}\right]$, whereas Collingbourne only proved the instability in the range $M \in \left[\frac{0.3L}{4\pi}, \frac{0.8L}{4\pi}\right]$.*

Remark. *Throughout this thesis we use the convention $G_N = c = 1$ unless stated otherwise.*

Chapter 2

Stability theory in general relativity

The aim of this thesis is to formulate, understand and analyse the stability problem of the Randall-Sundrum black string. The required background and tools are introduced in this chapter.

First of all, deriving the Randall-Sundrum model requires knowledge about the theory of general relativity. The concepts of general relativity that are important to us are defined in Section 2.1. General relativity describes the interaction between matter and the geometry or curvature of spacetime. This can be described using Lorentzian manifolds, where a metric tensor g solves the Einstein equations. Moreover, we show how symmetries of the system can be used to simplify a problem.

Once we have defined general relativity we can formulate the stability problem in Section 2.2. The idea behind stability theory is that a small change in initial conditions of the object has no big consequences on the evolution. Even though the Einstein equations form a system of non-linear coupled partial differential equations, it turns out that it is possible to set initial conditions on a hypersurface such that the Einstein equations determine the evolution through the entire manifold. Using this fact it is possible to define stability of a spacetime. We consider three types of stability: (non-linear) stability, linear stability and mode stability. The mode stability is the type that is studied in Chapter 4. The most important result of this section is that many mode stability analyses lead to a master equation of Schrödinger form, as in Eq. 1.1.

The left hand side of Eq. 1.1 can be viewed as a differential operator. In Section 2.3 we define spectral theory, which is the theory behind such operators. Results from spectral theory simplify the mode stability analyses. In particular, the following theorem which is proven in Section 2.3.3, makes the mode stability analyses in some cases almost trivial once we have the master equation.

Theorem 2.0.1. *If V is piecewise continuous, non-negative and bounded then the Schrödinger operator in Eq. 1.1 has no negative eigenvalues.*

Additionally, in Section 2.3.1 we derive Lem. 1.1.1, which is crucial when deriving the main result in Chapter 4.

2.1 General relativity

According to general relativity, matter interacts with the geometry of spacetime and causes curvature. Consequently, the geometry of spacetime becomes dynamic. On the other hand, matter is influenced by curvature as well. The dynamics of these interactions are governed by the Einstein equations. Lorentzian manifolds are used to describe this interaction. In this section, we define Lorentzian manifolds and curvature tensors to describe these interactions.

In particular, in Section 2.1.1 Lorentzian manifolds are introduced, which are central objects in the theory. They consist of a manifold M and a metric tensor g. The metric describes the curvature of the manifold. To see this we define several curvature tensors in Section 2.1.2. With these curvature tensors we can define a functional called the Einstein Hilbert action which represents the total curvature. In Section 2.1.3 we derive that the Einstein equations are obtained by varying this functional. The Einstein equation describe the interaction between matter and curvature. Finally, we look at how we can simplify general relativity problems by using symmetries of the systems we consider in Sections 2.1.4 and 2.1.5.

2.1.1 Lorentzian manifolds

General relativity describes the interaction between curvature and matter within a spacetime manifold. The central objects to describe the curvature are Lorentzian manifolds. In this section we define these manifolds and look at ways to construct them.

The curvature of a manifold is described by a metric.

Definition 2.1.1. *Let M be a manifold. A **metric tensor** is a non-degenerate, symmetric, bilinear form $g : TM \otimes TM \to \mathbb{R}$. g is **positive-definite** if $g(X, X) > 0$ for all non-zero $X \in TM$.*

A 2-tensor g is non-degenerate if for all $X \in T_pM$ there exists a $Y \in T_pM$ such that $g(X, Y) \neq 0$. For an orthogonal basis $\{E_1, \ldots, E_n\}$ of T_pM, it must hold that $g(E_i, E_i) \neq 0$. This can be used to assign a **signature** to a metric tensor g. Namely, if we define the quadratic form $q : TM \to \mathbb{R}$ by $q(X) = g(X, X)$, then for every orthogonal basis of T_pM, the map q produces n real numbers. Each of these numbers can either be positive or negative. We define the signature of the metric g as (p, q), where p is the amount of positive numbers and q the amount of negative numbers. Note that because of non-degeneracy and continuity, if M is connected, then the signature of g in a point p is consistent with the signature of g over the entire manifold.

Another consequence of the non-degeneracy of the metric is that g defines an identification of the tangent bundle TM with the cotangent bundle T^*M. Namely, a vector $X \in T_pM$ can be mapped to a covector in T_p^*M by the map

$$X \mapsto g(X, -). \tag{2.1}$$

Due to the fact that g is non-degenerate, this map is in fact a bijection. In a coordinate chart, if X^a is a vector field, we denote the covector associated to it by the map in Eq. 2.1 by $X_a = g_{ab}X^b$.

Definition 2.1.2. *A **semi-Riemannian manifold** (M, g) consists of a n-dimensional smooth manifold M together with a metric tensor g. We say (M, g) is a:*

- ***Riemannian manifold** if g has signature $(n, 0)$,*

- ***Lorentzian manifold*** *if g has signature $(n-1,1)$.*

If g has signature (p,q) with $q \neq 0$, then it is possible for vectors $X \in T_pM$ to have negative length $g(X,X) < 0$. We call vectors of negative length **timelike** and vectors of positive length **spacelike**. Due to continuity of the metric, if both positive and negative length vectors exist, then there must also exist non-zero vectors of zero length. Vectors of zero length are called **null** or **lightlike**.

The idea in general relativity is that nothing can move faster than light. Massive matter, such as electrons and protons or human beings, can only follow timelike trajectories, whereas massless particles move on lightlike trajectories. In our universe it seems like there is only one time-direction. Therefore, it is common in general relativity to focus on Lorentzian spacetimes. The prime example of a Lorentzian manifold is **Minkowski space**.

Example 2.1.3. *Minkowski space is the Lorentzian manifold $(\mathbb{R}^n, \eta)$, for which in Euclidean coordinates $(t, x^1, \ldots, x^n)$ the metric is given by*

$$\eta = diag(-1, 1, \ldots, 1).$$

Definition 2.1.4. *Let M be a manifold. We denote by $\mathcal{M}$ the space of all Lorentzian metrics on M.*

If we have a semi-Riemannian manifold (N, g) and a map $f : M \to N$, then f induces a metric on M by using the pullback. This **pullback metric** is defined by

$$f^*g(v,u) = g(dfv, dfu), \quad \text{for } v, u \in TM. \tag{2.2}$$

This works especially well if f is a diffeomorphism, because then f^*g is also non-degenerate and therefore a metric tensor. In particular, note that f^*g and g have the same signature. With this observation, Eq. 2.2 defines an **action** of the group of diffeomorphisms, which we denote by $\mathrm{Diff}(M)$, on the space of Lorentzian metrics $\mathcal{M}$ of M.

When (M, g') is another semi-Riemannian manifold we can compare g' and f^*g. This gives us a notion for when two semi-Riemannian manifolds are equivalent.

Definition 2.1.5. *Two semi-Riemannian manifolds (M, g') and (N, g) a diffeomorphism $f : M \to M'$ such that $f^*g = g'$ is called an **isometry**. If such an isometry exists then (M, g') and (N, g) are **isometric**.*

Definition 2.1.6. *Let (M, g) be a semi-Riemannian manifold. Then (M, g) is:*

- ***Homogeneous*** *if for every $p, q \in M$ there exists an isometry $f : M \to M$ such that $f(p) = q$.*
- ***Isotropic*** *at $p \in M$ if for any two tangent vectors $v, w \in T_pM$ such that $|v| = |w|$, there exists an isometry $f : M \to M$ such that $f_*(v) = w$.*
- ***Maximally symmetric*** *if it is homogeneous and isotropic everywhere.*

In this thesis we focus on a class of Lorentzian manifolds. In particular, we consider a class where the spacetimes are constructed by taking the product of two semi-Riemannian manifolds.

Definition 2.1.7. *A **warped product** $M \times_f N$ of two semi-Riemannian manifolds (M, g) and (N, h) with respect to a function $f : N \to \mathbb{R}$, is the manifold $M \times N$ with metric $h \oplus (f^2 \cdot g)$. f^2 is called the **warping factor**.*

2.1.2 The connection and curvature tensors

In the previous section we saw that a metric describes the curvature of the manifold. However, to improve our grip on this we can define curvature tensors, which are tensors that depend on the metric. In this section the necessary curvature tensors are defined.

In order to talk about the curvature of space we need to fix a connection ∇. For any vector bundle $\pi : E \to M$, let $\Gamma(E)$ be the space of sections

$$\Gamma(E) := \{s : M \to E | \pi \circ s(x) = x, \forall x \in M\}. \tag{2.3}$$

The connection can be viewed as a map $\nabla : \Gamma(E) \to \Gamma(T^*M \otimes E)$. We say a connection is **compatible** with the metric g if

$$\nabla_X g = 0, \quad \text{for all } X \in \Gamma(TM), \tag{2.4}$$

where $\Gamma(TM) := \{X : M \to TM | X(p) \in T_pM\}$ denotes the set of all **vector fields**. Additionally, we want the connection to be torsion free. For a connection we can define the torsion map $T : \Gamma(TM) \times \Gamma(TM) \to \Gamma(TM)$ by

$$T(X, Y) = \nabla_X Y - \nabla_Y X - [X, Y]. \tag{2.5}$$

Here $[X, Y]$ denotes the **Lie bracket**, and it is defined by

$$[X, Y](f) = X(Y(f)) - Y(X(f)), \quad \textbf{for } f \in C^\infty(M),\ X, Y \in \Gamma(TM).$$

A connection is **torsion-free** if $T[X, Y] = 0$ for all $X, Y \in \Gamma(TM)$. To find the connection we want, the following lemma from [26, P. 99] is useful.

Lemma 2.1.8. *For any Lorentzian manifold (M, g) there exists an unique connection ∇ on M which is both compatible with the metric g and torsion-free.*

This connection is called the **Levi-Civita connection**. In all cases we fix the connection to be this unique connection.

Given a coordinate chart and corresponding frame $\{E_a\}$ on a neighbourhood $\mathcal{U} \subset M$, we can define the **Christoffel symbols** $\Gamma \in \Gamma(T^*M^{\otimes 3})$ as

$$\Gamma_{abc} = g(E_a, \nabla_{E_b} E_c).$$

It is important to note that the Christoffel symbols can be viewed as a tensor only in a fixed frame. Under a coordinate transformation, the Christoffel symbol does not transform as would be expected from a tensor. For this reason we can also cannot compute the covariant derivative of the Christoffel symbols. However, the difference between two Christoffel symbols is a tensor.

For the Levi-Civita connection the Christoffel symbols can be expressed in a nice way.

Lemma 2.1.9. *Let (M, g) be a semi-Riemannian manifold, and let ∇ be the Levi-Civita connection. Furthermore, let (U, ϕ) be a local chart with coordinates x_i, $i = 1, \ldots, n$. Finally, let us denote*

$$g_{ij} = g(\frac{\partial}{\partial x_i}, \frac{\partial}{\partial x_j}). \tag{2.6}$$

Then

$$\Gamma_{abc} = \frac{1}{2} \left[\partial_c g_{ab} + \partial_b g_{ac} - \partial_a g_{bc}\right]. \tag{2.7}$$

Proof. For $X, Y, Z \in \Gamma(TM)$ we have

$$\nabla_X(g(Y,Z)) = \nabla_X g(Y,Z) + g(\nabla_X Y, Z) + g(Y, \nabla_X Z).$$

Due to the metric compatibility $\nabla_X g(Y,Z) = 0$. Furthermore, with this connection we can rewrite $g(Y, \nabla_X Z) = g(Y, \nabla_Z X) + g(Y, [X,Z])$, which we can use to get the following linear combination

$$\begin{aligned}\nabla_X(g(Y,Z)) + \nabla_Y(g(Z,X)) - \nabla_Z(g(X,Y)) =& 2g(\nabla_X Y, Z) + g(X,[Y,Z]) \\ &- g(Y,[Z,X]) - g(Z,[X,Y]).\end{aligned}$$

This can be rewritten to

$$\begin{aligned}g(Z, \nabla_X Y) = \frac{1}{2}\{&\nabla_X(g(Y,Z)) + \nabla_Y(g(Z,X)) - \nabla_Z(g(X,Y)) \\ &- g(X,[Y,Z]) + g(Y,[Z,X]) + g(Z,[X,Y])\}.\end{aligned} \tag{2.8}$$

We can express the vector fields using the coordinate chart by

$$X(x) = \sum_{i=1}^{n} f_i(x) \frac{\partial}{\partial x^i}. \tag{2.9}$$

Then the Lie-bracket of two vector fields X and Y expressed in the coordinate chart is given by

$$[X,Y] = \sum_{i,j=1}^{n} f_i(x) \frac{\partial g_j(x)}{\partial x^i} \frac{\partial}{\partial x^j} - g_i(x) \frac{\partial f_j(x)}{\partial x^i} \frac{\partial}{\partial x^j} \tag{2.10}$$

In particular, in a coordinate basis the Lie brackets will vanish for vector fields of the form $\frac{\partial}{\partial x_i}$, so we obtain the expression for the Christoffel symbols

$$\Gamma_{abc} = g(E_a, \nabla_b E_c) = \frac{1}{2}\left[\partial_b g_{ca} + \partial_c g_{ab} - \partial_a g_{bc}\right].$$

□

Another consequence of a curved spacetime is that covariant derivatives generally do not commute. To get a measure of how well they commute on vector fields we define the **Riemann tensor** $R \in \Gamma(T^*M^{\otimes 3} \otimes TM)$ as a $(1,3)$-tensor

$$R(X,Y)Z = \nabla_X(\nabla_Y Z) - \nabla_Y(\nabla_X Z) - \nabla_{[X,Y]} Z, \quad X, Y, Z \in \Gamma(TM). \tag{2.11}$$

Using the identification map in Eq. 2.1 the Riemann tensor can be transformed to a $(0,4)$-tensor, i.e. a section of $T^*M^{\otimes 4}$. Then it is defined by

$$R(X,Y,Z,W) = g(R(X,Y)Z, W), \quad X, Y, Z, W \in \Gamma(TM). \tag{2.12}$$

In a coordinate chart, there exists a useful expression for the Riemann tensor

$$\begin{aligned}R^a_{bcd} &= g(E^a, R(E_c, E_d)E_b) \\ &= \partial_c \Gamma^a_{bd} - \partial_d \Gamma^a_{bc} + \Gamma^a_{ce}\Gamma^e_{bd} - \Gamma^a_{de}\Gamma^e_{bc}.\end{aligned} \tag{2.13}$$

The commutation relation of the covariant derivative on tensors is different than for vector fields. However, it still depends on the Riemann tensor. This will be a useful relation later on.

Lemma 2.1.10. *Let $T \in \Gamma(T^*M \otimes T^*M)$, and let ∇ be the Levi-Civita connection. Then in any coordinate basis*

$$\left(\nabla_a, \nabla_b - \nabla_b \nabla_a\right) T_{cd} = -R^m_{cab} T_{md} - R^m_{dab} T_{mc}.$$

Proof. Note that the Christoffel symbol is not a tensor, therefore $\nabla_a \Gamma^b_{cd}$ does not make sense. However, $\nabla_a T_{bc}$ is a tensor. Therefore, we should start with the outer covariant derivative and work inwards.

$$\begin{aligned}
[\nabla_a, \nabla_b]\, T_{cd} =& \partial_a \nabla_b T_{cd} - \Gamma^k_{ac} \nabla_b T_{kd} - \Gamma^k_{ad} \nabla_b T_{ck} - \partial_b \nabla_a T_{cd} + \Gamma^k_{bc} \nabla_a T_{kd} + \Gamma^k_{bd} \nabla_a T_{ck} \\
=& - \left(\partial_a \Gamma^k_{bc}\right) T_{kd} + \left(\partial_b \Gamma^k_{ac}\right) T_{kd} - \left(\partial_a \Gamma^k_{bd}\right) T_{ck} + \left(\partial_b \Gamma^k_{ad}\right) T_{ck} \\
& - \Gamma^k_{al} \Gamma^l_{bc} T_{kd} + \Gamma^k_{bl} \Gamma^l_{ac} T_{kd} - \Gamma^k_{al} \Gamma^l_{bd} T_{ck} + \Gamma^k_{bl} \Gamma^l_{ad} T_{ck} \\
=& - R^k_{cab} T_{kd} - R^k_{dab} T_{ck}.
\end{aligned}$$

□

Another tensor that describes the curvature of the manifold is the **Ricci tensor** $\mathrm{Ric}_g \in \Gamma(T^*M \otimes T^*M)$. For an orthonormal frame of the tangent bundle $\{E_1, \ldots, E_n\}$ it is defined by

$$\mathrm{Ric}_g(X, Y) = \sum_{i=1}^{n} R(X, E_i, E_i, Y), \quad X, Y \in \Gamma(TM). \tag{2.14}$$

In a coordinate basis we denote it by

$$R_{ab} = R^c_{acb}. \tag{2.15}$$

The trace of the Ricci tensor gives the **Ricci scalar** or **scalar curvature**. This is an invariant of the metric. It is denoted by

$$\mathrm{scal}_g = \sum_{i=1}^{n} \mathrm{Ric}(E_i, E_i), \tag{2.16}$$

or in a coordinate chart by

$$\mathrm{scal}_g = g^{ab} R_{ab} = R^a_a. \tag{2.17}$$

The Ricci scalar describes the curvature of the manifold.

2.1.3 The Einstein-Hilbert action and Einstein equations

In the previous section, several curvature tensors were defined. In particular, we defined the scalar curvature. In this section we define a functional of the metric called the total curvature. It turns out that a physical metric is an extremal point of this functional. This gives us the Einstein equations.

By integrating the Ricci scalar over the entire manifold we get the total curvature, which gives a sense of how strongly curved the total space is. However, a **volume form** or n-form is necessary for integration. A natural candidate would be the volume form dV_g which in any oriented coordinate basis is described by

$$dV_g = \sqrt{|\det g|}\; dx^1 \wedge \cdots \wedge dx^n. \tag{2.18}$$

Lemma 2.1.11. *The volume form dV_g given in Eq. 2.18 is well-defined.*

Proof. In order to show that Eq. 2.18 is a definition for dV_g, we need to show that the expression is independent of the choice of coordinates, as long as they have the same orientation. Let (ϕ, U) be any chart with coordinates $x_1, \ldots, x_n$. Then we define the determinant of g in the chart ϕ to be $\det g = \det g_{ab}$. Note that this definition is not coordinate independent. Namely, if we have another chart (ϕ', V) with coordinates $x'_1, \ldots x'_n$, then the metric transforms as

$$g_{ab} \mapsto g'_{ab} = \frac{\partial x^c}{\partial x'^a} \frac{\partial x^d}{x'^b} g_{cd}. \tag{2.19}$$

let $A = d\phi \circ d\phi'^{-1}$ be the transition function of the coordinate transformation from x to x'. Then A can be represented as a matrix $A^b_a = \frac{\partial x^b}{\partial x'^a}$ which is the Jacobian of the coordinate transformation. Using the Jacobian, the metric transforms as $g'_{ab} = A^c_a g_{cd} A^d_b$. Therefore,

$$\det g'_{ab} = (\det A)^2 \det g_{ab}$$

Using this result, we can compare dV_g in the different charts

$$\begin{aligned} dV_g &= \sqrt{(-1)^q \det g} dx^1 \wedge \cdots \wedge dx^n \\ &= \det A \sqrt{(-1)^q \det g} dx'^1 \wedge \cdots \wedge dx'^n \\ &= \sqrt{(-1)^q \det g'} dx'^1 \wedge \cdots \wedge dx'^n. \end{aligned}$$

We conclude that the expression in Eq. 2.18 is independent of the choice of coordinates. □

If M is orientable, then all dV_g defined by coordinate basis of an oriented atlas will be identical, making dV_g the associated form of M. We are now ready to define the Einstein-Hilbert functional or total curvature.

Definition 2.1.12. *Let M be a manifold and let $\mathcal{M}$ denote the set of all Lorentzian metrics on M. Then the **Einstein-Hilbert** functional or **total curvature** is defined by*

$$\begin{aligned} S : \mathcal{M} &\to \mathbb{R}, \\ g &\mapsto \int_M scal_g \, dV_g. \end{aligned}$$

The total curvature gives an indication of how strongly curved the spacetime with metric g is. If two manifold are diffeomorphic, we cannot distinguish one from the other. Therefore, both manifolds describe the same physical situation and must have the same total curvature. However, the metric can still change under the action of a diffeomorphism. To prevent this to be a problem we would want the Einstein Hilbert action to be invariant under this action.

Theorem 2.1.13. *The Einstein Hilbert action*

$$S_{EH}(g) = \int scal_g \, dV_g \tag{2.20}$$

is invariant under the action of diffeomorphisms.

Proof. Let M, N be two manifolds and $f : N \to M$ a diffeomorphism between them. We want to show that

$$\int_M \mathrm{scal}_g \, dV_g = \int_N \mathrm{scal}_{g'} \, dV_{g'}, \tag{2.21}$$

where we used $g' = f^* g$. This equality follows from the coordinate invariance of the volume form dV_g. Namely, suppose we have a chart on $U \subseteq N$ and $f(U) \subseteq M$ with coordinates y^i and x^i respectively. Then

$$\begin{aligned} \int_{f(U)} \sqrt{\det g(x)} \mathrm{scal}_g(x) dx^1 \dots dx^n &= \int_U \sqrt{\det g(f(y))} \mathrm{scal}_g(f(y)) A(y) dy^1 \dots dy^n \\ &= \int_U \sqrt{\det g'(y)} \mathrm{scal}_{g'}(y) dy^1 \dots dy^n. \end{aligned}$$

Now if $\{U_i\}$ is a locally finite open cover of M, then there exist a partition of unit subordinate to this open cover, which is a set of functions $\eta_i : U_i \to \mathbb{R}$ such that $\sum_i \eta_i = 1$ everywhere.

Then

$$\int_M \mathrm{scal}_g \, dV_g = \sum_i \eta_i \int_{U_i} \sqrt{\det g(x)} \mathrm{scal}_g(x) dx^1 \dots dx^n$$
$$= \sum_i \eta_i \int_{f^{-1}(U_i)} \sqrt{\det g'(y)} \mathrm{scal}_{g'}(y) dy^1 \dots dy^n = \int_N \mathrm{scal}_{g'} \, dV_{g'}.$$

□

This theorem indeed shows that for a diffeomorphism $f : M \to N$ and a metric tensor g on N, that (N, g) and (M, f^*g) describe the same physical situation.

If the system does not contain any matter fields, then this system is in **vacuum**. In this case the full action of the system is given by the Einstein-Hilbert functional. If we include matter fields then there exists a **Lagrangian** which is a function of the matter fields $\{\phi_i\}_{i \in I}$, the covariant derivatives of these fields, and the metric. Then the **matter action** associated to the Lagrangian is defined by

$$S_{\mathrm{mat}}(g) = \int_M L \, dV_g. \tag{2.22}$$

The equations of motion of the fields are obtained by requiring that the action is stationary under variations of the fields. Applying this to the fields would give the Euler-Lagrange equations.

In general relativity, we are not only interested in the dynamics of the matter fields, but the metric is dynamical as well. Therefore, we want to obtain equations of motion of the metric g. The action in Eq. 2.22 also depends on the metric. Therefore, to obtain the equations of motion of the metric, we also have to vary the matter action. The contribution of the matter action is described by the **energy-momentum tensor** $T \in \Gamma(T^*M^{\otimes 2})$ which is defined by

$$T = -\frac{2}{\sqrt{-\det g}} \frac{\delta S_{\mathrm{mat}}}{\delta g}. \tag{2.23}$$

The total action is given by combining the Einstein-Hilbert functional with the action from the matter fields. Finally, to cover all possibilities a **cosmological constant** $\Lambda \in \mathbb{R}$ needs to be included as well. Altogether, the action becomes

$$S = \int_M \left[2M_p^{n-2} (\mathrm{scal}_g - 2\Lambda) + L \right] dV_g, \tag{2.24}$$

where n is the dimension of the spacetime and M_p denotes the n-dimensional Planck mass.

If we require this action to be stationary under variations of g we end up with the Einstein equations [26].

Definition 2.1.14. *The **Einstein equations** describing the dynamics of the metric tensor g_{ab} are*

$$R_{ab} - \frac{1}{2} scal_g \cdot g_{ab} + \Lambda \cdot g_{ab} = \frac{1}{2M_p^{n-2}} T_{ab}. \tag{2.25}$$

*The **Einstein vacuum equations** are the special case when $T = 0$, i.e. when no matter is present.*

Consider the case $T = 0$. Then by taking the trace of the Einstein equations we get the relation

$$\mathrm{scal}_g = \frac{2n}{n-2} \Lambda,$$

where n is the dimension of our space. If we define $\mu = \frac{2}{n-2}\Lambda$, then we can rewrite the vacuum Einstein equations from Eq. 2.25 to the form

$$R_{ab} = \mu\, g_{ab}. \tag{2.26}$$

Therefore, in vacuum the Ricci tensor is proportional to the metric.

Definition 2.1.15. *We call (M, g, Λ, L) an **Einstein manifold** with cosmological constant Λ and Lagrangian L, if (M, g) is a Lorentzian manifold and g solves the Einstein equations in Eq. 2.25. A Lorentzian manifold (M, g) is an Einstein manifold if there exists a $\mu \in \mathbb{R}$ such that*

$$Ric_g = \mu \cdot g. \tag{2.27}$$

Example 2.1.16. *The four-dimensional **Schwarzschild metric** of mass M, is given by the Lorentzian manifold $(\mathbb{R}^4, g_s)$ such that in spherical coordinates (t, r, θ, φ) the metric takes the form*

$$g_s = -\left(1 - \frac{r_s}{r}\right) dt^2 + \frac{1}{1 - \frac{r_s}{r}} dr^2 + r^2 d\theta^2 + r^2 \sin\theta\, d\varphi^2, \tag{2.28}$$

*where $r_s = 2M$ is called the **Schwarzschild radius**.*

The Schwarzschild metric is derived using Brikhoff's theorem [26, Section 5.2].

Lemma 2.1.17 (Birkhoff's theorem)**.** *Any spherically symmetric solution to the vacuum Einstein equations 2.27 with $\mu = 0$, is static. Therefore, there exists a frame in which the metric has the following form*

$$g = -f(r)^2 dt^2 + g(r)^2 dr^2 + r^2 d\Omega_2^2. \tag{2.29}$$

Using this result and plugging it into the Einstein equations, one can derive that $f(r) = g(r)^{-1}$ and that it must be of the form as in Eq. 2.28. Therefore, the Schwarzschild metric is the unique spherically symmetric solution to the vacuum Einstein equations with $\mu = 0$. The metric describes a spacetime around a static black hole.

Definition 2.1.18. *A **trapped surface** is a co-dimension 2 surface $S \subset M$, such that the two outward pointing light rays are converging.*

A spacetime contains a **black hole** if there exists a compact trapped surface. In the case of the Schwarzschild metric, note that at $r = r_s$ the factors in front of dt^2 and dr^2 change sign. Therefore, inside the compact surface $r = r_s$, r gets the role of time and all time- and lightlike trajectories are forced to $r = 0$. This makes the surface $r = r_s$ a trapped surface, since both outgoing light rays eventually reach the point $r = 0$. Therefore, the Schwarzschild metric describes a black hole.

The Schwarzschild metric has spherical symmetry, but there exist spacetimes with even more symmetries. Recall, the definition of maximally symmetric spaces in Def. 2.1.6. Weinberg showed that an Einstein manifold (M, g) that is maximally symmetric is locally unique [27, section 13.2].

Theorem 2.1.19. *Let $\mu \in \mathbb{R}$, then any two maximally symmetric metrics that solve Eq. 2.27 and have the same signature are locally equivalent.*

There are three different cases we can consider, $\mu < 0$, $\mu = 0$ or $\mu > 0$. In the case that $\mu = 0$, then the Ricci tensor vanishes, and therefore also the Ricci scalar. We call such spaces **Ricci flat**. Examples are Minkowski space which saw in Ex. 2.1.3, and the Schwarzschild metric which we will define in Section 3.2.6. However, it is important to note that the Schwarzschild

solution is not maximally symmetric. If $\mu > 0$ then the space is positively curved. A maximally symmetric example in this case is called **de Sitter space**. In this thesis we will focus on spaces with negative cosmological constant, $\mu < 0$. The maximally symmetric space in this case is called **Anti-de Sitter space**, we define this space in Section 3.1.2.

2.1.4 Gauge fixing

In the previous section we derived the Einstein equations. Recall that the Einstein Hilbert action is invariant under the action of diffeomorphisms from Theorem 2.1.13. This also applies to the Einstein equations. Consequently, a diffeomorphism $f : M \to N$ and (N, g, Λ, L) an Einstein manifold give rise to another Einstein manifold (M, f^*g, Λ, f^*L). This has as an advantage that we can choose a representation that fits the problem that we want to solve of the physical system that we want to describe. In this section we will show how we can manipulate the metric to make a suitable choice, which we call gauge fixing.

Definition 2.1.20. *Let (M, g, Λ, L) be an Einstein manifold. **Gauge fixing** is picking a representative*

$$g' \in \{\phi^* g | \phi : M \to M \text{is a diffeomorphism}\}. \tag{2.30}$$

Large parts of this thesis is focused on showing the stability or instability of spacetimes. The theory of stability will be discussed in Section 2.2, but it turns out that we want to study to behaviour of **linear perturbations** of the metric. Such a linear perturbation can be seen as a point $(g, h) \in T\mathcal{M}$, the tangent space of all Lorentzian metrics on M. We can represent this by a metric $g \in \mathcal{M}$ and a symmetric 2-tensor $h \in \Gamma(\mathrm{Sym}^2(T^*M))$. For simplicity we will use the suggestive notation $g + h$ for the point (g, h).

Gauge fixing can also be used on this linear level. To do this, we have to approximate the diffeomorphism on the linear level. This can be used to our advantage by choosing a gauge that simplifies the problem. If we use diffeomorphisms that we control, then we can transform the problem to a nice form.

Let $X \in \Gamma(TM)$ be a vector field, then X generates diffeomorphisms from M to itself. These diffeomorphisms are generated by the flow of X. The **flow** of X is a map $\phi_X : M \times \mathbb{R} \to M$. In [28, P. 209] the flow is defined by the differential equation

$$\begin{aligned} \frac{d}{dt}\phi_X(x,t)|_{t=t_0} &= X(\phi_X(x,t_0)), \\ \phi_X(x,0) &= x. \end{aligned} \tag{2.31}$$

Definition 2.1.21. *Let $f : M \to M$ be a diffeomorphism and $X \in \Gamma(TM)$. We say that f is **generated** by X if $f(x) = \phi_X(x, 1)$, where ϕ_X is the flow of X.*

Note that not for every $X \in \Gamma(TM)$, the flow $\phi_X(x, 1)$ exists, because the flow could diverge already for a time smaller than 1.

Definition 2.1.22. *A **gauge transformation** is a diffeomorphism generated by a vector field $X \in \Gamma(TM)$.*

Gauge transformations are in fact diffeomorphisms that slightly move our system. Therefore, according to theorem 2.1.13 gauge transformations do not change the physics of the system. It turns out that because of this property, gauge transformations can be a useful tool to simplify a problem. This is because a diffeomorphism not only changes the coordinates, but it also

transforms the metric. Once we have transformed the metric in a desired form we can fix this gauge to filter 'unphysical' degrees of freedom out of the problem. Not choosing the right gauge might lead to divergencies that only arise due to a bad choice of gauge. These degrees of freedom are called unphysical because we can get rid of them without changing the physics of the problem.

For our purpose we are only interested in the linear order of the transformation of the metric. Let $g+h$ be a perturbed metric, where g is a metric tensor of a manifold M and h a 2-tensor. Then how does the metric transform under gauge transformations?

Lemma 2.1.23. *Let $(M, \hat{g})$ be a Lorentzian manifold and let $g = \hat{g} + h$ be a perturbed metric, where h is a symmetric 2-tensor. Under a gauge transformation generated by $X \in \Gamma(TM)$, the 2-tensor h transforms as*

$$h \mapsto h' = h - \mathcal{L}_X \hat{g}. \tag{2.32}$$

Proof. Let X be a small vector field. Recalling how the metric transforms from Eq. 2.19 we get

$$\begin{aligned} g'_{ab}(x') &= (\delta^c_a - \partial_a X^c)(\delta^d_b - \partial_a X^d)(g_{cd}(x') - X^\gamma \partial_\gamma g_{cd}(x')) \\ &\approx g_{ab}(x') - (\partial_a X^c) g_{cb}(x') - (\partial_b X^c) g_{ca}(x') - X^c \partial_c g_{ab}(x') \\ &= g_{ab}(x') - \hat{\nabla}_a X_b(x') - \hat{\nabla}_b X_a(x'). \end{aligned} \tag{2.33}$$

It turns out that we can rewrite this in a coordinate invariant way using the **Lie derivative** along a vector field X, denoted by $\mathcal{L}_X$. The Lie derivative $\mathcal{L}_X : \Gamma(E) \to \Gamma(E)$ can be defined on the sections of any vector bundle $E \to M$, and is defined by

$$\mathcal{L}_X T = \frac{d}{dt}|_{t=0} \phi_X(t)^* T, \quad T \in \Gamma(E),$$

where $\phi_X(t)$ denotes the diffeomorphism induced by the flow of X at time t. The Lie derivative of g along any vector field X is given by

$$(\mathcal{L}_X \hat{g})_{ab} = \hat{\nabla}_a X_b + \hat{\nabla}_b X_a, \tag{2.34}$$

where $\hat{\nabla}$ denote the covariant derivatives with respect to the background metric $\hat{g}$. Note that indeed $\mathcal{L}_X g \in \Gamma(\mathrm{Sym}^2(T^*M))$. Combining Eq. 2.33 and 2.34 find that we can express the transformation of the perturbed metric in a coordinate invariant form

$$g' = g - \mathcal{L}_X \hat{g}. \tag{2.35}$$

Writing $g' = \hat{g} + h'$, we can subtract $\hat{g}$ from both sides of Eq. 2.35 to see how h transforms. This gives the desired expression in Eq. 2.32. □

We conclude that gauge transformations are a way to linearly transform the metric. This is used in Chapter 4 to simplify the analyses of the mode stability.

2.1.5 Stationary spacetimes

In Lem. 2.1.23 we derived that the metric linearly transforms with the Lie derivative $\mathcal{L}_X g$. A natural thing to ask is what happens in the case that $\mathcal{L}_X g = 0$. In this case a vector field conserves the metric g. We call this a Killing vector field and this indicates that this vector field represents a symmetry of the Lorentzian manifold. In this section we derive that if a timelike Killing vector field exists, then there exists a chart such that the metric is time-independent.

Definition 2.1.24. *Let (M, g) be a Lorentzian manifold. A **Killing vector field** of g is a vector field $K \in \Gamma(TM)$ that preserves the metric*

$$\mathcal{L}_K g = 0. \tag{2.36}$$

In a coordinate chart an equivalent definition is

$$\nabla_{(a} K_{b)} = 0. \tag{2.37}$$

where the brackets denote the symmetric part of $\nabla_a K_b$. So for any $(0,2)$-tensor T the symmetric part is defined by

$$T_{(ab)} = \frac{1}{2}\left(T_{ab} + T_{ba}\right). \tag{2.38}$$

Equation 2.37 is also called **Killing's equation**. It turns out that not only the Lie derivative vanishes, but we can actually find a metric that is independent of the Killing field.

Lemma 2.1.25. *Let (M, g) be a spacetime manifold and $K \in \Gamma(TM)$. K is a Killing vector field if and only if around any $p \in M$ there exists a coordinate chart with coordinates $\{x^1, \ldots, x^n\}$ such that $K = \partial_1$ and the metric is independent of x^1 in this chart.*

For the proof of this lemma, we will use a general result for vector fields which is theorem 9.22 from Lee [28].

Theorem 2.1.26. *Let V be a smooth vector field on a smooth manifold M, and let $p \in M$ be a point such that $V(p) \neq 0$. Then there exist smooth coordinates $\{x^1, \ldots, x^n\}$ on some neighbourhood of p in which V has coordinate representation ∂_1.*

Now we can prove lemma 2.1.25

Proof. Let K be a Killing vector field. According to theorem 2.1.26 we can find coordinates x^a around every point $p \in M$ where $K(p) \neq 0$, such that $K = \partial_1$. Pick such a coordinate system, then K can also be written as $K^a = (\partial_1)^a = \delta^a_1$. If K satisfies Killing's equation 2.37, then in this coordinate chart the equation becomes

$$\partial_a K_b + \partial_b K_a = 2\Gamma^c_{ab} K_c.$$

Note that $K_a = g_{ab}K^b = g_{a1}$. Using this and the definition for the Christoffel symbol we find

$$\partial_a g_{b1} + \partial_b g_{a1} = g_{1c} g^{cd}(\partial_a g_{bd} + \partial_b g_{ad} - \partial_d g_{ab}).$$

Since $g_{1c}g^{cd} = \delta^d_1$, it follows that

$$\partial_1 g_{ab} = 0.$$

We conclude that the metric is independent of x^1.

Conversely, consider a metric g_{ab} independent of the coordinate x^{σ^*}, and define $K = \partial_{\sigma^*}$. Then by the same steps as in the first part of the proof we can see that K satisfies Killing's equation. □

Definition 2.1.27. *An Einstein manifold (M, g) is **stationary** if it admits a Killing vector field K that is asymptotically timelike. This means that there exists a surface such that outside of this surface the Killing vector field is timelike.*

Therefore, we can associate a time coordinate t to this Killing vector field in a stationary Einstein manifold. Then there exist coordinate charts such that the metric is time independent in these coordinates. In these coordinates the system is invariant under time translations. Stationary manifolds are convenient to do calculations with because of this time symmetry. In the next section we see that we require stationary manifolds to analyse mode stability.

To summarize, we have derived the Einstein equations and defined when a Lorentzian manifold is an Einstein manifold. Unfortunately, not all Einstein manifolds are physically realistic. For example, let (M, g) be a stationary Einstein manifold, then there exists a time-independent frame. However, in nature a stationary state does not exist. Due to quantum effects even the vacuum state is already very dynamic. Therefore, a stationary state can never be a true description of a physical state, because there will always be some dynamics. Nevertheless, as long as small perturbations on the manifold do not have a big impact on the evolution of the system, the solution can be used to approximate a physical system. This is the study of stability of a solution and we describe it in the next section.

2.2 Stability theory

Now that we understand Lorentzian manifolds and the Einstein equations, we can formulate the stability problem. For a manifold M and a Lagrangian L there may be many metric tensors that solve the Einstein equations. Sometimes there exist solutions that are particularly useful because of a certain symmetry or another desirable property. To study the behaviour of such a solution we also have to study the metric solutions 'close' to it. If there are nearby metrics that diverge from it eventually, then the solution is unstable. It is unlikely that unstable solutions describe physical systems, because if they occur, they probably only exist for short periods of time. To study the behaviour of these metrics we have to perturb the background metric and analyse the Einstein equations.

A stability problem can only be formulated if there exists a way to set initial conditions. Luckily, in general relativity there exist Cauchy surfaces and initial conditions can be set on these surfaces such that the evolution is determined by the Einstein equations. We derive this in Section 2.2.1. The definition of stability is stated in Section 2.2.2. There are quite some difficulties in proving stability of spacetimes. Therefore, we also consider two other types of stability. Namely, linear stability in Section 2.2.3 and mode stability in Section 2.2.4.

2.2.1 The Cauchy problem

In this section we derive how we can set initial conditions to define stability. It turns out that there exist Cauchy surfaces in Lorentzian manifolds that influence the entire manifold. To get a feeling of what is meant by stability, consider the following example of an ordinary differential equation.

Example 2.2.1. *Consider the ordinary differential equation*

$$\frac{dy}{dt} = 1 + y, \quad y(0) = 1. \tag{2.39}$$

This equation has a constant solution given by $y(t) = 1$. However, to see if it is stable we have to look at solutions that have slightly different initial conditions. Now take as initial conditions $y(0) = 1 + \epsilon$. With these initial conditions the solution is given by $y(t) = 1 + \epsilon e^t$. This solution diverges from the original solution for large t. Therefore the solution of 2.39 is unstable.

For ordinary differential equations, the definition for stability is quite intuitive. Namely, if $f : \mathbb{R} \to \mathbb{R}$ is a solution to a differential equation with initial conditions $f(0) = f_0$, then the differential equation is stable at f, if for any other solution $g : \mathbb{R} \to \mathbb{R}$ with initial condition $g(0) = g_0$, it holds that if $|f_0 - g_0|$ is small, then $|f - g|$ is small.

We want to construct a similar definition for metric solutions to the Einstein equations. However, for such a definition we have to be able to set initial conditions and have a notion for when two metrics are close to each other. Normally, we could use the boundary of our manifold to set boundary condition, but in many cases the space does not have a boundary. Therefore, in order to set some boundary conditions we need to find a hypersurface that influences the entire space. In other words, every geodesic should pass through this surface.

Definition 2.2.2. *Let (M, g) be a Lorentzian manifold. A map $\gamma : (0, 1) \to M$ is an **inextensible Cauchy curve** in (M, g) if*

1. *γ is differentiable,*
2. *$\gamma(t)$ is timelike for each $t \in I$,*
3. *$\gamma(t)$ does not approach a limit as t approaches 0 or 1.*

The collection of all inextensible timelike curves describes is the collection of all paths that a particle could possibly take in the manifold M. If we can find a hypersurface such that each curve crosses the hypersurface exactly once, then we could choose such a surface to set the initial conditions, since every path would be influenced by these conditions.

Definition 2.2.3. *A subset $S \subset M$ is called a **Cauchy surface** if every inextensible differentiable timelike curve in (M, g) has exactly one point of intersection with S. If (M, g) admits a Cauchy surface, then we call (M, g) **globally hyperbolic**.*

Using Cauchy surfaces, perturbations of the metric can be defined. Suppose $(M, \hat{g}, L)$ is an Einstein manifold with Cauchy surface S. Then we view $\hat{g}$ has a background metric. If a metric g is specified with inital data on S in the form of $g|_S$ and $\nabla_X g|_S$ with X a vector field not tangent to S, then the Einstein equations fully determine g on the rest of the manifold uniquely up to diffeomorphisms. This may be surprising since the Einstein equations are a set of very non-linear partial differential equations, but this is one of the beautiful aspects of general relativity and the working of it is explained by Hawking and Ellis [29, chapter 7]. This initial value problem is called the **Cauchy problem**.

Let $(S, \hat{g})$ be an Einstein manifold. Another Einstein manifold (M, α, g) is called a **development** of $(S, \hat{g})$ if there exists an embedding $\alpha : S \to M$ such that $\alpha^* g = \hat{g}$. Another development (M', α', g') of $(S, \hat{g})$ is an **extension** of M if there exists a diffeomorphism ϕ of M into M', which leaves S pointwise fixed and such that $\phi^* g' = g$. With these definition Hawking and Ellis [29, Section 7.6] prove the following theorem.

Theorem 2.2.4. *Let $(S, \hat{g})$ be initial data such that $\hat{g}$ satisfies the constraint equations [29, Eq. 7.17 and 7.18], then there exists a unique (up to a diffeomorphism) development (M, α, g) that is an extension of any other development.*

For this maximal extension $\alpha(S)$ is a Cauchy surface of M. We do not prove this theorem. However, we give some intuition why it is only necessary to specify the metric along the surface S.

Let (M, g) be a maximal development of $(S, g|_S)$. Suppose $\phi : M \to M$ is a diffeomorphism that keeps S pointwise fixed. Then this gives an induced map ϕ^* which takes g at $p \in S$ to

$\phi^* g$. For $n \in T_p^* M$ which is orthogonal to S and normalized such that $n_a g^{ab} n_b = -1$, we can give any value to $n_a \phi_* g^{ab}$ by choosing the right diffeomorphism ϕ [29]. Consequently, the components $n_a g^{ab}$ are insignificant. Similarly, we can give $n_a X^c \nabla_c \phi^* g^a_b$ any value we want, so not all components of $X^c \nabla_c g_{ab}|_S$ are relevant as well.

This setup with initial data gives rise to an interesting question. Namely, if we choose the initial data $(S, \hat{g})$ and $(S, \hat{g}')$ such that $\hat{g}$ and $\hat{g}'$ are close, is the development (M, g) also close to the development (M', g')? If g does not change much under a slight change of initial conditions, then we call (M, g) stable. There are some difficulties though. Due to the invariance under diffeomorphisms and different coordinates, it can occur that a slightly deformed metric diverges from g even when (M, g) is stable. This is merely a consequence of a bad choice of gauge. However, such occurrences make the search for stability much more difficult.

2.2.2 Non-linear stability

With these Cauchy surfaces we can formulate stability of an Einstein manifold. This allows us to set initial conditions and derive what happens if we slightly alter the inital conditions. Similar to example 2.2.1 we want to call a spacetime unstable, if there exists a metric which is close to the original metric on a Cauchy surface, but which diverges asymptotically. For a physically realistic metric, small perturbations need to remain small. Therefore, we would want any metric that is close to it initially, to stay close to it.

Definition 2.2.5. *Let (M, g, L) a globally hyperbolic Einstein manifold and $S \subset M$ a Cauchy surface. (M, g, L) is **(non-linearly) stable** if for any $\epsilon > 0$ there exists a $\delta > 0$ such that if (M, g', L) is an Einstein manifold and $||g' - g||_S < \delta$, then there exists a $f \in Diff(M)$ such that $||f^* g' - g||_M < \epsilon$.*

Here $||.||_S$ and $||.||_M$ denote some norm on the jet bundle of 2-tensors over the Cauchy surface S and manifold M, respectively. It is not possible to give an general expression for these norms, since these depend on the situation and the tools that can be used to solve the problem. We call (M, g) **unstable** if it is not stable.

Unfortunately, the study of stability is extremely complicated since it requires the full understanding of the six coupled non-linear differential equations coming from the Einstein equations. This number is even bigger for higher dimensional spaces. Additionally, there is the problem of gauge fixing. By choosing the wrong gauge it is possible that metrics that are actually close to each other appear far apart. In simple spaces such as Minkowski space, the gauge choices are easier to understand than in more complicated spaces. Stability has only been solved in a few cases, for example for Minkowski space [30] and for slowly rotating Kerr black holes [31].

2.2.3 Linear stability

Due to the difficulties with stability, there exists a weaker notion of stability which does not necessarily imply stability, but can highlight some of the aspects and can be useful for the full proof. This weaker form of stability is linear stability and is described in this section. In the case of linear stability, we linearize the Einstein equations around the background metric and consider metrics that solve this linearized equation. This way we avoid having non-linear partial differential equations that we have to solve and only have to solve linear equations. In order to linearize the Einstein equations, we need to determine how the curvature tensors transform under perturbations.

Recall that the difference between two connections is a 1-form that takes values in the space of two tensors. Therefore, we can represent the transformation of the connection or Christoffel symbol under a linear perturbation $g = \hat{g} + h$ as $\Gamma = \hat{\Gamma} + \delta\Gamma$, where $\delta\Gamma \in \Gamma(TM \otimes T^*M^{\otimes 2})$.

Lemma 2.2.6. *Let $(M, \hat{g})$ be a Lorentzian manifold. Under a perturbation $g = \hat{g} + h$, the Christoffel symbols transform as $\Gamma^c_{ab} = \hat{\Gamma}^c_{ab} + \delta\Gamma^c_{ab}$ with*

$$\delta\Gamma^c_{ab} = \frac{1}{2}\hat{g}^{cd}\left(\hat{\nabla}_a h_{bd} + \hat{\nabla}_b h_{da} - \hat{\nabla}_d h_{ab}\right), \tag{2.40}$$

where $\hat{\nabla}$ denotes the covariant derivative with respect to the background metric $\hat{g}$.

Proof. If we only consider terms linear in h then

$$\begin{aligned}\Gamma^c_{ab} &= \frac{1}{2}(\hat{g}^{cd} - h^{cd})\left[\partial_a(\hat{g}_{bd} + h_{bd}) + \partial_b(\hat{g}_{da} + h_{da}) - \partial_d(\hat{g}_{ab} + h_{ab})\right] \\ &\approx \hat{\Gamma}^c_{ab} - \hat{g}^{cd}\hat{\Gamma}^i_{ab}h_{di} + \frac{1}{2}\hat{g}^{cd}\left(\partial_a h_{bd} + \partial_b h_{da} - \partial_d h_{ab}\right),\end{aligned} \tag{2.41}$$

where $\hat{\Gamma}$ denotes the Christoffel symbol associated to the background metric $\hat{g}$. Using the symmetries of the Christoffel symbols can derive that

$$\hat{\nabla}_a h_{bc} + \hat{\nabla}_b h_{ca} - \hat{\nabla}_c h_{ab} = \partial_a h_{bc} + \partial_b h_{ca} - \partial_c h_{ab} - 2\hat{\Gamma}^d_{ab}h_{cd}. \tag{2.42}$$

Applying Eq. 2.42 to Eq. 2.41 gives the desired result. □

Recall that $\delta\Gamma$ is tensorial. Therefore, the covariant derivative of $\delta\Gamma^c_{ab}$ exists, even though this was not possible for the Christoffel symbol $\hat{\Gamma}$. We can apply this to determine how the Riemann tensor varies.

Lemma 2.2.7. *Let $(M, \hat{g})$ be a Lorentzian manifold. Under a perturbation $g = \hat{g} + h$, the Riemann tensor transforms as*

$$\delta R^a_{bcd} = \hat{\nabla}_c\delta\Gamma^a_{bd} - \hat{\nabla}_d\delta\Gamma^a_{bc}. \tag{2.43}$$

Proof. This follows from

$$\begin{aligned}\delta R^a_{bcd} =& \partial_c\delta\Gamma^a_{bd} - \partial_d\delta\Gamma^a_{bc} + \delta\Gamma^a_{cm}\hat{\Gamma}^m_{bd} + \hat{\Gamma}^a_{cm}\delta\Gamma^m_{bd} - \delta\Gamma^a_{dm}\hat{\Gamma}^m_{bc} - \hat{\Gamma}^a_{dm}\delta\Gamma^m_{bc} \\ =& \hat{\nabla}_c\delta\Gamma^a_{bd} - \hat{\nabla}_d\delta\Gamma^a_{bc}.\end{aligned}$$

□

The variation of the Riemann tensor in Eq. 2.43 is simple and will be useful. However, to determine how the Ricci tensor transforms we need the full expression in terms of h. Using the expression for the variation of the Christoffel symbol in Eq. 2.40 and substituting this into Eq. 2.43 we get

$$\delta R^a_{bcd} = \frac{1}{2}\hat{g}^{am}\left(\hat{\nabla}_c\hat{\nabla}_b h_{dm} + \hat{\nabla}_c\hat{\nabla}_d h_{bm} - \hat{\nabla}_c\hat{\nabla}_m h_{bd} - \hat{\nabla}_d\hat{\nabla}_b h_{cm} - \hat{\nabla}_d\hat{\nabla}_c h_{bm} + \hat{\nabla}_d\hat{\nabla}_m h_{bc}\right). \tag{2.44}$$

Unfortunately, the covariant derivative does not commute on $(0,2)$-tensors. Instead, recall Lem. 2.1.10 to rewrite Eq. 2.44 to

$$\delta R^a_{bcd} = \frac{1}{2}\hat{g}^{am}\left(\hat{\nabla}_c\hat{\nabla}_b h_{dm} - \hat{\nabla}_c\hat{\nabla}_m h_{bd} - \hat{\nabla}_d\hat{\nabla}_b h_{cm} + \hat{\nabla}_d\hat{\nabla}_m h_{bc} - \hat{R}^n_{bcd}h_{mn} - \hat{R}^n_{mcd}h_{bn}\right). \tag{2.45}$$

Lemma 2.2.8. *Let $(M, \hat{g})$ be a Lorentzian manifold. Under a perturbation $g = \hat{g} + h$, the Ricci tensor transforms as*

$$\delta R_{ab} = \frac{1}{2}\left(-\hat{\Box} h_{ab} - \hat{\nabla}_a \hat{\nabla}_b h + \hat{\nabla}_{(a}\hat{\nabla}^c h_{b)c} - 2\hat{R}_{acbd}h^{cd} + 2\hat{R}^c_{(a}h_{b)c}\right). \tag{2.46}$$

Here $\hat{\Box} = \hat{g}^{ab}\hat{\nabla}_a\hat{\nabla}_b$ denotes the wave operator.

Proof. Using that $\delta R_{ab} = \delta R^c_{acb}$ and Eq. 2.45 we get

$$\delta R_{ab} = \frac{1}{2}\left(\hat{\nabla}^c\hat{\nabla}_a h_{bc} - \Box h_{ab} - \hat{\nabla}_b\hat{\nabla}_a h + \hat{\nabla}_b\hat{\nabla}^c h_{ac} - \hat{R}_{acbd}h^{cd} + \hat{R}^c_b h_{ac}\right) \tag{2.47}$$

We can rewrite this expression using the fact that the trace is a scalar valued quantity, so the covariant derivative commutes

$$\hat{\nabla}_a\hat{\nabla}_b h = \hat{\nabla}_b\hat{\nabla}_a h. \tag{2.48}$$

Additionally, using again Lem. 2.1.10

$$\hat{\nabla}^c\hat{\nabla}_a h_{bc} = \hat{\nabla}_a\hat{\nabla}^c h_{bc} + [\hat{\nabla}^c, \hat{\nabla}_a]h_{bc} = \hat{\nabla}_a\hat{\nabla}^c h_{bc} - \hat{R}_{acbd}h^{cd} + \hat{R}^c_a h_{bc}. \tag{2.49}$$

Combining Eq. 2.47, 2.48 and 2.49 leads to the expression in Eq. 2.46. □

So for a perturbed metric $g = \hat{g} + h$ the Ricci tensor takes the form

$$R_{ab} = \hat{R}_{ab} + \delta R_{ab} = \hat{R}_{ab} - \frac{1}{2}\Delta_L h_{ab}.$$

We call $\Delta_L : \Gamma(T^*M \otimes T^*M) \to \Gamma(T^*M \otimes T^*M)$ the **Lichnerowicz operator** [18] and using Lem. 2.2.8 it is given by

$$\Delta_L h_{ab} = \hat{\Box}\, h_{ab} + \hat{\nabla}_a\hat{\nabla}_b h - 2\hat{\nabla}_{(a}\hat{\nabla}^c h_{b)c} + 2\hat{R}_{abcd}h^{cd} - 2\hat{R}^c_{(a}h_{b)c}. \tag{2.50}$$

Definition 2.2.9. *Let $(M, \hat{g})$ be an Einstein manifold. A perturbation $g = \hat{g} + h$ solves the **linearized Einstein equations** if and only if*

$$\Delta_L h = 0. \tag{2.51}$$

Definition 2.2.10. *Let $(M, \hat{g})$ be an Einstein manifold and $\Sigma \subset M$ a Cauchy surface. The spacetime $(M, \hat{g})$ is **linearly stable** if any perturbed metric $g = \hat{g} + h$ that is close to $\hat{g}$ on Σ and solves the linearized Einstein equations, has h decaying sufficiently fast in time with respect to an appropriate frame of (M, g).*

This definition is again vague. What does sufficiently fast decay mean for example? In non-linear stability we need full control over the perturbed metric. Due to the non-linear terms in the Einstein equation it necessary to not only bound the perturbation but also know the decay of the curvature tensors and their derivatives. By contrast, in the linear theory, any sort of control over the solutions is satisfactory. Additionally, the problem again depends on some choices. In particular, a frame of the background space needs to be chosen and a gauge needs to be fixed. According to [31] the strategy to prove linear stability is as follows:

- Find components of the metric that are invariant under gauge transformations as in Eq. 2.32 for which the linearized Einstein equation 2.51 become simple, decoupled, wave equations.
- Analyse the components and derive at least one of the properties:

  - There are no exponentially growing modes.
  - The component is bounded for all times.
  - The component decays in time.

- Find a vector field X such that after a gauge transformation all gauge dependent components inherit the above property.

In many cases solving the linearized Einstein equation is still very difficult. As shown in [18, P. 7], in vacuum we can simplify the problem by working in a smart gauge.

Definition 2.2.11. *The **transverse traceless** gauge of a metric $g + h$ is defined by*

$$\nabla_a h^a_b = 0, \tag{2.52}$$
$$h = g^{ab} h_{ab} = 0. \tag{2.53}$$

We derive how to get to the transverse traceless gauge for each case specifically. In this gauge, Eq. 2.50 simplifies to

$$\Delta_L h_{ab} = \hat{\Box} h_{ab} + 2\hat{R}_{acbd} h^{cd} - 2\hat{R}^c_{(a} h_{b)c}. \tag{2.54}$$

In non-vacuum it is still possible to fix the gauge such that

$$\hat{\nabla}_a h^a_b - \frac{1}{2}\hat{\nabla}_b h = 0, \tag{2.55}$$

just not each term separately [18]. This will still simplify the Lichnerowicz operator to the form in Eq. 2.54. Even with this simplification the problem can be hard to solve. This is because h depends on all coordinates.

2.2.4 Mode stability

The final simplification that we can make is to reduce the complexity of the coordinate dependencies. Namely, we can only consider perturbations of a certain complex frequency ω. This works especially well in the case of stationary spacetimes. The stability of modes is called mode stability. In this section we define mode stability and show the existence of a useful master equation for mode stability problems.

To get a mode decomposition of the perturbation we use the Laplace transform.

Definition 2.2.12. *A **mode decomposition** of a 2-tensor h is given by the Laplace transformation [32]*

$$h(t, x^i) = \int e^{-i\omega t} \chi(\omega, x^i) d\omega, \tag{2.56}$$

*where x^i denote the spatial coordinates. We call $e^{-i\omega t}\chi(\omega, x^i)$ a **mode** of h.*

The Laplace transformation can be viewed as a Fourier transformation with complex frequency ω. This splitting of the t variable is a decomposition into modes, where ω represents the frequency of the mode, but a complex frequency rather than a real frequency. Consequently, if the imaginary part is non-zero, a mode grows or decays over time. The mode grows if $\operatorname{Im}\omega > 0$ and decays if $\operatorname{Im}\omega < 0$. If the background space is stationary, then in the time-independent frame, the Lichnerowicz operator is time-independent as well. Therefore, in this frame, we get independent equations for each mode and it is possible to analyse the modes separately.

Namely, if we insert the decomposition in Eq. 2.56 into the linearized Einstein equation 2.51 we get

$$\Delta_L h_{ab} = \int \Delta_L \left(e^{-i\omega t}\chi_{ab}(\omega, x^i)\right) d\omega \tag{2.57}$$

In particular, if $\Delta_L e^{-i\omega t}\chi_{ab}(\omega, x^i) = 0$ for each ω, then h_{ab} solves the linearized Einstein equations. This is a nice first step in studying the stability problem. If the background metric admits other symmetries as well it is possible to separate other variable of χ. We will discuss this in more detail when considering specific spacetimes.

Definition 2.2.13. *Let (M, g) be an Einstein manifold. We say (M, g) has **mode stability** if all mode solutions to*

$$\Delta_L e^{-i\omega t} h_{ab}(\omega, x^i) = 0, \tag{2.58}$$

have $\operatorname{Im}\omega \leq 0$.

Unfortunately, mode stability does not imply linear stability and vice versa. This is caused by the interactions between different modes that may cause or cancel instabilities. This can be seen by looking at Eq. 2.57. Observe that $\Delta_L h_{ab} = 0$ does not imply that $\Delta_L \left(e^{-i\omega t}\chi_{ab}(\omega, x^i)\right) = 0$ for all $\omega \in \mathbb{C}$. Therefore, even if all mode solutions have $\operatorname{Im}\omega \leq 0$, there can still be linear perturbations h that contain growing modes. On the other hand, if there is a mode solution with $\operatorname{Im}\omega > 0$, then this can still be canceled in the integral of Eq. 2.56, such that the linear perturbation h is still stable. Nevertheless, in most cases proving mode stability does support the understanding of the linear stability problem.

In Eq. 2.58 every time derivative gets replaced by a factor $(-i\omega)$. In many cases the resulting equation can then be rewritten to a Schrödinger type equation

$$-\frac{d^2\psi}{dx^2} + V(x)\psi = \omega^2\psi, \tag{2.59}$$

where V is a potential. This changes the problem to an eigenvalue problem. If we view the left hand side of Eq. 2.59 as a differential operator, then the (M, g) is modally stable if this differential operator does not admit any negative eigenvalue. This is because if $\omega^2 \geq 0$, then $\omega \in \mathbb{R}$, thus $\operatorname{Im}\omega = 0$. Conversely, if $\omega^2 < 0$, then ω is imaginary. Therefore, in this case there is an unstable mode.

The next section is about spectral theory. Here we define a class of operators called self-adjoint operators. For such operators we can define the spectrum, which intuitively describes the set of eigenvalues of the operator. If the spectrum contains negative elements, then there exist unstable modes, whereas if the spectrum contains only positive elements, then all modes are stable. In the next section we state Theorem 2.3.16, which is useful for proving the existence of negative elements in the spectrum.

Mode stability is the first step on the long route to proving non-linear stability. In this thesis the focus is on studying the mode stability of different black hole spacetimes. We look at the mode stability of the Schwarzschild solution in four dimensions in Section 4.1 and we uncover a regime where unstable modes appear in the case of a black string in five dimensions in Section 4.2. We use this instability to find which black holes are stable in Randall-Sundrum in Section 4.3. However, first we define Randall-Sundrum and look at its properties in the next chapter.

2.3 Spectral theory

In the previous section we saw that in many cases a mode stability problem can be reduced to a Schrödinger type equation. The frequencies of the modes correspond to eigenvalues of

the Schrödinger operator, which means that we need to study the eigenvalues of this equation. By identifying the left hand side of Eq. 2.59 with an operator, we can use spectral theory to analyse the spectrum of this operator. In this section we define spectral theory, which is the theory behind such operators. Furthermore, we derive some important results to analyse the spectrum of differential operators. Most of the definitions come from the book by Simon and Reed [33, Sections 8.1 - 8.3].

In Section 2.3.1 we define the useful class of differential operators called self-adjoint operators. For a self-adjoint operator A we can define the spectrum, which is the set of $\lambda \in \mathbb{C}$ for which $A - \lambda I$ is not bijective. In Section 2.3.2 we derive that for well-behaved potentials, the Schrödinger operator as in Eq. 2.59 is self-adjoint. This allows us to use the results from this section for the stability analyses in Chapter 4. Finally, we state the spectral theorem and prove Theorem 2.0.1 in Section 2.3.3. In the end we derive the following theorem.

Theorem 2.3.1. *Suppose the mode stability problem of a spacetime (M, g) can be rewritten to a master equation of the form of Eq. 2.59. If V is*

- *Piecewise continuous,*
- *bounded,*
- *non-negative,*

then (M, g) is modally stable.

2.3.1 Self-adjoint operators

In this section we make definitions that allow us to view the left hand side of Eq. 2.59 as a differential operator. For this we need to define Hilbert spaces and linear maps or operators on Hilbert spaces. Furthermore, we define a class of operators with useful properties called self-adjoint operators. As an example we take the Laplacian, which is an important operator for Section 2.3.2.

Most functional spaces are infinite dimensional linear spaces.

Definition 2.3.2. *A **Hilbert space** $\mathcal{H}$ is a real or complex inner product space that is complete.*

Example 2.3.3. *An important example of a Hilbert space is $L^2(\mathbb{R})$ which consists of functions $f : \mathbb{R} \to \mathbb{R}$ which are square integrable, i.e. for which*

$$||f||_{L^2}^2 = \int_{-\infty}^{\infty} f(x)^2 \, dx < \infty.$$

This norm is induced by the inner product on L^2 given by

$$\langle f, g \rangle_{L^2} = \int_{-\infty}^{\infty} f(x) g(x) \, dx \quad f, g \in L^2(\mathbb{R}).$$

We can act on this Hilbert space with linear operators. Let $\mathcal{H}$ be a Hilbert space, then a map $A : D(T) \subset \mathcal{H} \to \mathcal{H}$ is a **linear operator** if

$$T(\alpha f + \beta g) = \alpha T(f) + \beta T(g), \tag{2.60}$$

for all $f, g \in \mathcal{H}$ and $\alpha, \beta \in \mathbb{R}$. Here $D(T)$ is a linear subspace of $\mathcal{H}$ called the domain of T. We say that T is **densely defined** if $D(T)$ is dense in $\mathcal{H}$. We denote the **set of linear operators** by $\mathcal{L}(\mathcal{H})$.

Example 2.3.4. *The smooth functions with compact support denoted by $C_0^\infty(\mathbb{R})$ form a dense subset of $L^2(\mathbb{R})$.*

Since not all functions $f \in L^2(\mathbb{R})$ are continuous, let alone differentiable, it is not trivial that we can act with differential operators on $L^2(\mathbb{R})$. However, we can define a weak derivative. The **weak derivative** of a function $f \in L^2(\mathbb{R})$ is a function $g \in L^2(\mathbb{R})$ such that

$$\int_{-\infty}^{\infty} f\, h'\, dx = \int_{-\infty}^{\infty} g\, h\, dx, \quad \text{for all } h \in C_0^\infty(\mathbb{R}). \tag{2.61}$$

Similarly, the k-th weak derivative is defined by taking k derivatives of h.

Example 2.3.5. *The Sobolev spaces $H^k(\mathbb{R})$ represent the square integrable functions that have k weak derivatives. They are defined by*

$$H^k(\mathbb{R}) = \{f \in L^2(\mathbb{R}) |\, f \textit{is } k \textit{ times weakly differentiable}\}.$$

The inner product is given by

$$\langle f, g\rangle_{H^2} = \sum_{i=0}^{k} \langle f^{(i)}, g^{(i)}\rangle_{L^2},$$

where $f^{(i)}$ denotes the i-th weak derivative of f.

The following lemma on Sobolev spaces will later be useful [34][Chapter 8].

Lemma 2.3.6. *Suppose $f \in H^k(\mathbb{R})$ for $k \in \mathbb{N}$ then f is bounded and*

$$\lim_{x\to\infty} f(x) = 0, \quad \lim_{x\to-\infty} f(x) = 0. \tag{2.62}$$

With Sobolev spaces it is possible to define differential operators.

Example 2.3.7. *Consider the Hilbert space $L^2(\mathbb{R})$. An example of a densely defined operator is the one-dimensional Laplacian, $\Delta = -\frac{d^2}{dx^2}$ with $D(\Delta) = H^2(\mathbb{R})$. Note that since the smooth functions with compact support form a subset of $H^2(\mathbb{R})$, we see that indeed Δ is densely defined.*

For densely defined operators we can define the adjoint.

Definition 2.3.8. *Let $T \in \mathcal{L}(\mathcal{H})$ be densely defined. Let $D(T^*)$ be the set of $f \in \mathcal{H}$ for which there exists a $g \in \mathcal{H}$ with*

$$\langle Th, f\rangle = \langle h, g\rangle \quad \textit{for every } h \in D(T). \tag{2.63}$$

For each such f we define $T^* f = g$. The operator T^* is called the adjoint of T.

Since T is densely defined there is a unique g that satisfies Eq. 2.63. Namely, suppose that $g, g' \in \mathcal{H}$ both satisfy Eq. 2.63 and $g \neq g'$. Then there must be a $h \in \mathcal{H}$ such that $\langle h, g\rangle \neq \langle h, g'\rangle$. However, since T is densely defined we have a sequence $\{h_n\}$ such that $\lim_{n\to\infty} h_n = h$, for which by definition we have $\langle h_n, g\rangle = \langle h_n, g'\rangle$ for all n. This means that both sides have the same limit, which contradicts our assumption that $\langle h, g\rangle \neq \langle h, g'\rangle$.

Definition 2.3.9. *A densely defined operator T on a Hilbert space $\mathcal{H}$ is called* ***symmetric*** *if $T \subset T^*$, that is, if $D(T) \subset D(T^*)$ and $Tf = T^* f$ for all $f \in D(T)$. Equivalently, T is symmetric if and only if*

$$\langle Tf, g\rangle = \langle f, Tg\rangle \quad \textit{for all } f, g \in D(T).$$

Definition 2.3.10. *T is called **self-adjoint** if $T = T^*$, that is, if T is symmetric and $D(T) = D(T^*)$.*

Theorem 2.3.11. *The one-dimensional Laplacian $\Delta = -\frac{d^2}{dx^2}$ with $D(\Delta) = H^2(\mathbb{R})$ is self-adjoint.*

Proof. Consider the one-dimensional Laplacian $\Delta = -\frac{d^2}{dx^2}$ with $D(\Delta) = H^2(\mathbb{R})$. Using integration by parts, we have for all $f, g \in H^2(\mathbb{R})$

$$\begin{aligned}\langle f, \Delta g\rangle &= -\int_{-\infty}^{\infty} fg''dx \\ &= -f(x)g'(x)|_{x=-\infty}^{\infty} + \int_{-\infty}^{\infty} f'g'dx \\ &= \left(f'(x)g(x) - f(x)g'(x)\right)|_{x=-\infty}^{\infty} - \int_{-\infty}^{\infty} f''gdx \\ &= \langle \Delta f, g\rangle.\end{aligned}$$

In the last equality we used Lem. 2.3.6. It follows that Δ is symmetric. Proving self-adjointness now boils down to showing that $D(\Delta) = D(\Delta^*)$. Let $f \in D(\Delta^*)$ then there exists a $g \in L^2(\mathbb{R})$ such that

$$\int_{-\infty}^{\infty} f(\Delta h)dx = \int_{-\infty}^{\infty} ghdx, \quad \text{for all } h \in D(\Delta). \tag{2.64}$$

In particular, since $C_0^\infty(\mathbb{R}) \subset D(\Delta) = H^2(\mathbb{R})$ it follows that Eq. 2.64 holds for all $h \in C_0^\infty(\mathbb{R})$. Therefore, g is the second weak derivative of f. Consequently, $f \in H^2(\mathbb{R})$ and we conclude that $D(\Delta) = D(\Delta^*)$ and thus that Δ is self-adjoint. □

Suppose that an operator $T : D(T) \to \mathcal{H}$ can be extended. In other words that there exists an operator $S : D(S) \to \mathcal{H}$ with $D(T) \subset D(S)$ and $T\phi = S\phi$ for $\phi \in D(T)$. Then the domain of the adjoint would decrease $D(S^*) \subset D(T^*)$. So if T is symmetric and S a symmetric extension we have

$$D(T) \subset D(S) \subset D(S^*) \subset D(T^*). \tag{2.65}$$

Therefore, a self-adjoint operator does not have a symmetric extension.

Definition 2.3.12. *Let $T \in \mathcal{L}(\mathcal{H})$. We say T is **closed** if its graph $G = \{(f, Tf) \in \mathcal{H} \times \mathcal{H} | f \in \mathcal{H}\}$ is closed.*

Lemma 2.3.13. *Let $T \in \mathcal{L}(\mathcal{H})$ be densely defined. Then T^* is closed.*

Proof. Let $\{f_n\} \subset D(T^*)$ such that $f_n \to f$ and $T^* f_n \to g$. Then for every $h \in D(T)$ we have

$$(h, T^* f_n) = (Th, f_n). \tag{2.66}$$

Now taking the limit $n \to \infty$ on both sides of Eq. 2.66 gives $(h, g) = (Th, f)$. Since this is true for every $h \in D(T)$, and $D(T)$ is dense in $\mathcal{H}$, we can conclude that indeed $f \in D(T^*)$ and $T^* f = g$. □

Combining the result of Lem. 2.3.13 and Theorem 2.3.11 it follows that Δ with $D(\Delta) = H^2(\mathbb{R})$ is closed. Since Δ is self-adjoint and its adjoint is closed.

Definition 2.3.14. *A symmetric operator T is called **essentially self-adjoint** if its closure $\overline{T}$ is self-adjoint. If T is closed, a subset $D \subset D(T)$ is called a **core** of T if $\overline{T|_D} = T$.*

For closed operators we can analyse the spectrum of eigenvalues. Recall from linear algebra that a linear map A had eigenvalue λ if there exist an eigenvector v with $Av = \lambda v$, in other words when $\ker(A-\lambda I) \neq \{0\}$. For linear operators $T \in \mathcal{L}(\mathcal{H})$ the story is a bit different. Now there is not necessarily an eigenvector corresponding to each eigenvalue. However, we can still analyse for which $\lambda \in \mathbb{C}$ the map $T - \lambda I$ is a bijection.

Definition 2.3.15. *Let $T \in \mathcal{L}(\mathcal{H})$ be closed. A complex number λ is in the **resolvent set** of T if $T - \lambda I$ is a bijection from $D(T)$ to $\mathcal{H}$ with a bounded inverse. We denote the resolvent set by $\rho(T)$. If $\lambda \in \rho(T)$, then $R(\lambda) = (T - \lambda I)^{-1}$ is called the **resolvent** of T at λ.*
*We say λ is in the **spectrum** $\sigma(T)$ if λ is not in the resolvent set.*

In equations such as Eq. 1.1, the spectrum of the operator on the left hand side can tell a lot about the stability of the system. In particular, to determine the infimum of the spectrum the following theorem from [35, Theorem 2.19] is useful.

Theorem 2.3.16. *Let $A : D(A) \subset \mathcal{H} \to \mathcal{H}$ be self-adjoint. Then*

$$\inf \sigma(A) = \inf_{f \in D(A),\, ||f||=1} \langle f, Af \rangle. \tag{2.67}$$

This theorem is especially useful in proving the existence of unstable modes. In order to prove that there exist a $E \in \sigma(A)$ with $E < 0$, there only needs to exist a $f \in D(A)$ such that $\langle f, Af \rangle = 0$.

2.3.2 The Schrödinger operator

In the previous section we stated the definition of self-adjoint operators and derived some useful properties of these operators. The operators that are of interest of us when proving mode stability are operators of the form of Eq. 2.59. In this section we introduce the Schrödinger operator and show in Cor. 2.3.20 that this operator is self-adjoint if the potential is bounded and piecewise continuous.

Definition 2.3.17. *Let $V : \mathbb{R} \to \mathbb{R}$ be a map such that $V \cdot f \in L^2(\mathbb{R})$ for any $f \in L^2(\mathbb{R})$. We call an operator $A : H^2(\mathbb{R}) \to L^2(\mathbb{R})$ of the form*

$$A = -\frac{d^2}{dx^2} + V(x), \tag{2.68}$$

*a **Schrödinger operator** with **potential** V.*

We are mainly interested in self-adjoint Schrödinger operators. This can be proven using the Kato-Rellich theorem.

Definition 2.3.18. *Let $\mathcal{H}$ be a Hilbert space, $A : D(A) \subset \mathcal{H} \to \mathcal{H}$ a self-adjoint operator and $B : D(B) \subset \mathcal{H} \to \mathcal{H}$ a symmetric operator with $D(A) \subset D(B)$. We say that B is A-bounded if there exist constants $\alpha, \beta \geq 0$ such that*

$$||Bx|| \leq \alpha ||Ax|| + \beta ||x||$$

for all $x \in D(A)$, and we say that α is an A-bound of B

Theorem 2.3.19 (Kato-Rellich)**.** *If B is A-bounded with A-bound smaller than 1, then $A + B$ is self-adjoint on $D(A)$, and essentially self-adjoint on any core of A.*

Let $\Delta = -\frac{d^2}{dx^2}$ denote the one-dimensional Laplacian with $D(\Delta) = H^2(\mathbb{R})$. Let $V : \mathbb{R} \to \mathbb{R}$ be a bounded and piecewise continuous potential with bound $V_{\max}$. Then $V : L^2(\mathbb{R}) \to L^2(\mathbb{R})$ can be viewed as an operator that maps $u \in L^2(\mathbb{R})$ to

$$(Vu)(x) = V(x)u(x). \tag{2.69}$$

With this construction V is a bounded operator, since

$$||Vu|| \leq V_{\max}||u||. \tag{2.70}$$

Consequently, using Def. 2.3.18, V has 0 Δ-bound.

Corollary 2.3.20. *Let $V : \mathbb{R} \to \mathbb{R}$ be bounded and piecewise continuous, and let $A = \Delta + V$ be the Schrödinger operator with potential V. Then A is self-adjoint on $D(A) = H^2(\mathbb{R})$, and essentially self-adjoint on any core of Δ.*

If the potential V is non-negative, then the Schrödinger operator has even additional nice properties.

Definition 2.3.21. *An operator T on a Hilbert space $\mathcal{H}$ is* ***non-negative*** *if*

$$(f, Tf) \geq 0 \quad \forall f \in D(T).$$

We denote this by $T \geq 0$.

Now suppose V is non-negative and let $0 \neq f \in C_0^\infty(\mathbb{R})$. For the Schrödinger operator A with potential V it holds that

$$\begin{aligned}(f, Af) &= \int_{-\infty}^{\infty} -f(x)\frac{d^2 f(x)}{dx^2} + V(x)f(x)^2\, dx \\ &= \int_{-\infty}^{\infty} \left(\frac{df(x)}{dx}\right)^2 + V(x)f(x)^2\, dx > 0.\end{aligned}$$

Since $C_0^\infty(\mathbb{R})$ is a core of A, it holds that $(f, Af) \geq 0$ for all $f \in D(A)$.

Corollary 2.3.22. *If V is non-negative then the Schödinger operator of Eq. 2.68 is non-negative.*

2.3.3 The spectral theorem

In the previous section we have defined the Schrödinger operator and saw that it is self-adjoint for well-behave potentials. In this section we derive the spectral theorem. With this theorem we can act with functions on self-adjoint operators to generate new operators. With the spectral theorem we can prove the main result of this section.

Theorem 2.3.23. *Let A be a self-adjoint non-negative operator on a Hilbert space $\mathcal{H}$. Then $\sigma(A) \subseteq [0, \infty)$.*

For a self-adjoint operator A on a Hilbert space $\mathcal{H}$, we can define a map from the bounded Borel functions to the set of self-adjoint operators on $\mathcal{H}$. The intuition behind this map is that for a self-adjoint operator A we can find a set of eigenvalues $\{\lambda_n\}$ and a corresponding set of eigenfunctions $\{\psi_n\}$. If we now have a bounded Borel function h, we can define a new linear operator $h(A)$ on this set of eigenfunctions by $h(A)\psi_n = h(\lambda_n)\psi_n$. Since A is self-adjoint this can be made into a well-defined operator on the Hilbert space.

Theorem 2.3.24 (functional spectral theorem)**.** *Let A be a self-adjoint operator on $\mathcal{H}$. Then there is a unique map $\hat{\phi}$ from the bounded Borel functions on $\mathbb{R}$ into $\mathcal{L}(\mathcal{H})$ so that*

1. *$\hat{\phi}$ is an algebraic homomorphism, i.e. $\hat{\phi}(f \circ g) = \hat{\phi}(f) \circ \hat{\phi}(g)$.*
2. *$\hat{\phi}$ is norm continuous, that is, $||\hat{\phi}(h)||_{\mathcal{L}(\mathcal{H})} \leq ||h||_\infty$.*
3. *Let $h_n(x)$ be a sequence of bounded Borel functions with $h_n(x) \xrightarrow[n\to\infty]{} x$ for each x and $|h_n(x)| \leq |x|$ for all x and n. Then, for any $\psi \in D(A)$, $\lim_{n\to\infty} \hat{\phi}(h_n)\psi = A\psi$.*
4. *If $h_n(x) \to h(x)$ pointwise and if the sequence $||h_n||_\infty$ is bounded, then $\hat{\phi}(h_n) \to \hat{\phi}(h)$ strongly.*
5. *If $A\psi = \lambda\psi$, then $\hat{\phi}(h)\psi = h(\lambda)\psi$.*
6. *If $h \geq 0$, then $\hat{\phi}(h) \geq 0$.*

It is also common to use the notation $h(A)$ instead of $\hat{\phi}(h)$. Note that the identity map $i : \mathbb{R} \to \mathbb{R}$ indeed also maps $i(A) = A$. The spectrum of the new operator relates to the spectrum of A.

Theorem 2.3.25. *Let f be a bounded Borel function. Then we have the inclusion:*

$$\sigma(f(A)) \subset \overline{f(\sigma(A))}.$$

In particular, for a measurable set $\Omega \subset \mathbb{R}$ we can consider the characteristic function

$$\chi_\Omega(x) := \begin{cases} 0 & \text{if } x \notin \Omega \\ 1 & \text{if } x \in \Omega \end{cases}. \tag{2.71}$$

We can then define operators $P_\Omega = \chi_\Omega(A)$.

Definition 2.3.26. *A family of projection operators $\{P_\Omega\}$ indexed over measurable sets $\Omega \subset \mathbb{R}$ is called a projection-valued measure (p.v.m.) if it has the following properties:*

1. *Each P_Ω is an orthogonal projection.*
2. *$P_\emptyset = 0$, $P_{(-\infty,\infty)} = I$.*
3. *If $\Omega = \bigcup_n \Omega_n$, with $\Omega_n \cap \Omega_m = \emptyset$ if $n \neq m$, then $P_\Omega = \lim_{N\to\infty} \sum_{n=1}^N P_{\Omega_n}$.*
4. *$P_{\Omega_1} P_{\Omega_2} = P_{\Omega_1 \cap \Omega_2}$.*

Lemma 2.3.27. *The family of operators $\{P_\Omega\}$ indexed over measurable sets $\Omega \subset \mathbb{R}$ is a p.v.m.*

Note that some operators P_Ω may be zero. Namely, if $\Omega \cap \sigma(A) = 0$, then by Theorem 2.3.25 it follows that $\sigma(P_\Omega) \subset \{0\}$. Nevertheless, if $\{P_\Omega\}$ is a p.v.m. then for any $f \in \mathcal{H}$, $\langle f, P_\lambda f\rangle$ defines a measure. Integration with this measure will generate an operator again. One can show that for a Borel function h it holds that

$$\langle f, h(A)f\rangle = \int_{-\infty}^{\infty} h(\lambda) d\langle f, P_\lambda f\rangle. \tag{2.72}$$

This gives us a correspondence between p.m.v. and self-adjoint operators.

Theorem 2.3.28. *There is a one-to-one correspondence between self-adjoint operators A and projection-valued measures $\{P_\Omega\}$ on $\mathcal{H}$, given by*

$$A = \int_{-\infty}^{\infty} \lambda \, dP_\lambda$$

With this theorem we want to work towards our main result.

Proof of Theorem 2.3.23. Let P_Ω be the p.m.v. associated to A. Assume that there exists a $\lambda \in \sigma(A)$ with $\lambda < 0$. Then there exist $a < b < 0$ and let $f \in \mathcal{H}$ such that $P_{(a,b)} f = f$. Then

$$\begin{aligned}(Af, f) &= \int_{-\infty}^{\infty} \lambda \, d(P_\lambda f, f) \\ &= \int_{-\infty}^{\infty} \lambda \, d(P_\lambda P_{(a,b)} f, f). \end{aligned} \tag{2.73}$$

Note that because of property 4 of Def. 2.3.26, it holds that for every $\lambda \notin [a, b]$ there exists a $\delta > 0$ such that $P_{(\lambda-\delta,\lambda+\delta)} P_{(a,b)} = 0$. Therefore, Eq. 2.73 becomes

$$(Af, f) = \int_a^b \lambda \, d(P_\lambda f, f). \tag{2.74}$$

In this equation we have that because of property 6 of Theorem 2.3.24 $(P_{(\lambda+\epsilon,\lambda-\epsilon)} f, f)$ is positive, whereas λ is negative in the range (a, b). This would mean that $(Af, f) < 0$ which contradicts our assumption that A is positive. Therefore, such a non-zero f does not exist which means that $P_{(a,b)} = 0$ for all $a < b < 0$. If $(a, b) \cap \sigma(A) \neq \emptyset$ somewhere then $P_{(a,b)} \neq 0$, so we conclude that $\sigma(A) \subseteq [0, \infty)$. □

This theorem makes the mode stability analyses in some cases much simpler. Once we have derived a master equation of Schrödinger form, we only need to check whether the potential is:

- Piecewise continuous,
- bounded,
- non-negative.

If all these three apply then it follows from Cor. 2.3.20 that the Schrödinger operator is self-adjoint. Furthermore, by combining Cor. 2.3.22 and Theorem 2.3.23 we conclude that the master equation only has positive eigenvalues. This proves the mode stability of the problem. In particular, we have now proven Theorem 2.3.1.

Chapter 3

The Randall-Sundrum model

In the previous chapter we defined everything we need to formulate the stability problem. We want to apply this to analyse the stability of the Randall-Sundrum black string. This chapter is dedicated to defining Randall-Sundrum models and in particular deriving the black string solution. Furthermore, we derive some properties of Randall-Sundrum models to show why this model can potentially answer open question in theoretical physics.

In Section 3.1 we give some motivation behind the model. The Randall-Sundrum model gives a solution to the hierarchy problem, which is the problem that we do not have a natural explanation for the huge difference between the electroweak scale and the Planck scale. Additionally, we explain the idea behind the AdS/CFT correspondence. This conjecture says that every Anti-de Sitter space is equivalent to a lower dimensional conformal field theory. This idea of another theory existing on the boundary of a negatively curved space has a lot of similarities with the Randall-Sundrum model.

After giving motivation behind the model, we define the model in Section 3.2. The Randall-Sundrum model is a five-dimensional space where the extra dimension is warped. On the boundaries there are two 3-branes. We consider two types of models RS1 and RS2. In RS1 the branes are separated by a finite constant distance. In RS2 one of the branes is pushed to infinity such that effectively there is only one brane. The most important result of this section is Theorem 3.2.14 which gives an easy way to construct Randall-Sundrum models. Any Ricci flat metric $g^{(4)}$ on $\mathbb{R}^4$ and parameters $\kappa, y_c > 0$ generate a Randall-Sundrum models. In particular, we use this to construct black hole solutions using the Schwarzschild metric.

In Section 3.3 we derive properties of the Randall-Sundrum model. First of all, we show how RS1 offers a solution to the hierarchy problem. In particular, we derive that we need $\kappa y_c \sim 35$ to solve the hierarchy problem. Furthermore, we show that it indeed natural to assume that the branes are separated by a constant distance. Additionally, the Randall-Sundrum model reproduces four-dimensional gravity, even if the extra dimension is infinite. We end this chapter with a discussion on why we expect the RS black string to be unstable. This is caused by a singularity in the RS2 model.

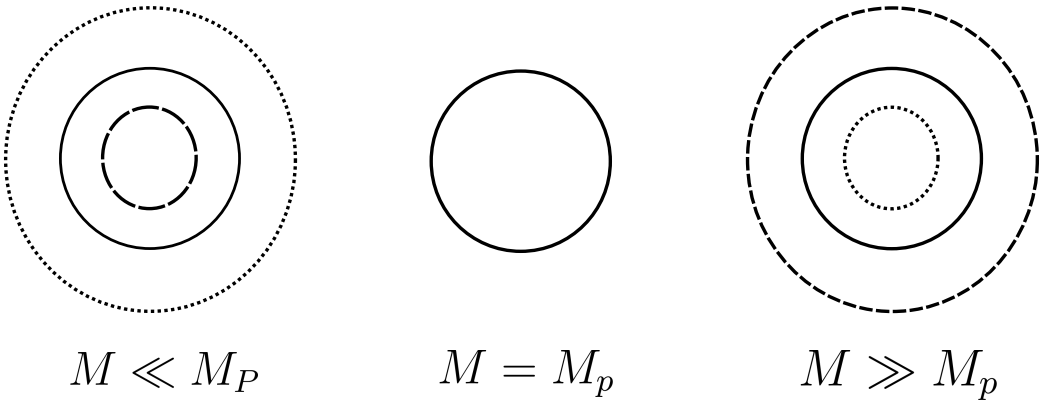

Figure 3.1: The ratio between the Schwarzschild radius (dashed line), the Compton length (solid line) and the Planck length (dotted line) for different mass ranges. Note that when the mass is equal to the Planck mass, all three lengths coincide.

3.1 Motivation

In this section we give some motivation to define the Randall-Sundrum model. Later in Section 3.2 we derive that the Randall-Sundrum model is a negatively curved warped spacetime. In Section 3.1.1 we state the hierarchy problem. Flat higher-dimensional spaces can potentially solve this problem, but this fails in five-dimensions since this would require a huge fifth dimension. To solve this problem, one can consider warped extra dimensions. In Section 3.1.2 we define Anti-de Sitter space. Later we show that Randall-Sundrum represents a slice of Anti-de Sitter space. Moreover, recently there have been developments in the AdS/CFT correspondence. This is discussed in Section 3.1.3. Similar to the AdS/CFT correspondence, there is a theory defined on the boundary of the space in the Randall-Sundrum model.

3.1.1 The hierarchy problem

In this section we describe the hierarchy problem and how it can be solved by including extra dimensions. The hierarchy problem is related to the huge difference between the electroweak scale and the Planck scale. This can be explained by the presence of extra dimensions. However, we show in this section that this fails in the case of one flat extra dimension, because the gravitational potential would disagrees with our observations.

In the last several decades theoretical physicists have been searching for a theory that combines GR and quantum theory. GR is an exact theory, meaning that if we would know the position and momenta of all particles at a certain point in time, we could in principle compute their positions and momenta at all other times. On the other hand, quantum theory is a theory of probabilities. In this theory we can only compute the probability that the system evolves from a certain configuration into another configuration.

These theories both work well in their own regimes, GR on very large cosmic scales and quantum theory on the miniscule particle level. There are regimes however, where the two theories meet, and contradict each other. To combine the two, requires a theory of quantum gravity. Even though, it is not yet known how we could construct this theory, there are ideas

how quantum gravity could be defined. One of the ideas is that there exists a spin-2 particle called the **graviton** that mediates the gravity interactions. This is a hypothetical particle, but if it would exist it would be almost impossible to detect [36]. It is similar to the photon, which is the particle that mediates electromagnetic interactions. Due to the fact that the photon is a massless particle, the electromagnetic interaction is relatively strong over long distances. Gravity is another force that is relatively strong over long distances, so we expect the graviton to be massless too.

It is possible to quantize gravity as an **effective field theory**, and this method works well on normal energy scales [37]. In the effective field theory, higher order curvature terms are also included in the action

$$S = \int d^4x\sqrt{-g}\left(4M_p^{n-2}\Lambda + 2M_p^{n-2}R + c_1\mathrm{scal}_g^2 + c_2 Ric_g \cdot Ric_g + \dots\right), \tag{3.1}$$

where the dots represent terms with higher power of scal_g, Ric_g and R. The higher orders become more relevant on smaller length scales and on higher energy scales. In an effective field theory, we cut off this summation at a certain power of the curvature terms. Since these higher order curvature terms become small on scales of huge lengths and small energies, this approximation works very well in most regimes.

However, there are places in the universe where energy scales are too high and the effective theory breaks down. For example, near the horizon of a small black hole, or at the big bang which is the origin of the universe. At these places singularities form in GR, which is a point in spacetime of infinite curvature. Therefore, all geodesics stop at this singularity and time and space stop to exist. This is an impossible phenomena in quantum theory, because a singularity has precise position and momentum, whereas in quantum theory the uncertainty principle forbids this. Furthermore, in the effective theory higher order curvature terms become relevant at these high energy levels. Therefore, the effective field theory fails to give a valid description at these regimes.

We can ask ourselves at what length scale GR starts to fail and we really need to include a full theory of quantum gravity. Both GR and quantum theory have their own characteristic length scales. In GR each massive object has a **Schwarzschild radius** r_s, which is given by

$$r_s = \frac{2G_N M}{c^2}, \tag{3.2}$$

where M is the mass of the object, G_N is Newton's gravitational constant and c the speed of light. If an object is smaller than its Schwarzschild radius, then it forms a black hole.

On the other hand, in quantum theory each massive particle has a **Compton wavelength**

$$L_C = \frac{\hbar}{Mc}, \tag{3.3}$$

where again M is the mass of the particle and $\hbar$ is the reduced Planck constant. At length scales comparable to the Compton wavelength, the energies of quantum fluctuations become comparable to the energy of the source. In other words, at these lengths we cannot neglect quantum effects anymore.

These two length scales meet at the **Planck length** $r_s = L_p = L_C$. At this scale the mass is equal to the **Planck mass** $M_p^2 = \frac{\hbar c}{2G_N}$. This means that the Planck mass is a lower bound for the mass of black holes as well as an upper bound for the mass of elementary particles. Take for example a point source of $M \gg M_p$, then a horizon would form at $r_s \gg L_p$, way before quantum effects come into play. It would not make sense to call this an elementary particle. Similarly, if we approach a point particle with $M \ll M_p$, then we will encounter

strong quantum effects way before we reach the horizon. Therefore, we cannot describe this horizon and we cannot call it a black hole. These different scales can also be seen in Fig. 3.1.

We conclude that we have found a natural candidate for the upper bound of the mass of elementary particles, $M_p \approx 1.22 \times 10^{19}\text{GeV}$. Now this gives rise to a question which describes the **hierarchy problem**. In 2012, the Higgs boson was discovered [38], it is the heaviest boson we know and it is responsible for giving mass to other particles through interactions. For example, the W and Z bosons, the particles that are responsible for mediating the weak interaction, get their mass through interactions with the Higgs boson. Due to their mass the weak interaction is only strong on very small distances. The electromagnetic force is mediated by the photon, which is a massless particle. Therefore, electromagnetic interactions are still relatively strong at long distances. At the electroweak scale $M_{\text{EW}} \approx 159.5GeV$, the W and Z bosons lose their mass, and the electromagnetic and weak force merge into one fundamental force.

We would expect fundamental scales such as the Planck and electroweak scale to be of the same order. However, note that the electroweak scale is an order of 10^{17} smaller than the Planck mass. This feels unnatural. Additionally, the electroweak scale is related to the mass of the Higgs boson. Due to the Weisskopf phenomenon, which is explained in more detail in [39, Chapter 3], quantum fluctuations would influence the mass we would observe for the Higgs boson. If μ is the mass of the Higgs boson, then quantum fluctuations should give an uncertainty to the mass of $\delta\mu = f\Lambda$, where f is some dimensionless coupling and Λ some cutoff scale. The only natural candidate for this cutoff scale is $\Lambda = M_p$, which an order of 10^{17} bigger then the electroweak scale. Therefore, to fix $\mu + \delta\mu$ to still be of the order of the electroweak scale, a huge fine-tuning for the coupling constant f is required. The lack of natural explanation for this observation is called the Hierarchy problem.

Definition 3.1.1. *The **Hierarchy problem** is the problem that we have no natural explanation for the fact that the electroweak scale is so much lower than the Planck scale.*

A possible solution to this problem could be that the Planck scale we just derived is not the real Planck scale and the true Planck scale is much lower. For example, if our universe consisted out of more than four dimensions, we would observe an effective four-dimensional Planck mass, whereas the global Planck mass could be much lower. We use the following lemma to illustrate this.

Lemma 3.1.2. *Consider an $4+n$-dimensional spacetime manifold $(M \times N, g)$, where M is a four-dimensional manifold, and N a closed n-dimensional manifold. Furthermore, suppose that the metric is a product metric $g = g^0 \oplus h$, where g^0 is a metric on M and h a Ricci flat metric on N. Then relation between the $4+n$-dimensional Planck mass $M_{p_{(4+n)}}$ and the effective four-dimensional Planck mass M_p is given by*

$$M_p^2 = Vol_n M_{p_{(4+n)}}^{2+n},$$

where Vol_n is the volume of (N, h).

Proof. The $4+n$-dimensional Ricci scalar R is equal to the effective 4-dimensional Ricci scalar R^0. The $4+n$-dimensional action is given by

$$\begin{aligned} S &= \int_M \int_N \sqrt{-\det g} 2M_{p_{(4+n)}}^{2+n} \left(\text{scal}_g - 2\Lambda\right) \, d^n y d^4 x \\ &= \int_M \int_N \sqrt{-\det(g^0)\det(h)} 2M_{p_{(4+n)}}^{2+n} \left(\text{scal}_{g^0}(x) - 2\Lambda\right) \, d^n y d^4 x \\ &= \int_M 2\text{Vol}_n M_{p_{(4+n)}}^{2+n} \left(\text{scal}_{g^0}(x) - 2\Lambda\right) \, d^4 x. \end{aligned}$$

Comparing this to the form of the four-dimensional action 2.24 we derive

$$M_p^2 = \mathrm{Vol}_n M_{p(4+n)}^{2+n}.$$

□

Using this result, we note that it is possible that the $4+n$-dimensional Planck mass is of the order of the Higgs mass, whereas in four dimensions we still observe the Planck mass. Now consider the case where we have n extra dimensions that are all compactified on a circle of radius L. Then $N = T^n$, where T^n is the n-dimensional torus. The volume of N is given by $\mathrm{Vol}_n = (2\pi L)^n$. With this volume the $4+n$-dimensional Planck mass would be of the order of the Higgs mass, if [40]

$$L \approx 10^{\frac{30}{n}-17}\mathrm{cm}.$$

In the case with one extra dimension, $n = 1$, this would imply that $L \approx 10^{13}$ cm, which is length similar to the size of our solar system. These are scales that we would be able to observe using experiments, because the extra dimensions influence the gravitational potential.

Lemma 3.1.3. *The $4+n$-dimensional gravitational potential is given by*

$$V(r) = -G_{4+n}\frac{M}{r^{n+1}}, \tag{3.4}$$

where M is the mass of the source, r the radial distance to the source and G_{4+n} the $4+n$-dimensional gravitational constant

Proof. We want the $4+n$-dimensional gravitational potential of a point particle of mass m located at the origin to solve the Poisson equation

$$\Delta_{4+n}V = 4\pi G_{4+n} M \delta^{3+n}(x^i), \tag{3.5}$$

where x^i denote only the spatial components of x. If we assume the potential to be time-independent and spherically symmetric then

$$\Delta_{4+n}V = (\frac{\partial^2}{\partial r^2} + \frac{N-1}{r}\frac{\partial}{\partial r})V.$$

We can simply check by substitution that

$$V = -G_{4+n}\frac{m}{r^{n+1}}$$

is a solution to Eq. 3.5. □

We conclude that in a higher dimensional universe, the gravitational potential would depend on a different power of r. Since the observations by Kepler and Newton it is already known that the gravitational potential is proportional to $1/r$ [41], so at first glance it seems like we can discard the idea of extra dimensions being present. Nevertheless, the story changes in the case of compact extra dimensions. Then the potential behaves as if there are an infinite amount of particles, all separated by the length of the extra dimension. For example, in the case of one extra dimension with radius L the potential would become

$$V(x,y) = -G_5 m \sum_{k=-\infty}^{\infty} \frac{1}{|x^i|^2 + (y - 2\pi L k)^2}, \quad x \in \mathbb{R}^4, y \in \mathbb{R}. \tag{3.6}$$

Assuming that the observer lives on the same y coordinate as the source, we can set $y = 0$.

Lemma 3.1.4. *In the region where $|x^i| \gg L$, the potential in Eq. 3.6 behaves as*

$$V(x, y = 0) = -\frac{G_5 m}{2rL}\left(1 + 2e^{-\frac{r}{L}} + \mathcal{O}(e^{-2\frac{r}{L}})\right), \tag{3.7}$$

where $r = |x^i|$. In the region where $|x^i| \ll R$, the potential 3.6 behaves as

$$V(x, y = 0) = -\frac{G_5 m}{\pi r^2} + \mathcal{O}(\frac{r}{L}). \tag{3.8}$$

Proof. After setting $y = 0$, it is shown in [9, P. 6] that the sum in Eq. 3.6 over k reduces to

$$V(x, y = 0) = -\frac{G_5 m}{2rL}\coth\Big(\frac{r}{2L}\Big). \tag{3.9}$$

For $a \in \mathbb{R}$ we can rewrite $\coth a$ as

$$\coth a = \frac{1 + e^{-2a}}{1 - e^{-2a}}.$$

Therefore, in the limit $a \to \infty$, we can approximate

$$\coth a = 1 + 2e^{-2a} + \mathcal{O}(e^{-4a}).$$

Returning to Eq. 3.9, we conclude that in the limit $r \gg L$

$$V(x, y = 0) = -\frac{G_5 m}{2rL}\left(1 + 2e^{-\frac{r}{L}} + \mathcal{O}(e^{-2\frac{r}{L}})\right).$$

In the limit $a \to 0$ it holds that

$$\coth a = \frac{1}{a} + \mathcal{O}(a^{-2}).$$

Consequently, in the region $r \ll L$ the potential 3.9 behaves as

$$V(x, y = 0) = -\frac{G_5 m}{\pi r^2} + \mathcal{O}(\frac{r}{L}).$$

□

If our universe would be five-dimensional with the radius of the extra dimension equal to $L = 10^{13}$ cm, then for any distance r on Earth we would have that $r \ll L$. Therefore, using Lem. 3.1.4 the gravitational potential would behave as Eq. 3.8. This is in disagreement with our observations.

Instead, we would expect the extra dimension to be relatively small compared to ordinary distances on Earth. Therefore, expect the potential to be of the form as in Eq. 3.7. Using experiments in the LHC we can put a bound on the size of the extra dimensions. So far tabletop experiments have restricted the size for one extra dimension to $L < 160\,\mu$m [42]. In order to retrieve the ordinary gravitational potential from the five-dimensional one in Eq. 3.7, we would need the five-dimensional Newton's constant to be equal to

$$G_5 = 2LG_4. \tag{3.10}$$

To conclude, we derived that the hierarchy problem can be solved by including extra compact dimensions. In the flat five-dimensional case the extra dimension would need to be of the order 10^{13} cm to offer a solution. However, the gravitational potential would disagree with our observations for such a large extra dimension. What about a five-dimensional space where the extra dimension is warped? This is what is Randall and Sundrum considered. As we will see later in this chapter, it is possible to solve the hierarchy problem with a small extra dimension if this extra dimension is curved.

3.1.2 Anti-de Sitter space

In the last section we concluded that we are interested in a curved five-dimensional space. Recall, that the vacuum Einstein equations 2.27 requires the Ricci tensor to be proportional to the metric by a factor that depends the cosmological constant Λ. We will later derive that Randall-Sundrum requires the space to be negatively curved, so $\Lambda < 0$. When $\Lambda < 0$ there exists a maximally symmetric Lorentzian solution to the Einstein vacuum equations. This solution is called Anti-de Sitter space. In this section we will define Anti-de Sitter space.

Definition 3.1.5. *Consider the semi-Riemannian manifold $(\mathbb{R}^{n+2}, g)$, where in Euclidean coordinates g is of the form*

$$ds^2 = -{dx_0}^2 + {dx_1}^2 + \cdots + {dx_n}^2 - {dx_{n+1}}^2.$$

*$n+1$-dimensional **Anti-de Sitter** space, or AdS_{n+1}, is defined by embedding the hyperboloid in $\mathbb{R}^{n+2}$ defined by the equation*

$$-{x_0}^2 - {x_{n+1}}^2 + {x_1}^2 + \cdots + {x_n}^2 = -\mu^2.$$

We can use the **Poincaré patch** to describe the half space of Anti-de Sitter space. This coordinate system is defined by

$$\begin{aligned} x^0 &= \frac{z}{2}\left(1 + \frac{\mu^2 + \vec{y}^2 - t^2}{z^2}\right), \\ x^a &= \frac{\mu}{z} y^a, && \text{for } 1 \le a \le n-1, \\ x^n &= \frac{z}{2}\left(1 - \frac{\mu^2 - \vec{y}^2 + t^2}{z^2}\right), \\ x^{n+1} &= \frac{\mu}{z} t. \end{aligned}$$

Where $y \in \mathbb{R}^{n-1}$, $t \in \mathbb{R}$ and $z > 0$. In these coordinates the induced metric on AdS_{n+1} is given by

$$ds^2 = \frac{\mu^2}{z^2}\left(-dt^2 + \delta_{ab} dy^a dy^b + dz^2\right) \tag{3.11}$$

Definition 3.1.6. *Let M be a semi-Riemannian manifold and g and h two metrics on M. We say g and h are **conformally equivalent** if there exists a smooth real valued function f on M, such that $g = f^2 \cdot h$, in that case f is called the **conformal factor**.*
*Let (M, g) and (N, h) be two semi-Riemannian manifolds. A diffeomorphism $\phi : M \to N$ is called a **conformal map** if $\phi^* g$ is conformally equivalent to h.*

Using this definition we see that in this Poincaré patch the half space of Anti-de Sitter is conformally equivalent to the half space of Minkowski. Consequently, on a z slice, it is possible to conformally embed n-dimensional Minkowski space in AdS_{n+1}.

In the next subsection we define the AdS/CFT correspondence, which says that a so called conformal field theory can be defined on the conformal boundary of AdS. To be able to see this boundary, we have to compactify AdS. This **conformal compactification** AdS space using the Penrose procedure [43]. This can be achieved using another coordinate patch defined by

$$\begin{aligned} x^0 &= \mu \sin\left(\frac{t}{\mu}\right) \cosh\left(\frac{r}{\mu}\right), \\ x^a &= \mu \Omega^a \sinh\left(\frac{r}{\mu}\right), \\ x^{n+1} &= \mu \cos\left(\frac{t}{a}\right) \cosh(r), \end{aligned}$$

where $\Omega \in S^{n-1} \subset \mathbb{R}^n$, $t \in [0, 2\pi\mu)$ and $r \geq 0$. In these coordinates the induced metric is

$$ds^2 = \mu^2 \left[-\cosh^2(\frac{r}{\mu})dt^2 + dr^2 + \sinh^2(\frac{r}{\mu})d\Omega_{n-1}^2 \right], \tag{3.12}$$

where $d\Omega_{n-1}$ is the standard metric on S^{n-1}. Note that the r coordinate is not compactified yet. To compactify r as well we redefine $\tan\left(\frac{\rho}{\mu}\right) = \sinh\left(\frac{r}{\mu}\right)$, where now $\rho \in [0, \frac{\pi\mu}{2})$. With this new coordinate Eq. 3.12 transforms to

$$ds^2 = \frac{\mu^2}{\cos^2(\frac{\rho}{\mu})} \left[-dt^2 + d\rho^2 + \sin^2(\frac{\rho}{\mu})d\Omega_{n-1}^2 \right]. \tag{3.13}$$

Looking at this metric we note that there exists a null geodesic starting at the origin, which can reach spatial infinity, i.e. $\rho = \frac{\pi\mu}{2}$, and return within a finite amount of time. This is depicted in Fig. 3.2. A consequence of this is that energy cannot escape to spatial infinity. Instead there seems to be a boundary at $\rho = \frac{\pi\mu}{2}$. Furthermore, any point in the diagram in Fig. 3.2 corresponds to a $n-1$ sphere in the full AdS_{n+1} model. Therefore, in the case $n = 2$, every point corresponds to circle S^1, so the AdS_3 space is compactified inside the interior of a cylinder $D^2 \times [0, 2\pi\mu)$ of radius $\frac{\pi\mu}{2}$.

Also for higher n the Penrose diagram in Fig. 3.2 represents a higher dimensional cylinder. To study the boundary, note that in these coordinates AdS_{n+1} is conformally equivalent to a flat solid cylinder. The interior of the cylinder corresponds to the Anti-de Sitter space, while the boundary of the cylinder is called the **conformal boundary**.

Definition 3.1.7. *Let (M, g) be a semi-Riemannian manifold and let N be a manifold with boundary and h a metric tensor on N. Then $(\partial N, h|_{\partial N})$ is a **conformal boundary** of (M, g) if there exists a conformal map $f : M \to \mathring{N}$.*

The boundary at $\rho = \frac{\pi\mu}{2}$ in Fig. 3.2 is the conformal boundary of AdS_{n+1}. According to the AdS/CFT correspondence we can define a conformal field theory on this boundary that is equivalent to the AdS space. We explain this in the next section.

3.1.3 AdS/CFT correspondence

Recent research in physics focuses a lot on studying conformal field theories on conformal boundaries, especially on the conformal boundary of AdS.

Definition 3.1.8. *A **conformal field theory** is a quantum field theory that is invariant under conformal transformations.*

In 1999, it was discovered that there exists a duality between $n+1$-dimensional AdS theories and n-dimensional CFTs [44]. An AdS theory is an Einstein manifold that asymptotically looks like Anti-de Sitter space, and therefore has the same conformal boundary. However, it can be the case that internally it looks completely different from AdS. Two theories are equivalent or **dual** to each other if there exists a map between the quantities and configurations of the theories that is conserved over time [45]. This means that both theories are different ways to describe the same phenomena and dynamics. This discovery then lead to the AdS/CFT correspondence.

Conjecture 3.1.9. *Every n-dimensional CFT is dual to some $n+1$-dimensional AdS theory of gravity.*

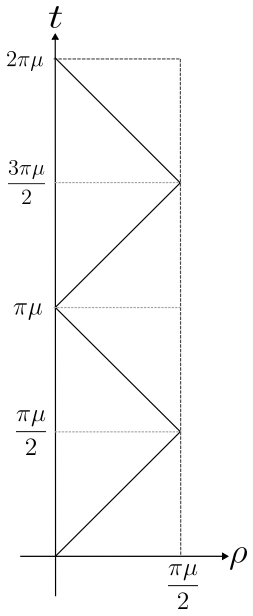

Figure 3.2: The Penrose diagram of Anti-de Sitter space with a light signal send from the origin as 45° lines. Here ρ is the compactified radial coordinate, and t the time coordinate which was already compact. As can be seen from the light trajectory, it is possible to reach spatial infinity and return to the origin in a finite amount of time. Every point inside the diagram corresponds to a $n-1$ sphere in the full model.

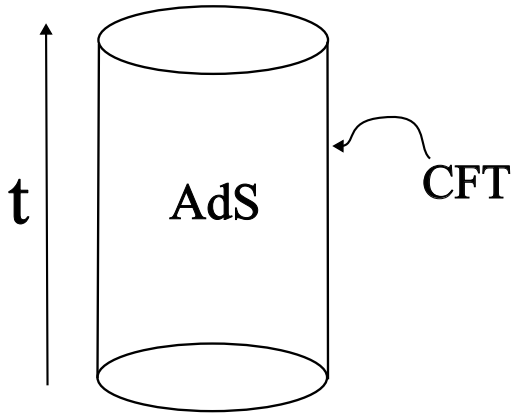

Figure 3.3: An intuitive picture of the AdS/CFT correspondence for $n = 2$. The AdS_3 theory is compactified in the interior of the cylinder and the CFT_2 is described on the boundary of the cylinder.

Consider the compactified AdS metric for $n = 2$ inside the cylinder. Then the 2-dimensional CFT lives on the boundary of the cylinder. This is illustrated in Fig. 3.3. Intuitively, in this correspondence the AdS theory is project on the conformal boundary, defining the CFT. Conversely, it is possible to reconstruct the AdS theory from all the information in the CFT on the boundary.

The AdS side of the correspondence will be represented by an **asymptotically Anti-de Sitter space**. An asymptotically AdS space represents an AdS space at spatial infinity and will therefore have a similar conformal boundary. However, matter and other structures may be present in the interior. The CFT lives on the conformal boundary and can be seen as a hologram of the AdS space [46].

An example of an asymptotically AdS space is the AdS black hole. The AdS/CFT correspondence could solve the information paradox for a AdS black hole. The **black hole information paradox** is explained in detail in [47, Sec. 2], but here follows a short explanation. Matter can fall into a black hole, and once matter disappears behind the horizon it can never return. Therefore, information is lost from the system. Nevertheless, in 1975 Hawking proved that black holes are not black after all, but instead slowly evaporate by emitting Hawking radiation [48]. Due to quantum effects, there is a constant creation and annihilation of virtual particle anti-particle pairs around the black hole. Sometimes, the anti-particle will fall into the black hole and the other virtual particle will not. Consequently, the particle that escapes becomes a real particle which is still entangled to the anti-particle. Additionally, the anti-particle makes the black hole lose mass, and it seems to an observer that the other particle came out of the black hole as radiation. Now information returns outside of the black hole, because of the entanglement between the particles. If this process continues, the black hole eventually completely evaporate. When the black hole disappears, the remaining particles can no longer be entangled with a particle inside the black hole. However, the information that was initially lost in the black hole was stored in this entanglement. After the black hole completely evaporated, what is left is radiation that contains no information about the initial state at all.

The system changes from a pure state into a mixed state. This contradicts with the principle of **unitarity**, which holds for both classical and quantum systems. This principle says that the state of a system at one point in time should determine its state at any other time. In general relativity the state on a Cauchy surface indeed should determine the state at any other time. In quantum mechanics the state of a system is described by the wave function. The wave function evolves by acting with a unitary operator on it. Therefore, using this operator, the wavefunction can be determined at any point in time.

There are attempts to solve this entanglement problem. However, this does not solve the information paradox due to the black hole no hair conjecture.

Conjecture 3.1.10. *A black hole has no hair, it is completely determined by its mass, angular momentum and charge.*

Therefore, all attempts still end up with the remaining radiation only containing information about the mass, angular momentum and charge of the black hole. When we consider a system where a black hole is formed through gravitational collapse of matter and then fully evaporates. It is impossible to reconstruct the initial state purely from the remaining radiation, because many initial states can evolve in a black hole with the same mass, angular momentum and charge. It seems as if information is lost!

The AdS/CFT correspondence solves the paradox, because even though the information paradox exists on the AdS side, we have unitarity on the CFT side of the duality. Therefore, to solve the paradox, we can map a final state on the AdS side to the CFT, then determine how this state evolved using the unitary operator. After applying the operator, the state can be

mapped back to the AdS side, to observe the initial state before the formation of the black hole.

The upshot is that, according to the above conjecture, there is some abstract boundary in AdS space that connects a lower dimensional CFT to the AdS theory. Since our universe appears four-dimensional, this result could be used to describe quantum processes using AdS_5, if we embed our universe on the conformal boundary. However, what if we embed our universe in a less abstract way? Namely as a 4-dimensional subspace of AdS_5. Such embeddings are called **3-branes**. As we will derive in the next section, but can already be seen in Eq. 3.11, it is possible to conformally embed Minkowski space into AdS with constant conformal factor. Therefore, the effective metric on the brane can even be the Minkowski metric. So if we embed a 4-dimensional world into AdS_5, do we still obtain 4-dimensional GR? And can we use any result from the AdS/CFT correspondence or can we learn anything from this new construction? These questions give some motivation to consider the Randall-Sundrum model.

3.2 The Randall-Sundrum model

In the previous section we looked at the hierarchy problem, which might be solved by considering warped spaces. Additionally, the AdS/CFT correspondence gave us the idea to consider theories living on the boundary of other spaces. In the Randall-Sundrum model this happens in the form of 3-branes. In this section we define the Randall-Sundrum model and derive metric solutions to the Einstein equations.

In Section 3.2.1 we state the assumptions behind the model and derive how the branes lead to extra terms in the action. In Section 3.2.2 we derive how the topology of Randall-Sundrum models can be viewed as an orbifold, which is useful in some of the later derivations. The curvature tensors are derived in Section 3.2.3. With this the Einstein equations are solved for the RS1 and RS2 models in Sections 3.2.4 and 3.2.5, respectively. In these subsections we derive the most important result of this section that gives an easy way to construct RS models. With this we construct a black hole solution called the black string in Section 3.2.6.

3.2.1 A warped structure and brane tension

In this subsection we make some assumptions on the structure of the Randall-Sundrum space and metric. There is an infinite amount of five-dimensional manifolds one can come up with and for each of those manifolds there are infinitely many four-dimensional manifolds that can be embedded in them. Nevertheless, based on observations and what we want to achieve we can make some logical assumptions that simplify the problem and allow us to derive some physical implications for the Randall-Sundrum scenario.

First of all, the four-dimensional subspace should represent our universe. Of course, we cannot be sure that our universe is infinite, it could for example still be a very large sphere. However, let us assume for now that it is infinite, because from our perspective it does seem that way. Then we want the four-dimensional manifold to be $M^4 = \mathbb{R}^4$. Another assumption that we make is that this brane is at the boundary of the five-dimensional space. Additionally, we want the five-dimensional space to have a simple topology such that we consider the two possibilities $M^5_{\text{RS1}} = \mathbb{R}^4 \times [0, 1]$ and $M^5_{\text{RS2}} = \mathbb{R}^4 \times [0, \infty)$. We call these models RS1 and RS2, respectively. A simple sketch of the different models can be seen in Fig. 3.4. We first focus on RS1, and from there derive the RS2 model.

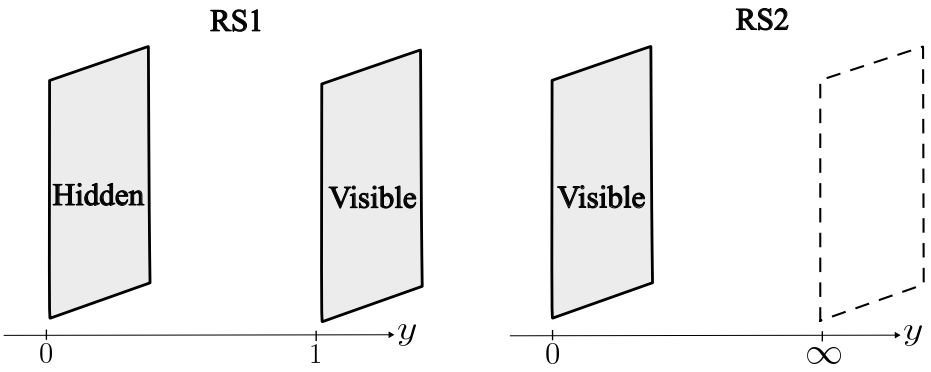

Figure 3.4: The branes and bulk space of the RS1 and RS2 model. Notice that in RS2 the visible brane is located at $y = 0$.

In RS1, we assume that there is another brane at the other boundary of M^5_{RS1}. If we choose Euclidean coordinates (x^0, x^1, x^2, x^3, y) then we fix the brane on which the standard model is located at $y = 1$, this brane is called the visible brane. The hidden brane is embedded at the other boundary at $y = 0$.

Secondly, we assume the geometry to be warped, so from Def. 2.1.7 the metric should be of the form

$$g = (f^2 \cdot \hat{g}) \oplus h, \tag{3.14}$$

where h is a metric on $[0, 1]$, $\hat{g}$ a metric on $\mathbb{R}^4$ and $f : [0, 1] \to \mathbb{R}$. In this way every slice of M^5 looks the same apart from some scaling by the function f. Recall the following elementary lemma.

Lemma 3.2.1. *Let $h = dy^2$ be the Euclidean metric on $[0, 1]$. Then for any Riemannian manifold $([0, 1], g)$ there exists a positive constant $y_c^2 \in \mathbb{R}$ such that $([0, 1], g)$ is isometric to $([0, 1], y_c^2 \cdot h)$.*

Proof. Let $([0, 1], g)$ be a Riemannian manifold. Then in Euclidean coordinates we can represent $g = g(x)^2 dx^2$, where $g(x) > 0$ for any $x \in [0, 1]$. Define $f : [0, 1] \to [0, 1]$ by

$$f(x) = \frac{\int_0^x g(y)dy}{y_c}, \tag{3.15}$$

where $y_c = \int_0^1 g(y)dy$. In this way, f is a diffeomorphism, because $f(x)$ is a smooth strictly increasing function and $f(0) = 0$ and $f(1) = 1$. Furthermore,

$$f_* g = g(x)^2 \left(\frac{df}{dx}\right)^{-2} dy^2 = y_c^2 \, dy^2. \tag{3.16}$$

□

Corollary 3.2.2. *A general warped metric on M^5_{RS1} is of the form*

$$g = e^{-2\sigma} \cdot \hat{g} \oplus y_c^2 \cdot h, \tag{3.17}$$

where $\sigma : \mathbb{R} \to \mathbb{R}$, $\hat{g}$ a metric tensor on $\mathbb{R}^4$, $y_c \in \mathbb{R}$, and h the Euclidean metric on $[0, 1]$.

Proof. We can apply Lem. 3.2.1 to the warped metric in Eq. 3.14. Additionally, it turns out that it is useful for our calculations to define $\sigma(y) = -\log f(y)$, such that a general warped metric is of the form as in Eq. 3.17. □

Thirdly, we assume that the branes have a **brane tension** which we will denote by $\lambda_{\text{hid}}, \lambda_{\text{vis}} \in \mathbb{R}$ for the hidden and visible brane, respectively. The brane tension describes the energy per unit volume of the brane. This energy influences the gravitational interactions and therefore has to be included in the action. In some theories the brane tension is considered to be variable, however we will assume that they are constant. Consequently, RS1 is a non-vacuum state and the Lagrangian is given by

$$L_{\text{RS1}} = -\lambda_{\text{hid}}\delta(y) + -\lambda_{\text{vis}}\delta(y-1), \tag{3.18}$$

where δ denotes the Dirac delta function. Due to the delta functions we only integrate the brane tension terms in the action over their corresponding brane. For this reason it is useful to define the **effective metrics**

$$g^{\text{hid}}(x) = g(x, y=0), \quad g^{\text{vis}}(x) = g(x, y=1), \tag{3.19}$$

With this Lagrangian the Randall-Sundrum action can be written as [7]

$$\begin{aligned} S_{\text{RS1}} &= S_{\text{grav}} + S_{\text{hid}} + S_{\text{vis}} \\ S_{\text{grav}} &= \int 2M_p^3 \left(scal_g - 2\Lambda\right) d\text{Vol}_g \\ S_{\text{hid}} &= -\int \lambda_{\text{hid}}\, d\text{Vol}_{g^{\text{hid}}} \\ S_{\text{vis}} &= -\int \lambda_{\text{vis}}\, d\text{Vol}_{g^{\text{vis}}}. \end{aligned} \tag{3.20}$$

Recall the definition of the energy-momentum tensor in Eq. 2.23. The energy-momentum tensor is obtained by varying the action in Eq. 3.20 with respect to the metric g. The following lemma is useful for the derivation.

Lemma 3.2.3. *The variation of the effective metrics with respect to the full metric is given by*

$$\frac{\delta\sqrt{-\det g^{vis}(x')}}{\delta g^{MN}(x,y)} = -\frac{1}{2}\sqrt{-\det g^{vis}(x)}\, g^{vis}_{ab}\delta^a_M\delta^b_N\delta^4(x-x')\delta(y-1).$$

Here $M, N = 0, 1, 2, 3, 5$ where 5 corresponds to the extra dimensional coordinate y, and $a, b = 0, 1, 2, 3$. Furthermore, δ^a_M are Kronecker delta functions and $\delta^4(x-x')$ and $\delta(y-1)$ are the four- and one-dimensional Dirac delta function, respectively. Recall that a prime feature of a functional derivative is that

$$\frac{\delta\phi^{a\ldots b}_{c\ldots d}(x)}{\delta\phi^{k\ldots l}_{m\ldots n}(y)} = \delta^a_k \ldots \delta^b_l\delta^m_c \ldots \delta^n_d\delta(x-y). \tag{3.21}$$

Proof. We can rewrite

$$\frac{\delta\sqrt{-\det g^{\text{vis}}(x')}}{\delta g^{MN}(x,y)} = \frac{\delta g^{ab}_{\text{vis}}(x)}{\delta g^{MN}(x,y)}\frac{\delta\sqrt{-\det g^{\text{vis}}(x')}}{\delta g^{ab}_{\text{vis}}(x)}. \tag{3.22}$$

Recalling the definition of g^{vis} from Eq. 3.19, and using the facts that

$$\begin{aligned} \frac{\delta g^{AB}}{\delta g^{MN}} &= \delta^A_M\delta^B_N, \\ \frac{\delta\sqrt{-\det g(x')}}{\delta g^{MN}(x)} &= -\frac{1}{2}\sqrt{-\det g(x)}\, g_{MN}\delta^n(x-x'), \end{aligned}$$

we can rewrite the right hand side of Eq. 3.22 to

$$\frac{\delta\sqrt{-\det g^{\text{vis}}(x')}}{\delta g^{MN}(x,y)} = -\frac{1}{2}\sqrt{-\det g^{\text{vis}}(x)}\, g^{\text{vis}}_{ab}\delta^a_M\delta^b_N\delta^4(x-x')\delta(y-1).$$

□

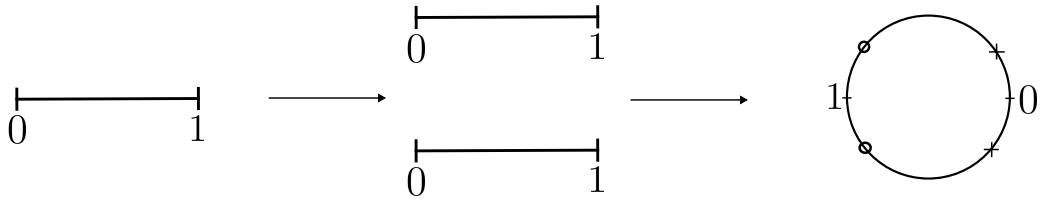

Figure 3.5: A scheme of the orbifolding procedure of the unit interval to the unit sphere. On the sphere the points at the circles or crosses are identified with each other.

We can apply Lem. 3.2.3 to both S_{hid} and S_{vis} to find the energy-momentum tensor.

Corollary 3.2.4. *In RS1 the energy-momentum tensor is given by*

$$T_{MN} = -\lambda_{hid}\frac{\sqrt{-\det g^{hid}}}{\sqrt{-\det g}}g^{hid}_{ab}\delta^a_M\delta^b_N\delta(y) - \lambda_{vis}\frac{\sqrt{-\det g^{vis}}}{\sqrt{-\det g}}g^{vis}_{ab}\delta^a_M\delta^b_N\delta(y-1). \tag{3.23}$$

Definition 3.2.5. *Let $\hat{g}$ be a metric tensor on $\mathbb{R}^4$, $\sigma : \mathbb{R} \to \mathbb{R}$ and $y_c, \lambda_{vis}, \lambda_{hid}, \Lambda \in \mathbb{R}$. The tuple $(\hat{g}, \sigma, y_c, \lambda_{vis}, \lambda_{hid}, \Lambda)$ is **RS1** if $(\mathbb{R}^4, g, \Lambda, L_{RS1})$ with g as in Eq. 3.17 and L_{RS1} as in Eq. 3.18 is an Einstein manifold.*

In the next subsection we use the energy-momentum tensor to solve the Einstein equations. By doing this we shall derive that there is a dependence between the brane tensions and the cosmological constant.

3.2.2 Randall-Sundrum as an orbifold

The usual topology of a five-dimensional space with compact extra dimension is $\mathbb{R}^4 \times S^1$. This was also the topology induced on the five-dimensional flat space in Section 3.1.1. This topology is not possible for the Randall-Sundrum model, because the branes are at the boundary of the extra dimension and S^1 has no boundary. In the literature it is common to still think of Randall-Sundrum as having this topology. For this we use the covering space of Randall-Sundrum and quotient out equivalent points using an action. This structure simplifies some of the calculations. This procedure turns the manifold into an orbifold.

Definition 3.2.6. *An n-dimensional **orbifold** is a Hausdorff topological space X, called the **underlying space**, with a covering by a collection of open sets U_i, closed under finite intersection. For each U_i, there is:*

- *an open subset V_i of $\mathbb{R}^n$, invariant under a faithful linear action of a finite group Γ_i,*
- *a continuous map ϕ_i of V_i onto U_i invariant under Γ_i, called an **orbifold chart**, which defines a homeomorphism between V_i/Γ_i and U_i.*

The interval $[0, 1]$ can be given an orbifold structure. Let $0 \leq i < j \leq 1$, we can cover the closed unit interval with open intervals of the form $U_{i,j} = (i, j)$, $U^0_j = [0, i)$ and $U^1_i(1 - i, 1]$. For the open intervals $U_{i,j}$ we define the opens $V_{i,j} = U_{i,j} \subset \mathbb{R}$ and $\phi_{i,j} : V_{i,j} \to U_{i,j}$ the

identity map and $\Gamma_{i,j}$ the trivial group. For open sets U_j^0 we define $V_j^0 = (-j, j) \subset \mathbb{R}$, with $\phi_j^0 : V_j^0 \to U_j^0$

$$\phi_j^0(x) = \begin{cases} x & \text{if } x \geq 0, \\ -x & \text{if } x < 0. \end{cases} \tag{3.24}$$

Additionally, $\Gamma_j^0 = \{1, -1\}$ with the action on $x \in V_j^0$ defined by $-1 \cdot x = -x$. Similarly, for opens U_i^1 we define $V_i^1 = (1 - i, 1 + i)$ with $\phi_i^1 : V_i^1 \to U_i^1$ defined by

$$\phi_i^1(x) = \begin{cases} x & \text{if } x \leq 1, \\ 2 - x & \text{if } x > 1. \end{cases} \tag{3.25}$$

Furthermore, we define the group $\Gamma_i^1 = \{1, -1\}$ with the action on $x \in V_i^1$ defined by $-1 \cdot x = 2 - x$.

Lemma 3.2.7. *The unit interval* $[0, 1]$ *with the above defined structure is an orbifold.*

Proof. The covering of $[0, 1]$ by the sets $U_{i,j}$, U_j^0 and U_i^1 is clearly closed under finite intersections. Furthermore, to each open set U we have associated an open set $V \subset \mathbb{R}$ which is invariant under an action of a finite group Γ. Lastly, the map ϕ defines a homeomorphism between V/Γ and U. □

This construction also gives an orbifold structure on $\mathbb{R}^4 \times [0, 1]$, since $\mathbb{R}^4$ has a canonical orbifold structure as a manifold, we can apply the above construction to the interval. In Fig. 3.5 it can be seen how the interval is turned into an orbifold. In the next subsection we will use this orbifold structure. A consequence of this is that we can lift the map $\sigma : [0, 1] \to \mathbb{R}$ to a map $\tilde{\sigma} : (-1, 2) \to \mathbb{R}$ which has the following orbifold symmetries

$$\tilde{\sigma}(-y) = \tilde{\sigma}(y), \quad \tilde{\sigma}(1 - y) = \tilde{\sigma}(1 + y). \tag{3.26}$$

3.2.3 Curvature tensors

In the previous sections we defined the RS1 model $(g^0, \sigma, y_c, \lambda_{\text{vis}}, \lambda_{\text{hid}}, \Lambda)$. To Check whether such a tuple indeed is RS1, we need to study the Einstein equations. For this we need to compute the Ricci tensor and scalar for a warped metric as in Eq. 3.17. This is done in this section.

First we compute the Christoffel symbols.

Lemma 3.2.8. *Let* $(g^0, \sigma, y_c, \lambda_{vis}, \lambda_{hid}, \Lambda)$ *be RS1. Then the non-trivial Christoffel symbols are given by*

$$\begin{aligned} \Gamma^c_{ab} &= {\Gamma^0}^c_{ab}, \\ \Gamma^5_{ab} &= \frac{\sigma'}{y_c^2} e^{-2\sigma} {g^0}_{ab}, \\ \Gamma^c_{a5} &= -\sigma' \, \delta^c_a. \end{aligned}$$

Disregarding those that can be constructed using symmetries from these Christoffel symbols.

Here $a, b, c = 0, 1, 2, 3$, and 5 denotes the extra dimensional component. Γ^0 denotes the Christoffel symbol induced by the metric g^0, and $\sigma' = \frac{\partial \sigma}{\partial y}$.

Proof. The Christoffel symbols can be computed from Eq. 2.7. Using that $g^{c5} = 0$ we indeed see that $\Gamma^c_{ab} = \Gamma^{0\,c}_{ab}$. For the second identity we have

$$\Gamma^5_{ab} = -\frac{1}{2} g^{55} \partial_5 g_{ab} = \frac{\sigma'}{y_c^2} e^{-2\sigma} g^0{}_{ab}.$$

Similarly, for the last identity

$$\begin{aligned} \Gamma^c_{a5} &= \frac{1}{2} g^{cb} \partial_5 g_{ab} \\ &= -\sigma' g^{cd} g_{ab} = -\sigma' \, \delta^c_a. \end{aligned}$$

□

Using the Christoffel symbols we can compute the Riemann tensor.

Lemma 3.2.9. *Let $(g^0, \sigma, y_c, \lambda_{vis}, \lambda_{hid}, \Lambda)$ be RS1. Then the non-trivial components of the Riemann tensor are*

$$\begin{aligned} R^a_{bcd} &= R^{0\,a}_{\quad bcd} - \frac{\sigma'^2}{y_c^2} \, e^{-2\sigma} \left(\delta^a_c g^0{}_{bd} - \delta^a_d g^0{}_{bc} \right), \\ R^5_{a5b} &= \frac{1}{y_c^2} e^{-2\sigma} g^0{}_{ab} \left(\sigma'' - \sigma'^2 \right), \\ R^a_{5b5} &= \delta^a_b \left(\sigma'' - \sigma'^2 \right). \end{aligned}$$

Here we disregarded the components that can be constructed from the above using symmetries.

In this lemma $R^{0\,a}_{\quad bcd}$ denotes the Riemann tensor of the semi-Riemannian manifold $(\mathbb{R}^4, g^0)$.

Proof. Using the definition of the Riemann tensor 2.13 and Lem. 3.2.8, we can derive

$$\begin{aligned} R^a_{bcd} &= \partial_c \Gamma^a_{bd} - \partial_d \Gamma^a_{bc} + \Gamma^a_{cM} \Gamma^M_{bd} - \Gamma^a_{dM} \Gamma^M_{bc} \\ &= R^{0\,a}_{\quad bcd} + \Gamma^a_{c5} \Gamma^5_{bd} - \Gamma^a_{d5} \Gamma^5_{bc} \\ &= R^{0\,a}_{\quad bcd} - \frac{\sigma'^2}{y_c^2} \, e^{-2\sigma} \left(\delta^a_c g^0{}_{bd} - \delta^a_d g^0{}_{bc} \right). \end{aligned}$$

For the second equality we have

$$\begin{aligned} R^5_{a5b} &= \partial_5 \Gamma^5_{ab} - \Gamma^5_{bc} \Gamma^c_{a5} \\ &= \frac{1}{y_c^2} e^{-2\sigma} g^0{}_{ab} \left(\sigma'' - 2\sigma'^2 \right) + \frac{\sigma'^2}{y_c^2} e^{-2\sigma} g^0{}_{ab} \\ &= \frac{1}{y_c^2} e^{-2\sigma} g^0{}_{ab} \left(\sigma'' - \sigma'^2 \right). \end{aligned}$$

Finally, for the third equality

$$\begin{aligned} R^a_{5b5} &= -\partial_5 \Gamma^a_{b5} - \Gamma^a_{5c} \Gamma^c_{5b} \\ &= \sigma'' \delta^a_b - \sigma'^2 \delta^a_c \delta^c_b \\ &= \delta^a_b \left(\sigma'' - \sigma'^2 \right). \end{aligned}$$

□

Next we compute the Ricci tensor.

Lemma 3.2.10. *Let $(g^0, \sigma, y_c, \lambda_{vis}, \lambda_{hid}, \Lambda)$ be RS1. Then the non-trivial components of the Ricci tensor are given by*

$$R_{ab} = {R^0}_{ab} + \frac{1}{y_c^2} e^{-2\sigma} g^0_{ab} \left(\sigma'' - 4\sigma'\right),$$
$$R_{55} = 4\sigma'' - 4\sigma'^2.$$

Here ${R^0}_{ab}$ denotes the Ricci tensor of the semi-Riemannian manifold $(\mathbb{R}^4, g^0)$.

Proof. Using the definition of the Ricci tensor in Eq. 2.15 we find

$$R_{ab} = R^c_{acb} + R^5_{a5b}$$

Applying Lem. 3.2.9 this becomes

$$\begin{aligned} R_{ab} &= {R^0}_{ab} - 3\frac{\sigma'^2}{y_c^2} e^{-2\sigma} {g^0}_{ab} + \frac{1}{y_c^2} e^{-2\sigma} {g^0}_{ab} \left(\sigma'' - \sigma'^2\right) \\ &= {R^0}_{ab} + \frac{1}{y_c^2} e^{-2\sigma} g^0_{ab} \left(\sigma'' - 4\sigma'\right). \end{aligned}$$

Where we used that $\delta^c_c = 4$. Likewise, for the (55) component

$$R_{55} = R^c_{5c5} = 4\sigma'' - 4\sigma'^2.$$

□

Finally, we can compute the Ricci scalar.

Lemma 3.2.11. *Let $(g^0, \sigma, y_c, \lambda_{vis}, \lambda_{hid}, \Lambda)$ be RS1. Then the Ricci scalar is*

$$R = e^{2\sigma} R^0 + \frac{1}{y_c^2} \left(8\sigma'' - 20\sigma'^2\right).$$

Here R^0 denotes the Ricci scalar of the semi-Riemannian manifold $(\mathbb{R}^4, g^0)$.

Proof. Using Lem. 3.2.10 and the definition of the Ricci scalar in 2.17 it directly follows that

$$\begin{aligned} R &= e^{2\sigma} R^0 + \frac{4}{y_c^2} \left(\sigma'' - 4\sigma'^2\right) + \frac{4}{y_c^2} \left(\sigma'' - \sigma'^2\right) \\ &= e^{2\sigma} R^0 + \frac{1}{y_c^2} \left(8\sigma'' - 20\sigma'^2\right). \end{aligned}$$

□

Now that we have the expressions for all the curvature tensors, we can solve the Einstein equations in the next section.

3.2.4 Solving the Einstein field equations

In this subsection we solve the Einstein equations for a metric that satisfies the assumptions that derived in Section 3.2.1. To summarize, we are considering the warped spacetime $M^5 = \mathbb{R}^4 \times [0, 1]$ with a metric tensor of the form as in Eq. 3.17 and energy-momentum tensor as in Eq. 3.23. It turns out that if we solve the Einstein equations for a Ricci flat metric g^0, many of the quantities in Def. 3.2.5 are related.

Theorem 3.2.12. *Let $(g^0, \sigma, y_c, \lambda_{vis}, \lambda_{hid}, \Lambda)$ be RS1. If g^0 is Ricci flat then:*

1. $\Lambda < 0$,
2. $24M_p^3\sqrt{\frac{-\Lambda}{6}} = \lambda_{hid} = -\lambda_{vis}$,
3. $\sigma(y) = y_c|y|\sqrt{\frac{-\Lambda}{6}}$.

Using the lemmas from Section 3.2.3 can compute the Einstein equation for a RS1 model. The **RS1 Einstein equations** are given by

$$R_{ab} - \frac{1}{2}Rg_{ab} + \Lambda g_{ab} = -\frac{1}{4M_p^3}\big(\lambda_{\text{hid}}\frac{\sqrt{-\det g^{\text{hid}}}}{\sqrt{-\det g}}g^{\text{hid}}_{ab}\delta^a_M\delta^b_N\delta(y) + \lambda_{\text{vis}}\frac{\sqrt{-\det g^{\text{vis}}}}{\sqrt{-\det g}}g^{\text{vis}}_{ab}\delta^a_M\delta^b_N\delta(y-1)\big). \tag{3.27}$$

The non-trivial components of this equation are the (55)-component and any other (ab)-component where $a, b = 0, 1, 2, 3$. From the (55)-component we get the equation

$$-\frac{1}{2}y_c^2R^0 + 6\sigma'^2 + y_c^2\Lambda = 0. \tag{3.28}$$

From the (ab)-components we get the equations

$$e^{2\sigma}R^0{}_{ab} + \left[-\frac{R^0}{2} + \frac{\left(6\sigma'^2 - 3\sigma''\right)}{y_c^2} + \Lambda\right]g^0{}_{ab} = -\frac{g^0{}_{ab}}{4y_c\,M_p^3}\left(\lambda_{\text{hid}}\,\delta(y) + \lambda_{\text{vis}}\,\delta(y-1)\right). \tag{3.29}$$

Now suppose that g^0 is Ricci flat. Then $R^0 = 0 = R^0{}_{ab}$, for every $a, b = 0, 1, 2, 3$. Therefore, we can rewrite Eq. 3.28 and 3.29 to

$$\sigma'^2 = -y_c^2\frac{\Lambda}{6} \tag{3.30}$$

$$\sigma'' = \frac{y_c}{12M_p^3}\left(\lambda_{\text{hid}}\,\delta(y) + \lambda_{\text{vis}}\,\delta(y-1)\right) \tag{3.31}$$

Here we used Eq. 3.28 to get rid of some terms in Eq. 3.29. The solution to Eq. 3.30 that respects the orbifold symmetries 3.26 at $y = 0$ and $y = 1$ is

$$\sigma(y) = \begin{cases} -y_c y\sqrt{\frac{-\Lambda}{6}} & \text{if } y < 0, \\ y_c y\sqrt{\frac{-\Lambda}{6}} & \text{if } 0 \le y \le 1, \\ y_c(2-y)\sqrt{\frac{-\Lambda}{6}} & \text{if } y > 1. \end{cases} \tag{3.32}$$

For simplicity we will denote this by $\sigma = y_c|y|\sqrt{\frac{-\Lambda}{6}}$. Note that this requires a negative cosmological constant. Consequently, the five-dimensional space will have similar properties as AdS space.

If we take the second derivative of 3.32 then due to the orbifold symmetry

$$\sigma''(y) = 2y_c\sqrt{\frac{-\Lambda}{6}}\left(\delta(y) - \delta(y-1)\right) \tag{3.33}$$

Comparing Eq. 3.33 to Eq. 3.31 we can relate Λ to the brane tensions $\lambda_{\text{hid/vis}}$

$$24M_p^3\sqrt{\frac{-\Lambda}{6}} = \lambda_{\text{hid}} = -\lambda_{\text{vis}}. \tag{3.34}$$

Consequently, the hidden brane has positive brane tension and the visible brane has negative brane tension. We can use the relation in Eq. 3.34 to replace the three constants in the model with one constant. For this we define the **curvature scale** κ as

$$\Lambda = -6\kappa^2, \quad \lambda_{\text{hid}} = -\lambda_{\text{vis}} = 24M_p^3\kappa. \tag{3.35}$$

Going back to Lem. 3.2.11, we can see why κ is called the curvature scale. Namely, away from the branes, for a Ricci flat g^0 we have $R = -20\frac{\kappa^2}{y_c^2}$. Therefore, for higher κ the space is more strongly curved. The warping factor scales with κ as well, since from Eq. 3.32 we can rewrite σ to

$$\sigma(y) = y_c|y|\kappa. \tag{3.36}$$

Therefore, the metric becomes

$$g = e^{-2y_c|y|\kappa}g^0 \oplus y_c^2 h \tag{3.37}$$

Definition 3.2.13. *The tuple (g^0, y_c, κ) is **flat RS1**, if g^0 is a Ricci flat metric tensor on $\mathbb{R}^4$ and $y_c, \kappa \in \mathbb{R}$.*

Theorem 3.2.14. *If (g^0, y_c, κ) is flat RS1, then $(g^0, y_c|y|\kappa, y_c, 24M_p^3\kappa, -24M_p^3\kappa, -6\kappa^2)$ is RS1.*

With this result, it is possible to construct many RS1 spaces. Namely, any Ricci flat metric and constants $y_c, \kappa \in \mathbb{R}$ will generate a RS1 space. In Chapter 2 we already saw two examples of Ricci flat spaces.

Example 3.2.15. *Let η be the Minkowski metric on $\mathbb{R}^4$. Then (η, y_c, κ) is for any $y_c, \kappa \in \mathbb{R}$. We call these spaces **standard RS1**.*

In the original Randall-Sundrum paper, the focus is on standard RS1 spaces. The advantage of these spaces is that they admit Poincaré symmetry on the branes and are therefore easy to work with. The other Ricci flat space we considered was the Schwarzschild black hole. In Section 3.2.6 we focus on this RS black hole solution.

Lemma 3.2.16. *Consider standard RS1 (η, y_c, κ). Then this manifold can be embedded into AdS_5.*

Proof. In the standard coordinates on $\mathbb{R}^4 \times [0, 1]$, the metric g in this RS1 model becomes

$$ds^2 = e^{-2\kappa y_c|y|}\eta_{ab}dx^a dx^b + y_c^2 dy^2. \tag{3.38}$$

Recall the AdS metric in the Poincaré patch in Eq. 3.11. For the Poincaré coordinate patch we denote the coordinates by (x', z) where $x' \in \mathbb{R}^4$ and $z > 0$. We can define a map $f : (\mathbb{R}^4, g) \to AdS_5$ which on these coordinate charts is defined by

$$f(x, y) = (x, \frac{1}{\kappa}e^{\kappa y_c|y|}).$$

Let's denote $z = \frac{1}{\kappa}e^{\kappa y_c|y|}$, then in the image of f it holds that $\frac{1}{\kappa} \leq z \leq \frac{e^{\kappa y_c}}{\kappa}$. Furthermore, the induced metric is given by

$$f_*g = \frac{1}{\kappa^2 z^2}\left(\eta_{ab}dx^a dx^b + dz^2\right). \tag{3.39}$$

This corresponds to the AdS_5 metric in the Poincare patch 3.11. We conclude that standard RS1 can be embeded in AdS_5. □

For this reason RS is also called a **slice of AdS$_5$**.

3.2.5 The infinite Randall-Sundrum model

So far we focused on RS1 models, consisting of two four-dimensional branes at the boundary of a finite fifth dimension. RS2 consists of only one brane, the visible brane, in a semi-infinite five-dimensional space. Luckily, the construction of RS2 works very similarly to the construction of RS1. To transform RS1 into RS2, we first map the interval $f : [0, 1] \to [0, y_c]$. The idea is to follow the same steps and in the end take the limit $y_c \to \infty$. With this limit one of the branes disappears to infinity. Since it would not be desirable to make the visible brane disappear, the location of the two branes needs to be swapped. The RS2 action is of similar form as the action in Eq. 3.20, where now the gravitational action is given by

$$S_{\text{grav}} = \int d^4x \int_0^{y_c} dz \sqrt{-\det g}\{-\Lambda + 2M_p^3 R\} \tag{3.40}$$

Where $z = y_c y$ is the new coordinate. Additionally, the branes are swapped, so the definitions of the reduced metric are modified to $g^{\text{vis}}(x) = g(x, z = 0)$ and $g^{\text{hid}}(x) = g(x, z = y_c)$.

Definition 3.2.17. *Let g^0 be a metric tensor on $\mathbb{R}^4$, $\sigma : \mathbb{R} \to \mathbb{R}$ and $\lambda_{vis}, \lambda_{hid}, \Lambda \in \mathbb{R}$. The tuple $(g^0, \sigma, \lambda_{vis}, \lambda_{hid}, \Lambda)$ is **RS2** if $(\mathbb{R}^4, g, S_{RS2})$ with g as in Eq. 3.17 and S_{RS2} as in Eq. 3.40 is an Einstein manifold.*

Following the same steps as in the previous sections, there exist many solutions when g^0 is Ricci flat.

Definition 3.2.18. *The tuple (g^0, κ) is **flat RS2**, if g^0 is a Ricci flat metric tensor on $\mathbb{R}^4$ and $\kappa \in \mathbb{R}$.*

Just like for RS1, the cosmological constants and brane tensions are related. The difference is however, that in RS2 the visible brane has positive brane tension. Let (g^0, y_c, κ) be flat RS2, then the RS2 metric g has the following form

$$g = e^{-2\kappa|z|} g^0 \oplus dz^2. \tag{3.41}$$

The **standard RS2** space (η, κ) can also be embedded in AdS_5, where now the z coordinate in the Poincaré patch is valued between $\frac{1}{\kappa} \leq z < \infty$. The visible brane is located at $z = \frac{1}{\kappa}$.

3.2.6 Black strings

Now that we found a simple way to construct RS spaces, it makes sense to look for Randall-Sundrum black hole solutions. In four-dimensions the simplest black hole is described by the Schwarzschild solution g_s from Ex. 2.1.16. The Schwarzschild metric is Ricci flat which makes it a natural candidate for RS. With Cor. 3.2.14 it follows that (g_s, y_c, κ) is flat RS1. We call this solution the **RS1 black string**. We call it a string instead of a hole, because it only forms a black hole on the 3-brane. This black hole is stretched out along the direction of the extra dimension. The result resembles the shape of a cylinder or string, as can be seen in Fig. 3.6. The RS metric for the black string in spherical coordinates is given by

$$g = e^{-2\kappa y_c|y|} \left[-\left(1 - \frac{r_s}{r}\right) dt^2 + \frac{1}{1 - \frac{r_s}{r}} dr^2 + r^2 d\theta^2 + r^2 \sin\theta \, d\varphi^2 \right] + y_c^2 dy^2. \tag{3.42}$$

These results also apply to RS2. However, we will now derive that there is some unwanted behaviour for the RS2 black string.

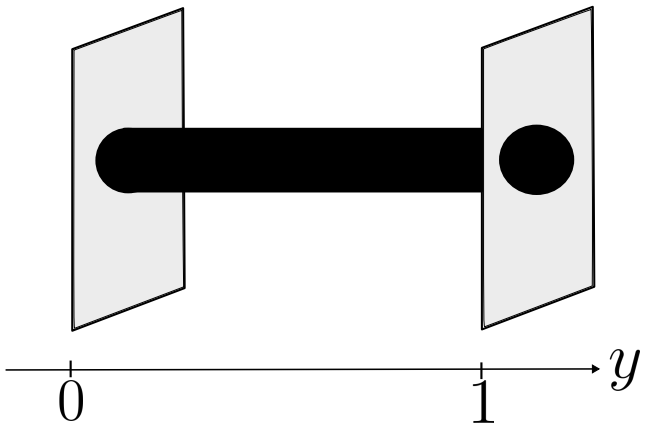

Figure 3.6: A schematic picture of the RS1 black string solution.

Lemma 3.2.19. *The effective four-dimensional black hole mass at a constant y-slice is*

$$M_* = Me^{-\kappa y_c y}.$$

Proof. Let us fix a $y \in [0, 1]$. Then using Eq. 3.42, we can rescale the t and r coordinate to

$$r = e^{\kappa y_c |y|}\hat{r},$$
$$t = e^{\kappa y_c |y|}\hat{t}.$$

Applying this rescaling to Eq. 3.42 leads to a metric that resembles the Schwarzschild metric

$$g = -(1 - \frac{2M}{\hat{r}}e^{-\kappa y_c|y|})d\hat{t}^2 + \frac{1}{1 - \frac{2M}{\hat{r}}e^{-\kappa y_c|y|}}d\hat{r}^2 + \hat{r}^2 d\theta^2 + \hat{r}^2 \sin^2\theta d\varphi^2 + dy^2. \tag{3.43}$$

Reading off the mass from Eq. 3.43 gives $M_* = Me^{-\kappa y_c|y|}$. □

A consequence of this result is that the mass of the black hole on the visible brane seems smaller as y_c increases. Consequently, in RS2, the black hole appears massless near the AdS horizon. This is a weird phenomenon. In Section 3.3.4 we derive that the metric also becomes singular at the AdS horizon.

Finally, it is important to note that a spherical black hole solution is hard to construct in RS. To illustrate this consider the most natural candidate, a five-dimensional Schwarzschild-AdS black hole, whose metric in spherical coordinates is given by

$$ds^2 = -U(r)dt^2 + U(r)^{-1}dr^2 + r^2\left(d\chi^2 + \sin^2\chi d\Omega^2\right), \tag{3.44}$$

where $d\Omega^2$ is the standard metric on S^2 and

$$U(r) = 1 - \frac{2M}{r} + r^2\kappa^2.$$

If we consider the RS2 case, with only one brane with positive tension present, then we should be able to write the position of the brane by $\chi = \chi(r)$. However, there only exist spherical solutions in the non-vacuum case [17]. We are only interested in vacuum solutions since these describe the system in its final state after gravitational collapse on the brane.

3.3 Properties of the Randall-Sundrum model

Now that we defined the Randall-Sundrum model, we can look at the most important properties of Randall-Sundrum. As explained in Section 3.1.1, this model was originally introduced as a new way of solving the hierarchy problem. We derive how the hierarchy problem is solved in Section 3.3.1. Then we show that not much fine-tuning is necessary to construct a model that solves the hierarchy problem in Section 3.3.2. Additionally, if we believe that Randall-Sundrum models could represent our universe, it is required that four-dimensional gravity is retrieved on the brane. In other words that the gravitational potential is proportional to r^{-1}. This is proven in Section 3.3.3. Finally, it turns out that there is a singularity at $z = \infty$ in the RS2 black string in Section 3.3.4. This is a big hint for the existence of an instability in the RS black string.

3.3.1 Solution to the hierarchy problem

The original motivation behind the Randall-Sundrum model is that it offers an original solution to the hierarchy problem [7]. In Section 3.1.1 we saw that the hierarchy problem can be solved by adding compact flat extra dimensions. Due to the extra dimensions, it is possible that the Planck scale is of the same order as the electroweak scale, but the effective four-dimensional Planck scale is much higher.

The solution of Randall and Sundrum works the other way around. The idea is that in the five-dimensional space, the electroweak scale and Planck scale are of the same order. In this model the effective four-dimensional Planck scale is still of the same order as the Planck scale. Due to the warping, the effective electro-weak scale greatly decreases on the visible brane. Namely, in this section we shall prove that the observed electroweak scale is an order $e^{-\kappa y_c}$ lower than the five-dimensional electroweak scale.

Lemma 3.3.1. *In flat RS the relation between the five-dimensional Planck scale M_{p_5} and the effective four-dimensional Planck scale M_p is given by*

$$M_p^2 = \frac{M_{p_5}^3}{2\kappa}\left(1 - e^{-2\kappa y_c}\right). \tag{3.45}$$

Proof. Consider the gravitational part of the RS action

$$S_g = \int d^4x \int_0^1 dy \sqrt{-\det g}\, 2M_{p_5}^3 \left(R - 2\Lambda\right). \tag{3.46}$$

Next we use that in flat RS the metric is warped $g = e^{-\kappa y_c |y|} g^0 \oplus y_c^2 \cdot h$ for some metric tensor g^0 on $\mathbb{R}^4$. Therefore,

$$\begin{aligned} \det g &= e^{-8\kappa y_c |y|} y_c^2 \det g^0, \\ R &= e^{2\kappa y_c |y|} R^0 - 20\kappa^2. \end{aligned}$$

For now we focus on the curvature term only, since from there we can read off the Planck mass. The action in terms of the four-dimensional metric is now

$$S_g = \int d^4x \int_0^1 dy \sqrt{-\det g^0}\, 2M_{p_5}^3 e^{-2\kappa y_c |y|} y_c R^0.$$

Note that g^0 is independent of the y-coordinate. By evaluating the y-integral, the effective four-dimensional action is obtained,

$$S_g = \int d^4x \sqrt{-\det g^0}\, \frac{M_{p_5}^3}{\kappa}\left(1 - e^{-2\kappa y_c}\right) R^0. \tag{3.47}$$

Comparing Eq. 3.47 to the standard Einstein-Hilbert action 2.24 with vanishing cosmological constant, we derive the desired relation 3.45. □

From this result we derive that if both M_{p_5} and κ are of the Planck scale and κy_c is relatively big, then M_p^2 is of the Planck scale. Another interesting consequence is that in the flat limit, i.e. when $\kappa \to 0$, we retrieve the relation for a flat extra dimension

$$M_p^2 = y_c M_{p_5}^3 = V_1 M_{p_5}^3$$

Lastly, we note that in the RS2 model this construction also works, but the exponential term vanishes.

Even though the Planck scale is not altered by the warping, it greatly influences fields that are restricted to the brane. To illustrate this we will take a look at the Higgs field, which is the field related to the Higgs Boson. The action of the Higgs field has the following form

$$S = \int \left(g_{\text{vis}}^{ab} \partial_a H^\dagger \partial_b H - \lambda (H^2 - v_0^2)^2 \right) d\text{Vol}_{g^{\text{vis}}}, \tag{3.48}$$

where $\lambda \in \mathbb{R}$ is a coupling constant and $H^\dagger$ denotes the complex conjugate of the field H. The second term in the integral, the term without derivatives, represents a potential. The **vacuum expectation value** of the Higgs field is the minimum of this potential, and it is the value the Higgs field takes in the absence of particles. For the action in Eq. 3.48 the vacuum expectation value is v_0.

The electroweak scale is related to the vacuum expectation value v_0 of the Higgs field H, which is also the mass of the Higgs boson. Unlike other known scalar fields, the Higgs field has a non-zero expectation value in vacuum. Since the Higgs field is part of the standard model, it is restricted to the visible brane. So v_0 represents the vacuum expectation value in the RS model, but as we will derive in the following lemma, it is possible that the effective vacuum expectation value observed on the visible brane is much lower.

Lemma 3.3.2. *Let v_0 be the vacuum expectation value of the Higgs field H in the flat RS1 model $(\hat{g}, y_c, \kappa)$. Then an observer on the visible brane will observe an effective vacuum expectation value of the Higgs field of $v_0 e^{-\kappa y_c}$.*

Proof. Let $\hat{g}$ be the four-dimensional metric. Then we can use the definition of g_{vis} from Eq. 3.19 to express g_{vis} in terms of the four-dimensional metric $\hat{g}$. The action in Eq. 3.48 then becomes

$$S = \int d^4x \sqrt{-\det g^0} e^{-2\kappa y_c} \left(g^{0^{ab}} \partial_a H^\dagger \partial_b H - \lambda e^{-2\kappa y_c} \left(H^2 - v_0^2 \right)^2 \right).$$

Next we can rescale the field by $H = e^{\kappa y_c} h$, then the action for this new field is

$$S = \int d^4x \sqrt{-\det g^0} \left(g^{0^{ab}} \partial_a h^\dagger \partial_b h - \lambda \left(h^2 - v_0^2 e^{-2\kappa y_c} \right)^2 \right). \tag{3.49}$$

Note that Eq. 3.49 closely resembles the four-dimensional action for the Higgs field as we know it. However, now the vacuum expectation value $\hat{v}_0$ in four dimensions relates to the five dimensional expectation value by

$$\hat{v}_0 = v_0 e^{-\kappa y_c}.$$

□

Note that the ratio between the mass of the Higgs particle and the effective mass of the Higgs particle on the brane is the same as the ratio between the mass of the black string and the

black hole on the brane. So it seems that we can generalize the result of Lem. 3.3.2 to any mass parameter m_0 [7]. If we assume v_0 to be of the Planck scale and we want our observed vacuum expectation value of the Higgs field to be around 1 TeV, then we need $e^{\kappa y_c}$ to be of the order 10^{16}. Therefore, in this model the hierarchy problem is translated to a new type of hierarchy, now between the curvature scale κ and the size of the extra dimension y_c. To solve the hierarchy problem we demand $\kappa y_c \approx 35$, which is a much smaller hierarchy.

3.3.2 Fixing the distance between the branes

In the previous subsection we derived how the length of the extra dimension y_c has to be tuned to solve the hierarchy problem. The RS1 model gives a much more natural explanation for the huge ratio between the electroweak scale and the Planck mass than we are able to do with the four-dimensional standard model. However, we still have to show whether the RS1 model is natural as well. In particular, one of the assumptions we made in the construction of the model in Sec. 3.2.1 is that the metric is warped. Consequently, we ended up with a space where the extra dimension has a constant length y_c. However, is this a natural assumption to make? If a lot of fine-tuning is required to construct a model that solves the hierarchy problem, it is not really a solution because it just moves the problem to another fine-tuning problem. Therefore, in this section we show that not much fine-tuning is required to construct a standard RS model with $\kappa y_c \sim 35$.

Without the assumption of the branes being separated by a constant distance, y_c should be replaced by a scalar field $T(x)$. This field would only depend on x because using Lem. 3.2.1, the y-dependence can be integrated out. Therefore, an even more general metric would have the form

$$g = e^{-2\sigma}\hat{g} + T(x) \cdot h. \tag{3.50}$$

This can be interpreted as that the distance between the branes is not constant. Therefore, instead of the branes forming flat sheets as in Fig. 1.1, they would be more wrinkled, such that at some points they are closer to each other than at other points.

This field $T(x)$ would then fluctuate around a vacuum expectation value. This vacuum expectation value can be denoted by y_c. These fluctuations correspond to a field called the **radion**. For the assumptions to be valid, we need a mechanism to fix $T(x)$ to take the value of its vacuum expectation value. Goldberger and Wise succeeded in this using a potential associated to a bulk scalar field with interaction terms that are localized on the 3-branes [49]. In particular, without much fine tuning the minimum of the potential can be arranged such that $\kappa y_c \sim 35$. In this section we follow their derivation.

Consider a bulk scalar field Φ with the bulk action

$$S = \frac{1}{2}\int d^4x \int_0^1 dy \sqrt{-\det g}\left(g^{MN}\partial_M\Phi\partial_N\Phi - m^2\Phi^2\right),$$

where g_{MN} with $M, N = 0, 1, 2, 3, 5$ is standard RS. There are also interaction terms on the hidden and visible branes given by

$$S_{\text{hid}} = -\int d^4x \lambda_{\text{hid}} \sqrt{-\det g_{\text{hid}}}\left(\Phi^2 - v_{\text{hid}}^2\right)^2,$$
$$S_{\text{vis}} = -\int d^4x \lambda_{\text{vis}} \sqrt{-\det g_{\text{vis}}}\left(\Phi^2 - v_{\text{vis}}^2\right)^2.$$

These terms on the branes cause Φ to have a y-dependent vacuum expectation value $\Phi(y)$.

This value is determined by the equation of motion for Φ

$$\begin{aligned} 0 =& -\frac{1}{y_c^2}\partial_y\left(e^{-4\sigma}\partial_y\Phi\right) + m^2 e^{-4\sigma}\Phi + 4e^{-4\sigma}\lambda_{\text{hid}}\Phi(\Phi^2 - v_{\text{hid}})\frac{\delta(y)}{y_c} \\ &+ 4e^{-4\sigma}\lambda_{\text{vis}}\Phi(\Phi - v_{\text{vis}}^2)\frac{\delta(y-1)}{y_c}, \end{aligned} \tag{3.51}$$

where $\sigma(y) = \kappa y_c|y|$.

Lemma 3.3.3. *The above action and equations of motion for the field Φ yield an effective potential with minimum κy_c. With minimal fine tuning the value of this potential can be set to $\kappa y_c \sim 35$.*

Proof. First of all, Eq. 3.51 has a solution away from the branes given by

$$\Phi(y) = e^{2\sigma}\left(Ae^{\nu\sigma} + Be^{-\nu\sigma}\right), \tag{3.52}$$

with $\nu = \sqrt{4 + \frac{m^2}{\kappa^2}}$. The coefficients A and B are determined by the boundary conditions at the branes. By integrating the equation of motion over a infinitesimal region around the branes. This gives the conditions

$$\begin{aligned} 0 =& \kappa\left[(2+\nu)A + (2-\nu)B\right] - 2\lambda_{\text{hid}}\Phi(0)\left[\Phi(0)^2 - v_{\text{hid}}^2\right], \\ 0 =& \kappa e^{2\kappa y_c}\left[(2+\nu)e^{\nu\kappa y_c}A + (2-\nu)e^{-\nu\kappa y_c}B\right] + 2\lambda_{\text{vis}}\Phi(1)\left[\Phi(1)^2 - v_{\text{vis}}^2\right]. \end{aligned}$$

Rather than solving these equations, we focus on the limit when λ_{hid} and λ_{vis} are very large. In this limit the equations are solved when $\Phi(0) = v_{\text{hid}}$ and $\Phi(1) = v_{\text{vis}}$. Which is a realistic limit recalling that both these constants are of the order of the Planck scale. Additionally, we will assume κy_c to be relatively large, such that using Eq. 3.52 the coefficients are given by

$$\begin{aligned} A =& v_{\text{vis}}e^{-(2+\nu)\kappa y_c} - v_{\text{hid}}e^{-2\nu\kappa y_c}, \\ B =& v_{\text{hid}}\left(1 + e^{-2\nu\kappa y_c}\right) - v_{\text{vis}}e^{-(2+\nu)\kappa y_c}, \end{aligned}$$

where we neglected higher powers of $e^{-\kappa y_c}$. Finally, assuming $m/\kappa \ll 1$ it holds that $\nu \approx 2+\epsilon$, with $\epsilon = m^2/4\kappa^2$. Plugging Eq. 3.52 with these coefficients into the scalar field action and integrating over y yields the effective four-dimensional potential for y_c

$$\begin{aligned} V(y_c) =& \kappa\epsilon v_{\text{hid}}^2 + 4\kappa e^{-4\kappa y_c}\left(v_{\text{vis}} - v_{\text{hid}}e^{-\epsilon\kappa y_c}\right)^2\left(1 + \frac{\epsilon}{4}\right) \\ &- \kappa\epsilon v_{\text{hid}}e^{-(4+\epsilon)\kappa y_c}\left(2v_{\text{vis}} - v_{\text{hid}}e^{-\epsilon\kappa y_c}\right), \end{aligned} \tag{3.53}$$

where terms proportional to ϵ^2 are neglected, but $\epsilon\kappa y_c$ is not treated as small. Ignoring the terms proportional to ϵ the minimum of this potential is at

$$\kappa y_c = 4\frac{\kappa^2}{m^2}\log\left(\frac{v_{\text{hid}}}{v_{\text{vis}}}\right). \tag{3.54}$$

With the requirements that $\log(v_{\text{hid}}/v_{\text{vis}})$ is of order unity and m^2/κ^2 of order $1/10$ we end up with $\kappa y_c \sim 40$. □

Even though this shows that RS is physically possible, there are still quite some assumptions made in the proof. For example, it is assumed that the brane tensions are $\lambda_{\text{vis/hid}}$ are large, which is a fact that followed from the derivation of RS. Something that fails in standard RS is to retrieve a small positive effective cosmological constant on the brane, which is what we observe in our universe [50]. Hawking and Hertog have tried to construct a RS space which better represents our universe [51]. Once we alter some of the assumptions, the above lemma does

not hold anymore, and the scalar field T is generally not stabilized anymore. The excitations of this field then lead to the productions of radions, which serve as dark matter candidate [52].

To conclude, in this subsection we have seen that standard RS realistically offers a solution to the hierarchy problem. In another regime RS spaces could also offer a solution to other big open questions in theoretical physics, such as dark energy and dark matter.

3.3.3 Localizing the graviton

In Section 3.3.1 we showed how RS solves the hierarchy problem. We described the hierarchy problem as the open question why the Planck scale is so much bigger compared to the electroweak scale. For this reason the Randall-Sundrum model is a candidate model to describe our universe. If it is a true candidate, then four-dimensional gravity must be retrieved on the brane. In this section we will derive that due to the warping factor, the graviton is 'bound' to the brane with positive tension. Therefore, the gravitational potential is proportional to r^{-1} even for very large or even infinite extra dimensions.

Recall from Sec. 3.2.4 that in RS1, the hidden brane has positive tension and the visible brane has negative tension. Therefore, the absence of the graviton at the visible brane will be explanation for the fact that gravity seems so weak. On the other hand, in RS2 the visible brane has positive tension and the extra dimension is infinite. Therefore, from Lem. 3.1.3 we might expect that the gravitational potential is proportional to r^{-2}. However, The fact that the graviton is bound to the visible brane will ensure that four-dimensional gravity is recovered even though there is a infinite extra dimension in the model.

We make use of Kaluza-Klein theory to describe the graviton. Before defining the concepts of Kaluza-Klein theory, it is important to note that even though it looks similar to perturbation theory and we use some of the same techniques as we use later on in proving stability of spacetimes, it is not related to the stability proofs that will be done in the next chapter. Kaluza-Klein theory is a method to describe the dynamics of particles such as the graviton, photon and radion in five-dimensional spacetimes. It also works by perturbing a background metric $\hat{g}$ by a 2-tensor h,

$$g = g^0 + h. \tag{3.55}$$

However, now this perturbation h describes several fields. Namely the four-dimensional restriction h_{ab} where $a, b = 0, 1, 2, 3$ represents the gravitational field of the spin-2 graviton. Similarly, the h_{a5} component represents the electromagnetic field and the h_{55} component, as we saw in the previous subsection, a scalar field related to the radion. The equations of motion of these fields are obtained by the linearized Einstein equations. It is then possible to separate the fields into modes of different masses. The zero-modes or massless modes of the gravitation, electromagnetic and scalar field correspond with the graviton, photon and radion, respectively. We apply Kaluza-Klein theory to the RS1 and RS2 model, to find the wavefunction of the graviton.

Theorem 3.3.4. *In standard RS the wavefunction of the graviton peaks at the negative tension brane.*

Let g be the metric of standard RS with curvature scale κ and distance between the branes y_c. To obtain the linearized Einstein equations we first make use of a coordinate transformation to express our metric in a useful way. We introduce a coordinate z such that

$$e^{\kappa y_c|y|} y_c dy = dz,$$
$$e^{-2\kappa|y|} = \frac{1}{(1+\kappa|z|)^2}.$$

For this new coordinate it holds that $0 \leq z \leq \frac{1}{\kappa}(e^{\kappa y_c} - 1) = z_c$. Then the metric in standard coordinates from Eq. 3.38 transforms to

$$ds^2 = \frac{1}{(1+\kappa|z|)^2}\eta_{MN}dx^M dx^N = e^{-2A(z)}\eta_{MN}dx^M dx^N, \tag{3.56}$$

where we defined

$$A(z) = \log(1+\kappa|z|). \tag{3.57}$$

For later purposes we note that

$$A'(z) = \frac{\mathrm{sgn}(z)\kappa}{1+\kappa|z|}, \tag{3.58}$$

$$A''(z) = \frac{2\kappa}{1+\kappa|z|}\left(\delta(z) - \delta(z-z_c)\right) - \frac{\kappa^2}{(1+\kappa|z|)^2}. \tag{3.59}$$

Using this new coordinate we can rescale h such that the perturbed metric takes the form

$$g = e^{-2A(z)}(\eta + h). \tag{3.60}$$

To obtain the linearized Einstein equations we can apply the following result form [53].

Lemma 3.3.5. *Let g and $\tilde{g}$ be two conformally equivalent metric tensors on a n-dimensional manifold such that $g = e^{-2A}\tilde{g}$. Then the Einstein tensors of g and $\tilde{g}$ are related by*

$$G_{MN}(g) = \tilde{G}(\tilde{g}) + (n-2)\left[\tilde{\nabla}_M A\tilde{\nabla}_N A + \tilde{\nabla}_M\tilde{\nabla}_N A - \tilde{g}_{MN}\left(\tilde{\nabla}_R\tilde{\nabla}^R A - \tilde{\nabla}_R A\tilde{\nabla}^R A\right)\right], \tag{3.61}$$

where $\tilde{\nabla}$ denotes the covariant derivative with respect to $\tilde{g}$.

Furthermore, we simplify the problem by a convenient choice of gauge

Definition 3.3.6. *Let $(M, g+h)$ be a RS space with an effective four-dimensional background metric $\hat{g}$. The **RS gauge** is given by*

$$\begin{aligned} h_{5M} &= 0, \\ \nabla^a h_{ab} &= 0, \\ \hat{g}^{ab}h_{ab} &= 0, \end{aligned}$$

where $M = 0,1,2,3,5$ and $a,b = 0,1,2,3$.

Since h is a symmetric metric tensor, it originally had 15 degrees of freedom. In this gauge we reduce it to 5 degrees of freedom. This also corresponds to what we would expect from a five-dimensional spin-2 particle such as the graviton [54]. Furthermore, note that this gauge corresponds to setting the photon and scalar field to zero such that we are only left with the tensor component associated to the graviton.

If we apply Lem. 3.3.5 to the metric in Eq. 3.60, we find that the Einstein tensor associated to g is given by

$$\begin{aligned} G_{MN}(g) = \tilde{G}_{MN} + 3\big[&\partial_M A\partial_N A + \partial_M\partial_N A - \tilde{\Gamma}^R_{MN}\partial_R A \\ &- \tilde{g}_{MN}\left(\partial_R\partial^R A + \tilde{\Gamma}^R_{RS}\partial^S A - \partial_R A\partial^R A\right)\big], \end{aligned} \tag{3.62}$$

where $\tilde{\Gamma}$ are the Christoffel symbols associated to $\tilde{g} = \eta + h$. For now we focus on the G_{ab} components of the Einstein equation, where $a,b = 0,1,2,3$. Since A only depends on the z-coordinate the relevant Christoffel symbols are $\tilde{\Gamma}^5_{ab}$ and $\tilde{\Gamma}^R_{R5}$. In the RS gauge and using Lem. 2.2.6, the linearized form of these Christoffel symbols are given by

$$\tilde{\Gamma}^5_{ab} = -\frac{1}{2}\partial_z h_{ab}, \quad \tilde{\Gamma}^R_{R5} = 0. \tag{3.63}$$

Furthermore, in this gauge the Einstein tensor associated to $\tilde{g}$ becomes

$$\tilde{G}_{ab} = -\frac{1}{2}\partial_R \partial^R h_{ab}. \tag{3.64}$$

Combining Eq. 3.63 and 3.64 with the expression for the Einstein tensor in Eq. 3.62 we get that the Einstein tensor equals

$$G_{ab}(g) = -\frac{1}{2}\partial_R \partial^R h_{ab} + \frac{3}{2}\partial_z h_{ab} A' - 3(\eta_{ab} + h_{ab})\left(A'' - A'^2\right). \tag{3.65}$$

Recall the RS energy-momentum tensor in Eq. 3.23. We want to express this tensor in terms of the function $A(z)$. Using Eq. 3.35 the energy-momentum tensor can be written as

$$T_{ab} = -12M^3\left(A'' + A'^2\right)(\eta_{ab} + h_{ab}). \tag{3.66}$$

Finally, using Eq. 3.35 again, the cosmological constant term can be written as

$$\Lambda g_{ab} = -6A'^2(\eta_{ab} + h_{ab}). \tag{3.67}$$

Now we can plug Eq. 3.65, 3.66 and 3.67 into the Einstein equation 2.25 to find the equation of motion

$$\partial_R \partial^R h_{ab} - 3\partial_z h_{ab} A' = 0. \tag{3.68}$$

We would like to get rid of the term with a single derivative. For this we use the following lemma from [55, Lemma 6.4].

Lemma 3.3.7. *The substitution*

$$u = v\,\exp\left(-1/2\int_0^x p dx\right) \tag{3.69}$$

transforms

$$u'' + p(x)u' + q(x)u = 0 \tag{3.70}$$

into

$$v'' + \left(q - \frac{1}{2}p' - \frac{p^2}{4}\right)v = 0. \tag{3.71}$$

According to Lem. 3.3.7 this can be achieved by the rescaling

$$h \to e^{\frac{3}{2}A}h. \tag{3.72}$$

This transforms Eq. 3.68 to

$$\partial_R \partial^R h_{ab} + \left(\frac{3}{2}A'' - \frac{9}{4}A'^2\right)h_{ab} = 0. \tag{3.73}$$

In flat five-dimensional space with compact extra dimension of length L, the linearized Einstein equations would reduce to

$$\partial_R \partial^R \hat{h}_{ab} = 0. \tag{3.74}$$

Due to the translational symmetry in the flat case, it is possible to decompose h into a Fourier series

$$\hat{h}_{ab}(x,z) = \sum_{n\in\mathbb{Z}} \hat{h}^n_{ab}(x) e^{i\frac{n}{L}z}. \tag{3.75}$$

Plugging Eq. 3.75 into Eq. 3.74, we get a Klein-Gordon equation for the modes

$$\left(\partial_c \partial^c - m_n^2\right)\hat{h}^n_{ab}(x) = 0, \tag{3.76}$$

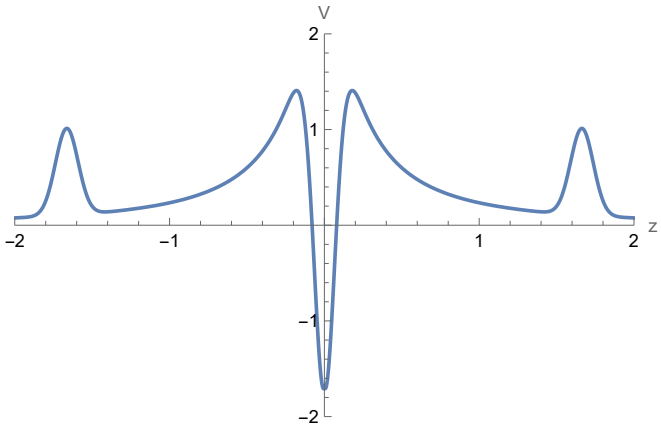

Figure 3.7: The potential in Eq. 3.79 plotted for the values $y_c = 1$, $\kappa = 1$. The low energy modes will be trapped inside the steep well at $z = 0$.

where $m_n = \frac{n}{L}$ are the masses. This is a decomposition in **Kaluza-Klein modes**. In the RS case we want to do something similar. However, now there is no translational symmetry in the z direction. Instead, we decompose the tensor h into Kaluza-Klein modes

$$h_{ab}(x,z) = \sum_{n=0}^{\infty} h^n_{ab}(x)\psi_n(z), \tag{3.77}$$

where the h^n_{ab} still solve the Klein-Gordon equation: $\partial_c\partial^c h^n_{ab} = m_n^2 h^n_{ab}$, for some mass spectrum $\{m_n\}$. However, now $\psi_n(z)$ represent wavefunctions of the graviton modes with mass m_n that solve the equation

$$\psi_n'' + \left(m_n^2 + \frac{3}{2}A'' - \frac{9}{4}A'^2\right)\psi_n = 0. \tag{3.78}$$

The zero-mode, corresponding to the graviton, is the $n = 0$ mode for which $m_0 = 0$. Therefore, we want to solve Eq. 3.78 for $n = 0$.

Note that Eq. 3.78 is a Schrödinger type equation with energy levels given by m_n^2 and a potential

$$\begin{aligned} V(z) =& \frac{9}{4}A'^2 - \frac{3}{2}A'' \\ =& \frac{15}{4}\frac{\kappa^2}{(1+\kappa|z|)^2} + \frac{3\kappa}{1+\kappa|z|}\left(\delta(z-z_c) - \delta(z)\right). \end{aligned} \tag{3.79}$$

This potential has the shape of a volcano as can be seen in Fig. 3.7. The mode functions ψ_n represent wavefunctions of the graviton and describes the probability distribution of its location for different energy levels or masses. Due to the deep well at $z = 0$ we expect the low mass modes to be trapped inside this well. Recall that we expect that the graviton is massless. Therefore, the zero-mode will be the most interesting for us.

Lemma 3.3.8. *The zero-mode graviton wavefunction is given by*

$$\psi_0(z) = \frac{1}{(1+\kappa|z|)^{\frac{3}{2}}}. \tag{3.80}$$

Proof. Before we solve Eq. 3.78, we have to determine the boundary conditions at the branes. This can be determined by integrating Eq. 3.78 in a small region around the visible and hidden

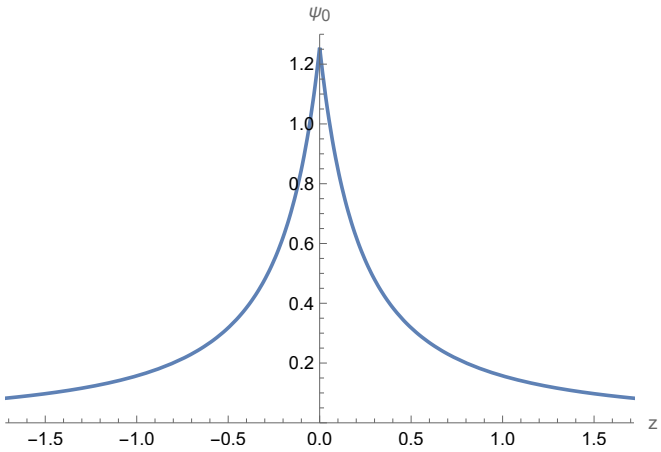

Figure 3.8: The wavefunction for the massless graviton mode in Eq. 3.80 for $y_c = 1$ and $\kappa = 1$.

brane. For the brane located at $z = 0$ we find

$$\begin{aligned} 0 =& \int_{0^-}^{0^+} \psi_n'' + \left(m_n^2 + \frac{3}{2}A'' - \frac{9}{4}A'^2 \right) \psi_n \\ =& \psi_n'(0^+) - \psi_n'(0^-) + 3\kappa\psi_n(0). \end{aligned} \tag{3.81}$$

According to the orbifold symmetry ψ is an even function. Therefore, $\psi'(z) = -\psi'(-z)$. Consequently, the boundary condition becomes

$$\psi_n'(0) = -\frac{3}{2}\kappa\psi_n(0). \tag{3.82}$$

Similarly, we can derive the boundary condition for the brane at $z = z_c$

$$\psi'(z_c) = -\frac{3\kappa}{2(1+\kappa z_c)}\psi_n(z_c). \tag{3.83}$$

Now we can check whether Eq. 3.80 solves Eq. 3.78 and adheres to the boundary conditions in Eq. 3.82 and 3.83. □

As can be seen in Fig. 3.8 the wavefunction of the zero-mode graviton peaks at the hidden brane located at $z = 0$. Therefore, matter at the visible brane only experiences the tail of the graviton wavefunction. This explains the weakness of gravity on the visible brane.

It is shown in [53, P. 20], the gravitational potential can be computed from the graviton modes. We can analyse this potential to see if RS gravity agrees with our observations.

Lemma 3.3.9. *The gravitational potential $V(r)$ in terms of graviton modes is given by*

$$V(r) = -\sum_{n=0}^{\infty} \frac{a_n^2}{4\pi} \frac{e^{-m_n r}}{r}, \tag{3.84}$$

where

$$a_n = \frac{e^{\frac{3}{2}A}\psi_n(z)}{2\sqrt{M^3}}. \tag{3.85}$$

Note that the zero-mode term dominates the potential in Eq. 3.84. If we plug in Eq. 3.80 the leading term of the potential is given by

$$\begin{aligned} V_0(r) &= -\frac{1}{16\pi M^3}\frac{1}{r} \\ &= -\frac{G_N}{r}. \end{aligned}$$

We conclude that this reproduces four-dimensional gravity. Note that this applies to both RS1 and RS2. Therefore, even though RS2 has infinite fifth dimension, as a consequence of the fact that the graviton is located close to the brane at $z = 0$, we still experience four-dimensional gravity on the brane.

3.3.4 Singularity of the black string

In the previous sections we have shown that the Randall-Sundrum model solves the Hierarchy problem with minimal fine-tuning and that four-dimensional gravity is retrieved on the brane. The final thing we require for RS to be a good model for our universe is the existence of solar mass black holes. In Section 3.2.6 we already constructed black hole solutions in the form of RS black strings. We noted that in RS2 the black string seems to become massless at $z = \infty$. In this section we derive that there is a singularity at $z = \infty$.

In 1999, another undesirable property was discovered by Chamblin, Hawking and Reall. They discovered that the black string is singular at the horizon [17, P. 4].

Lemma 3.3.10. *The square of the Riemann tensor of the black string is*

$$R_{MNKL}R^{MNKL} = 40\kappa^4 + \frac{48M^2e^{4\kappa y_c y}}{r^6} \tag{3.86}$$

The square of the Riemann tensor is singular both at the centre of the black string $r = 0$, and in RS2 at the AdS horizon $z = y_c y \to \infty$. A **singularity** is a point of infinite curvature. Any geodesic that reaches a singularity, stops at the singularity and can never leave it. The theory breaks down at a singularity. Note that the square of the Riemann tensor becomes infinite both at $r = 0$ and $z = \infty$, therefore there are singularities at these points.

The singularity of Eq. 3.86 at $r = 0$ is hidden behind the horizon of the black string. This type of singularity also occurs at regular black holes. Since it is unclear whether black hole solutions give a valid description of the interior of black holes, we do not worry about such a singularity too much. The singularity at $z = \infty$ is a so called **naked singularity**, not hidden behind any horizon and can be reached by anything. Since our theory breaks down at such a singularity, we want to avoid them in our theories. Therefore, this observation hints to an instability of the black string. This instability was first postulated by Chamblin, Hawking and Reall. To avoid the formation of the singularity they proposed that the black string would pinch off near the AdS horizon, forming a **black cigar**. A sketch of the black cigar can be seen in Fig. 3.9.

So far there is no exact solution for the black cigar, let alone for the transition from a black string to a black cigar. At first, there was even some debate about whether static solutions for black holes could exist. Due to effects of the AdS/CFT correspondence, it was argued that black holes would quickly evaporate [56]. Therefore, time-independent solutions could not exist. In 2011 however, the first numerical solutions were constructed for black holes in RS2 with a wide range of masses [57]. It turns out that large black holes behave as $\mathrm{AdS}_5/\mathrm{CFT}_4$

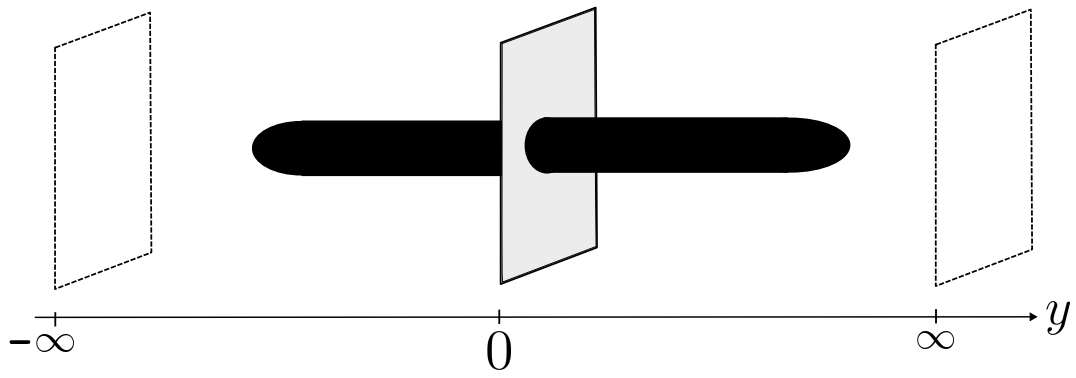

Figure 3.9: A schematic picture of the black cigar solution in the RS2 model.

solutions, whereas small black holes behave as if they are in flat extra dimensional space. Later in 2021, even numerical solutions for rotating black holes in RS2 were constructed [58].

We conclude that the RS2 black string seems unstable. In the state of the RS2 black string the forming of the singularity needs to be avoided. Therefore, when reaching this state it quickly pinches off close to the AdS horizon. In this process it transforms to a different state. Using the definition of stability in Def. 2.2.5, this describes an instability. If the RS2 black string is unstable, it would make sense if there are cases where the RS1 black string is unstable as well. We want solar mass black holes to exist in RS1, but they cannot exist for long periods of time if they turn out to be unstable. In the next chapter we therefore analyse the mode stability of the RS black string. Furthermore, we derive the masses for which black strings are stable in RS.

Chapter 4

Mode stability of black strings

In the previous chapter we defined the Randall-Sundrum model. This model offers a solution to the hierarchy problem. However, black holes seem to be unstable in this model. This chapter aims to analyse the mode stability of the RS black string. In this chapter, we apply results and techniques that were derived and explained in Chapter 2.

First of all, the mode stability of the Schwarzschild metric is analysed in Section 4.1. Due to the spherical symmetry of the Schwarzschild metric, the metric perturbations can be decomposed into modes of different angular momentum and parity. These different components are expressed in terms of Regge-Wheeler harmonics. These harmonics are also useful for decomposing the black string perturbations. We derive that the Schwarzschild metric has mode stability by using Theorem 2.3.1.

In five-dimensional flat space, there are two types of black holes: hyperspherical black holes and black strings. If the extra dimension is compact and the size L is large, then the hyperspherical black hole is entropically favourable over the black string. Therefore, we expect the black string to be unstable. In Section 4.2, we analytically prove the mode instability of the black string in five-dimensional flat space. After the deriving the master equation of Schrödinger form, we approximate the potential by an asymmetric finite well potential. This potential defines the asymmetric finite well operator. By computing the eigenfunctions with negative eigenvalues of this operator we obtain a set of test functions. We apply Theorem 2.3.16 and use this set of test functions to estimate the lowest eigenvalue of the master equation. In this way, we prove that the black string of mass M is unstable in the range $M \in \left[\frac{0.1L}{4\pi}, \frac{0.85L}{4\pi}\right]$.

In Section 4.3, we generalize the flat black string instability to warped spaces. First, we derive the master equation for the RS black string. Then we construct perturbations such that this master equation reduces to the same master equation as for the flat black string. Consequently, the results from Section 4.2 apply to these perturbations as well. We derive that there exists an upper bound M_0, such that RS1 black strings of mass M are modally unstable if $M < M_0$.

4.1 Mode stability of the Schwarzschild metric

In this section we prove the mode stability of the 4-dimensional Schwarzschild metric. We primarily follow the paper by Regge & Wheeler [20] where this has first been claimed. However, to finalize the proof we will also use a papers by Vishveshwara [21] and Zerilli [22], who proved

the mode stability more rigorously.

Recall the Schwarzschild metric from Eq. 2.28. Let us consider a perturbation of the Schwarzschild metric $g = g_s + h$. The spherical symmetry of the Schwarzschild metric allows us to decompose the perturbation tensor h into components of different angular momentum and parity. This decomposition will allow us to analyse the stability of each component separately instead of having to analyse the stability for general h. In Section 4.1.1 we derive this decomposition into so called Regge-Wheeler harmonics. In Section 4.1.2 we apply this decomposition to the perturbations of the Schwarzschild metric and simplify the problem using gauge transformations. Then we analyse the odd and even parity modes in Section 4.1.3.

4.1.1 Scalar, vector and tensor spherical harmonics

The Schwarzschild metric is spherically symmetric. For such spaces we want to use the symmetry to decompose scalars, vectors and tensors in to components of different angular dependence. In this section we derive a useful complete set of functions that does this.

Definition 4.1.1. *The **spherical harmonics** are scalar functions $Y : S^2 \to \mathbb{R}$, which are eigenfunctions of the Laplacian*

$$\Delta_{S^2} Y = \lambda Y. \tag{4.1}$$

We derive the scalar spherical harmonics, and we shall see that they have useful properties.

Let us start with the Laplace equation in spherical coordinates

$$\triangle f = \frac{1}{r^2}\frac{\partial}{\partial r}(r^2\frac{\partial f}{\partial r}) + \frac{1}{r^2\sin\theta}\frac{\partial}{\partial\theta}(\sin\theta\frac{\partial f}{\partial\theta}) + \frac{1}{r^2\sin^2\theta}\frac{\partial^2 f}{\partial\varphi^2} = 0, \tag{4.2}$$

For $f \in C^\infty(\mathbb{R}^3)$. Now we make the ansatz that we can split variables, so $f(r,\theta,\varphi) = R(r)Y(\theta,\varphi)$. Then we can rewrite Eq. 4.2 to

$$\frac{1}{R}\frac{\partial}{\partial r}(r^2\frac{\partial R}{\partial r}) = -\frac{1}{Y\sin\theta}\frac{\partial}{\partial\theta}(\sin\theta\frac{\partial Y}{\partial\theta}) - \frac{1}{Y\sin^2\theta}\frac{\partial^2 Y}{\partial\varphi^2}.$$

Note that the differential operator on the right hand side is the S^2 Laplacian. The left hand side is completely independent of θ and φ, and the right hand side is independent of r. So we must have that both sides are equal to some constant $\lambda \in \mathbb{R}$. Now we can again make a separation of variables by making the ansatz $Y = \Theta(\theta)\Phi(\varphi)$. Then we can rewrite the equation to

$$\lambda\sin^2\theta + \frac{\sin\theta}{\Theta}\frac{\partial}{\partial\theta}(\sin\theta\frac{\partial\Theta}{\partial\theta}) = -\frac{1}{\Phi}\frac{\partial^2\Phi}{\partial\varphi^2}. \tag{4.3}$$

Note that again the left hand side only depends on θ, whereas the right hand side only depends on φ. Therefore, both sides must be equal to some constant m^2. On first sight, m could be imaginary. However, consider the resulting differential equation

$$\frac{\partial^2\Phi}{\partial\varphi^2} = -m^2\Phi.$$

Then it follows that Φ is a linear combination of $e^{\pm im\varphi}$. If we demand that Φ is periodic and its period can be evenly divided by 2π, then m must be an integer.

Now going back to Eq. 4.3 we can rewrite it to the form

$$\frac{d}{d\theta}(\sin\theta\frac{d\Theta}{d\theta}) + \lambda\sin\theta\Theta = \frac{m^2}{\sin\theta}\Theta$$

Next, we define $P(\cos\theta) = \Theta(\theta)$ and $x = \cos\theta$. By this change of variables the above equation is equivalent to

$$\frac{d}{dx}\left((1-x^2)\frac{dP}{dx}\right) + \left(\lambda - \frac{m^2}{1-x^2}\right)P(x) = 0. \tag{4.4}$$

With complicated analysis [59], of which we will not go into detail here, one can show that solutions of this equation are regular on the sphere if and only if

$$\lambda = l(l+1), \quad \text{with } l = |m|, |m|+1, |m|+2, \ldots.$$

In that case Eq. 4.4 is solved by the associated Legendre Polynomials $P_{lm}(x)$.

Definition 4.1.2 (Legendre Polynomials)**.** *The associated Legendre polynomials $P^{lm}(x)$ are solutions to the differential equation*

$$\frac{d}{dx}\left((1-x^2)\frac{dP_{lm}}{dx}\right) + \left(l(l+1) - \frac{m^2}{1-x^2}\right)P_{lm}(x) = 0.$$

They can be expressed in the form

$$P^{lm}(x) = \frac{(-1)^m}{2^l l!}(1-x^2)^{m/2}\frac{d^{l+m}}{dx^{l+m}}(x^2-1)^l.$$

We can now define the spherical harmonics.

Lemma 4.1.3. *The spherical harmonics $Y_{lm} : S^2 \to \mathbb{R}$ are defined for every non-negative integer l and integer $m = -l, -l+1, \ldots, l$. They are given by*

$$Y_{lm}(\theta,\varphi) = N_{lm}P_{lm}(\cos\theta)e^{im\varphi},$$

with N_{lm} a normalization constant

$$N_{lm} = \sqrt{\frac{2l+1}{4\pi}\frac{(l-|m|)!}{(l+|m|)!}}.$$

The spherical harmonics have the following properties

1. *The spherical harmonics are eigenfunctions of the angular momentum operator*

$$r^2\triangle Y_{lm}(\theta,\varphi) = -l(l+1)Y_{lm}(\theta,\varphi), \quad r > 0.$$

2. *The spherical harmonics are orthonormal on the sphere*

$$\int Y_{lm}Y_{l'}^{m'*}d\Omega = \delta_{l,l'}\delta_{m,m'}$$

3. *The spherical harmonics form a complete set in $L^2(S^2)$*

$$\sum_{l=0}^{\infty}\sum_{m=-l}^{l} Y_{lm}(\theta,\varphi)Y_l^{m*}(\theta',\varphi') = \frac{1}{\sin\theta}\delta(\theta-\theta')\delta(\varphi-\varphi').$$

We say that Y^{lm} has an angular momentum l, with projection on the z-axis m. This has to do with the eigenvalues of the spherical harmonics when acted on by the corresponding operator. Using the completeness property of the spherical harmonics, any well-behaved function $f(r,\theta,\varphi)$ can be decomposed into spherical harmonics.

Lemma 4.1.4. *Let $f \in C^k(\mathbb{R}^3)$ for $k \geq 0$. Then we can decompose f into spherical harmonics*

$$f(r,\theta,\varphi) = \sum_{l=0}^{\infty} \sum_{m=-l}^{l} f_{lm}(r) Y_{lm}(\theta,\varphi), \quad \textit{with}$$
$$f_{lm}(r) = \int f(r,\theta,\varphi) Y^*_{lm}(\theta,\varphi) d\Omega.$$

Furthermore, for the coefficients it holds that $f_{lm} \in C^k(\mathbb{R})$.

Proof. For $f \in C^k(\mathbb{R}^3)$, in spherical coordinates we have that for constant radius $r_0 \geq 0$ the function $f(r_0,\theta,\varphi)$ is square integrable on S^2. Therefore, the f_{lm} are well defined. Furthermore, note that indeed

$$\begin{aligned} f(r,\theta,\varphi) &= \sum_{l=0}^{\infty} \sum_{m=-l}^{l} \int f(r,\theta',\varphi') Y_l^{m*}(\theta',\varphi') Y_{lm}(\theta,\varphi) d\Omega' \\ &= \int f(r,\theta',\varphi') \sum_{l=0}^{\infty} \sum_{m=-l}^{l} Y_{lm}(\theta,\varphi) Y_l^{m*}(\theta',\varphi') d\Omega' \\ &= \int \frac{f(r,\theta',\varphi')}{\sin\theta} \delta(\theta-\theta')\delta(\varphi-\varphi') d\Omega' = f(r,\theta,\varphi). \end{aligned}$$

We prove the regularity of f_{lm} by induction. First, we prove that f_{lm} is continuous if f is continuous. Let $r \geq 0$ and $\epsilon > 0$. Since f is continuous at r and S^2 is compact, there exists a $\delta > 0$ such that for any $|r' - r| < \delta$ it holds that

$$|f(r',\theta,\varphi) - f(r,\theta,\varphi)| < \frac{\epsilon}{\int |Y_{lm}| d\Omega} \tag{4.5}$$

Consequently, it also holds that

$$\begin{aligned} |f_{lm}(r') - f_{lm}(r)| &= \left| \int (f(r',\theta,\varphi) - f(r,\theta,\varphi)) Y_{lm}(\theta,\varphi) d\Omega \right| \\ &\leq \int |f(r;,\theta,\varphi) - f(r,\theta,\varphi)| |Y_{lm}(\theta,\varphi)| d\Omega < \epsilon. \end{aligned}$$

By induction it follows that if f is k-times differentiable, then so is f_{lm}. Since a derivative of f_{lm} can be moved inside of the integral and only effects f, then using the fact that $\frac{\partial^k f}{\partial r^k}$ is continuous it follows that $\frac{\partial^k f_{lm}}{\partial r^k}$ is continuous using the same procedure as above. □

We conclude that any scalar function can be written as a sum of spherical harmonics. A natural next step would be to try to express all vector and even tensor functions in terms of spherical harmonics. For this we will need to define vector and tensor spherical harmonics. These were first introduced by Regge and Wheeler in 1957 [20]. Later others, including Zerilli in 1970 [22], developed different definitions of vector and tensor spherical harmonics, each useful for a different application. Finally, in 1980 Kip Thorne [60] wrote a paper comparing all different definitions and showing how they relate to each other. In this section we focus on the definitions by Regge & Wheeler. Even though, these definitions might seem a bit out of the blue they are most useful to us in proving the stability of the Schwarzschild metric.

Regge & Wheeler structure the vector and tensor spherical harmonics in terms of parity. A parity transformation is a transformation where the coordinates are reflected in the origin, $(x,y,z) \mapsto (-x,-y,-z)$. On the 2-sphere we define the **parity map** $p : S^2 \to S^2$ that maps a point on the two sphere to the point on the opposite side

$$(\theta,\varphi) \mapsto p(\theta,\varphi) = (\pi - \theta, \varphi + \pi).$$

Note that under this parity transformation, the spherical harmonics transform as

$$\begin{aligned} p^* Y_{lm}(\theta,\varphi) &= Y_{lm}(\pi-\theta,\varphi+\pi) \\ &= N_{lm}\, P_{lm}(\cos(\pi-\theta))\, e^{im(\varphi+\pi)} \\ &= (-1)^m N_{lm}\, P_{lm}(-\cos\theta)\, e^{im\varphi}. \end{aligned}$$

Now looking at the expression from definition 4.1.2, we see that $P_{lm}(-x) = (-1)^{l+m} P_{lm}(x)$, so the spherical harmonics transform under the parity transformation as

$$p^* Y_{lm}(\theta,\varphi) = (-1)^{l+2m} N_{lm} P_{lm}(\cos\theta) e^{im\varphi} = (-1)^l Y_{lm}(\theta,\varphi).$$

It turns out that we can distinguish different vector and tensor spherical harmonics based on how they transform under the parity transformation.

Definition 4.1.5. *Let $A_{lm}(\theta,\varphi)$ be a scalar, vector, or tensor defined on the 2-sphere which is an eigenfunction of the S^2 Laplacian with eigenvalue $-l(l+1)$. We say A_{lm} has **even parity** if A_{lm} transforms under the parity transformation as*

$$p^* A_{lm}(\theta,\varphi) = (-1)^l A^{lm}(\theta,\varphi).$$

*A_{lm} has **odd parity** if it transforms under the parity transformation as*

$$p^* A^{lm}(\theta,\varphi) = (-1)^{l+1} A^{lm}(\theta,\varphi).$$

Now we can define the **Regge-Wheeler harmonics**, which is a set of scalar, vector and tensor spherical harmonics. From Lem. 4.1.3 it follows that the scalar spherical harmonics are just given by the regular spherical harmonics. Furthermore, we just derived that these have even parity. The **vector spherical harmonics** are sections on T^*S^2. For each non-negative integer l and $m = -l, -l+1, \dots, l$ there exist two types of opposite parity which in spherical coordinates are given by:

$$(\Psi_{lm})_a = \frac{\partial}{\partial x^a} Y_{lm}(\theta,\varphi), \qquad \text{even parity,} \tag{4.6}$$

$$(\phi_{lm})_a = \epsilon_a^{\ b} \frac{\partial}{\partial x^b} Y_{lm}(\theta,\varphi), \qquad \text{odd parity.} \tag{4.7}$$

Here $a, b = 2, 3$, where $x^2 = \theta$ and $x^3 = \varphi$. The tensor $\epsilon_\mu^{\ \nu}$ is defined by $\epsilon_2^{\ 2} = \epsilon_3^{\ 3} = 0$, $\epsilon_2^{\ 3} = -\frac{1}{\sin\theta}$ and $\epsilon_3^{\ 2} = \sin\theta$. For the tensor spherical harmonics we also need to introduce the 2-tensor γ_{ab} on the sphere, where in spherical coordinates $\gamma_{22} = 1$, $\gamma_{23} = \gamma_{32} = 0$ and $\gamma_{33} = \sin^2\theta$. The **tensor spherical harmonics** are sections of $Sym^2(T^*S^2)$, for non-negative integers l and $m = -l, -l+1, \dots, l$ they are given by

$$(\alpha_{lm})_{ab} = \nabla_a \nabla_b Y_{lm}(\theta,\varphi), \qquad \text{even parity,} \tag{4.8}$$

$$(\beta_{lm})_{ab} = \gamma_{ab} Y_{lm}(\theta,\varphi), \qquad \text{even parity,} \tag{4.9}$$

$$(\xi_{lm})_{ab} = \frac{1}{2}\left[\epsilon_a^{\ c}(\Psi_{lm})_{cb} + \epsilon_b^{\ c}(\Psi_{lm})_{ca}\right], \qquad \text{odd parity.} \tag{4.10}$$

Here again $a, b = 2, 3$. Thorne proved that any scalar, vector or tensor can be expressed in terms of Regge-Wheeler harmonics [60, P. 12].

Theorem 4.1.6. *Any scalar, vector, or symmetric 2-tensor on S^2 can be decomposed in terms of Regge-Wheeler harmonics. In particular, let $X \in \Gamma(TS^2)$, then there exist $u_{lm}, v_{lm} \in \mathbb{R}$ such that*

$$X = \sum_{l=0}^{\infty} \sum_{m=-l}^{l} u_{lm}\Psi_{lm} + v_{lm}\phi_{lm}. \tag{4.11}$$

Similarly, for any $T \in \Gamma(Sym^2(TS^2))$ there exist $U_{lm}, V_{lm}, W_{lm} \in \mathbb{R}$ such that

$$T = \sum_{l=0}^{\infty} \sum_{m=-l}^{l} U_{lm}\alpha_{lm} + V_{lm}\beta_{lm} + W_{lm}\xi_{lm}. \tag{4.12}$$

In the next sections we use these harmonics to decompose the perturbations.

4.1.2 Mode decomposition of perturbations to the Schwarzschild metric

With the Regge-Wheeler harmonics, we can decompose perturbations of the Schwarzschild metric and analyse the mode stability. The Schwarzschild metric describes the spacetime around black holes. We want to derive whether this metric is a stable spacetime configuration. We are quite sure that black holes exist and that they are stable. Therefore, if we believe the Schwarzschild metric is a good description, small perturbations of the metric should not have big consequences. Therefore, there should not be any exponentially growing modes.

Let $g = g^s + h$ be a perturbation of the Schwarzschild metric g^s, where $h \in \Gamma(\mathrm{Sym}^2(T\mathbb{R}^4))$. Due to the spherically symmetric background, the components of h of different angular momentum split in the linearized Einstein equations. It turns out that in order to prove stability, it is enough to separately prove stability for perturbations with different angular momentum l, projection to the z-axis m, and parity, with $l = 0, 1, 2, \dots$ and $m = -l, -l+1, \dots, l$.

Proposition 4.1.7. *A general perturbation $h \in \Gamma(Sym^2(T\mathbb{R}^4))$ which has angular momentum l, whose projection on the z-axis is m, and with odd parity is given by*

$$h_{ab} = \begin{pmatrix} 0 & 0 & -h_0(t,r)\frac{1}{\sin\theta}\frac{\partial}{\partial\varphi} & h_0(t,r)\sin\theta\frac{\partial}{\partial\theta} \\ 0 & 0 & -h_1(t,r)\frac{1}{\sin\theta}\frac{\partial}{\partial\varphi} & h_1(t,r)\sin\theta\frac{\partial}{\partial\theta} \\ * & * & h_2(t,r)\left(\frac{1}{\sin\theta}\frac{\partial^2}{\partial\theta\partial\varphi} - \frac{\cos\theta}{\sin^2\theta}\frac{\partial}{\partial\varphi}\right) & \frac{1}{2}h_2(t,r)\big(\frac{1}{\sin\theta}\frac{\partial^2}{\partial\varphi^2} + \cos\theta\frac{\partial}{\partial\theta} \\ & & & -\sin\theta\frac{\partial^2}{\partial\theta^2}\big) \\ * & * & * & -h_2(t,r)\left(\sin\theta\frac{\partial^2}{\partial\theta\partial\varphi} - \cos\theta\frac{\partial}{\partial\varphi}\right) \end{pmatrix} Y_{lm}. \quad (4.13)$$

Here the $*$ indicates components that are determined by the symmetry of the tensor. The perturbations of even parity will take the following form

$$h_{ab} = \begin{pmatrix} H_0(t,r) & H_1(t,r) & f_0(t,r)\frac{\partial}{\partial\theta} & f_0(t,r)\frac{\partial}{\partial\varphi} \\ H_1(t,r) & H_2(t,r) & f_1(t,r)\frac{\partial}{\partial\theta} & f_1(t,r)\frac{\partial}{\partial\varphi} \\ * & * & \left(K(t,r) + G(t,r)\frac{\partial^2}{\partial\theta^2}\right) & G(t,r)\left(\frac{\partial^2}{\partial\theta\partial\varphi} - \frac{\cos\theta}{\sin\theta}\frac{\partial}{\partial\varphi}\right) \\ * & * & * & G(t,r)\big(\frac{\partial^2}{\partial\varphi^2} + \sin\theta \\ & & & \cos\theta\frac{\partial}{\partial\theta}\big) + K(t,r)\sin^2\theta \end{pmatrix} Y_{lm}. \quad (4.14)$$

We refer to Eq. 4.13 as the odd type of perturbation and to Eq. 4.14 as the even type of perturbations.

Proof. In spherical coordinates we can decompose the tangent space as follows

$$T\mathbb{R}^4 = T\mathbb{R} \oplus T\mathbb{R}_{\geq 0} \oplus TS^2. \quad (4.15)$$

Therefore, the vector bundle $\mathrm{Sym}^2(T\mathbb{R}^4)$ will consist of blocks of the following form

$$\mathrm{Sym}^2(T\mathbb{R}^4) = \mathrm{Sym}^2(T\mathbb{R}) \oplus (T\mathbb{R} \otimes T\mathbb{R}_{\geq 0}) \oplus \left(T\mathbb{R} \otimes TS^2\right) \quad (4.16)$$

$$\oplus\, \mathrm{Sym}^2(T\mathbb{R}_{\geq 0}) \oplus \left(T\mathbb{R}_{\geq 0} \otimes TS^2\right) \oplus \mathrm{Sym}^2(TS^2). \quad (4.17)$$

There is an identification between $T\mathbb{R}$ and $\mathbb{R}$. Therefore, we can use scalar functions on $\mathbb{R}^4$ to represent sections on $\mathrm{Sym}^2(T\mathbb{R})$, $T\mathbb{R}$, $\mathrm{Sym}^2(T\mathbb{R}_{\geq 0})$ and $T\mathbb{R}_{\geq 0}$. Using Theorem 4.1.6

these scalars can be decomposed into spherical harmonics. Additionally, we can apply the same theorem to the sections on TS^2 and $\mathrm{Sym}^2(TS^2)$ to decompose these into Regge-Wheeler vector and tensor spherical harmonics, respectively.

Using the definitions from Section 4.1.1, we can now construct a general perturbation with angular momentum l, projection to the z-axis m and odd or even parity. In spherical coordinates this construction will precisely give the tensors in Eq. 4.13 and 4.14. □

Recall from Sec. 2.2 that for a stationary background space we can focus on proving mode stability. The Schwarzschild metric is independent of the time-coordinate t, so it is sensible to do a mode decomposition here. With Eq. 2.56 we split the perturbation in modes of different frequencies ω. As a consequence of the time translation symmetry it is possible to analyse the stability of the modes separately. For a mode of h the time dependence will be given by a factor $\exp(-i\omega t)$. So altogether, we can separately solve the linearized Einstein equations for the different modes of the perturbation, each mode with a specific frequency ω, l and m value, and parity. A general perturbation will then be a superposition of these modes with coefficients that fit the boundary conditions and initial values. However, recall from section 2.2 that having only stable modes does not imply linear stability. Namely, it is possible that this superposition is just a formal series and that it does not converge to a solution. Moreover, the integral in Eq. 2.56 does not necessarily have to consist purely out of modes that solve the linearized Einstein equations. It is possible that there are modes such that $\Delta_L e^{-i\omega t}\chi(\omega, x^i) \neq 0$, but in the integral it gets cancelled by another non-zero mode. Nevertheless, we focus on mode stability for now.

Proposition 4.1.8. *The Einstein equations will be independent of the projection to the z-axis m.*

Proof. Since the background is spherically symmetric, we can always apply a rotation such that the projection to the new z-axis is equal to any desired value. □

Therefore, we can specialize to $m = 0$, which will take away all φ dependency and is for that reason the most sensible choice.

Before computing the Einstein equations, we note that the perturbations can still be simplified by gauge transformations. For a small vector field $X \in \Gamma(T\mathbb{R}^4)$ the metric transforms as in Eq. 2.32. Keeping g_s fixed, the perturbation transforms as

$$h'_{ab} = h_{ab} + \nabla^s_a X_b + \nabla^s_b X_a, \tag{4.18}$$

where ∇^s denotes the covariant derivative with respect to the Schwarzschild metric. Since we do not want to disturb the angular momentum or parity of our perturbation, we only want to transform the perturbations using vector fields of the same angular momentum and corresponding parity. Using the splitting of $T\mathbb{R}^4$ in Eq. 4.15, we can split

$$\Gamma(T\mathbb{R}^4) = \Gamma(T\mathbb{R}) \otimes \Gamma(T\mathbb{R}_{\geq 0}) \otimes \Gamma(TS^2). \tag{4.19}$$

Therefore, the vector fields are decomposed in Regge-Wheeler harmonics by using scalar spherical harmonics for X_0 and X_1 and vector spherical harmonics for (X_2, X_3).

Lemma 4.1.9. *After a suitable gauge transformation, a general odd parity perturbation of angular momentum l and frequency ω takes the from*

$$h_{ab} = \begin{pmatrix} 0 & 0 & 0 & h_0(r) \\ 0 & 0 & 0 & h_1(r) \\ 0 & 0 & 0 & 0 \\ h_0(r) & h_1(r) & 0 & 0 \end{pmatrix} \times e^{-i\omega t} \sin\theta \frac{\partial}{\partial\theta} P_l(\cos\theta), \tag{4.20}$$

where P_l is a Legendre polynomial. An even parity perturbation is of the form

$$h_{ab} = \begin{pmatrix} H_0(t,r) & H_1(t,r) & 0 & 0 \\ H_1(t,r) & H_2(t,r) & 0 & 0 \\ 0 & 0 & K(t,r) & 0 \\ 0 & 0 & 0 & K(t,r)\sin^2\theta \end{pmatrix} \times e^{-i\omega t} P_l(\cos\theta). \tag{4.21}$$

Proof. Let us first focus on odd type perturberbations. Odd parity X_a will then have the form

$$X_0 = 0, \;\; X_1 = 0, \;\; X_a = \Lambda(t,r)\epsilon_a^b \frac{\partial}{\partial x^b} Y_{lm} \;\; (a,b = 2,3).$$

If we then compute covariant derivatives of this covector, we find that

$$\begin{aligned}
\nabla_2 X_2 &= \Lambda(t,r)\left(\frac{\cos\theta}{\sin^2\theta}\frac{\partial}{\partial\varphi} - \frac{1}{\sin\theta}\frac{\partial^2}{\partial\theta\partial\varphi}\right) Y_{lm}, \\
\nabla_2 X_3 &= \Lambda(t,r)\sin\theta\frac{\partial^2}{\partial\theta^2} Y_{lm}, \\
\nabla_3 X_2 &= \Lambda(t,r)\left(-\frac{1}{\sin\theta}\frac{\partial^2}{\partial\varphi^2} - \cos\theta\frac{\partial}{\partial\theta}\right) Y_{lm}, \\
\nabla_3 X_3 &= \Lambda(t,r)\left(\sin\theta\frac{\partial^2}{\partial\theta\partial\varphi} - \cos\theta\frac{\partial}{\partial\varphi}\right) Y_{lm}.
\end{aligned}$$

Consequently, by setting $\Lambda(t,r) = -\frac{1}{2}h_2(t,r)$ we can precisely cancel the contribution of the tensor spherical harmonic. Note that other covariant derivatives such as $\nabla_1 X_3$, will also not vanish. However, we can solve this by redefining h_1, such that after the redefinition the component of the perturbation did not change. With this gauge transformation in mind and by setting $m = 0$, a general perturbation of odd parity, with angular momentum l and frequency ω takes the form of Eq. 4.20.

Similarly, the even parity perturbations can also be simplified. Using the scalar spherical harmonics and the even vector spherical harmonics from Eq. 4.6, a gauge transformation of even parity, and of (l,m) type is of the following form

$$\begin{aligned}
X_0 &= M_0(t,r)Y_{lm}, \\
X_1 &= M_1(t,r)Y_{lm}, \\
X_2 &= M(t,r)\frac{\partial}{\partial\theta}Y_{lm}, \\
X_3 &= M(t,r)\frac{\partial}{\partial\varphi}Y_{lm}.
\end{aligned}$$

Note that we have three degrees of freedom, M_0, M_1 and M, which we want to use to cancel the factors of G, f_0 and f_1 in Eq. 4.14. By examining the covariant derivatives of the covector field X_a, the following equations need to be satisfied in order to cancel the desired terms

$$\begin{aligned}
\frac{\partial M}{\partial t} + M_0 &= -f_0, \\
\frac{\partial M}{\partial r} - \frac{2M}{r} + M_1 &= -f_1, \\
M &= \frac{-1}{2}G.
\end{aligned}$$

This simply leads to the following solution

$$M = \frac{-1}{2}G, \quad M_0 = \frac{1}{2}\frac{\partial G}{\partial t} - f_0, \quad M_1 = \frac{1}{2}\frac{\partial G}{\partial r} - \frac{G}{r} - f_1. \tag{4.22}$$

Here again, this gauge transformation also shifts the other terms. Nevertheless, no new terms are introduced, such that we can just redefine of the functions H_0, H_1, H_2 and K. Finally, just as in the odd case we set $m = 0$. With this the even perturbations can be written in the form of Eq. 4.21. □

Now that we have each mode in this simple form, we can compute the linear Einstein equations for each mode separately. This is done in the next section.

4.1.3 Mode stability of the Schwarzschild metric

In this section we solve the linearized Einstein equations 2.51 for odd and even parity perturbations of the Schwarzschild metric. We prove that all modes are stable for both types of parity. We combine this to prove that the Schwarzschild black hole has mode stability.

Theorem 4.1.10. *The Schwarzschild metric $(\mathbb{R}^4, g_s)$ has mode stability.*

To prove this theorem we first have to analyse the linearized Einstein equations of the Schwarzschild metric. We start with analysing the equations for odd parity modes.

Lemma 4.1.11. *The linearized Einstein equations of the Schwarzschild metric for odd parity modes can be rewritten into a* ***odd parity master equation*** *of the following form*

$$-\frac{d^2Q}{dr^{*2}} + V_{odd}\, Q = \omega^2 Q, \tag{4.23}$$

where

$$V_{odd}(r) = \left(1 - \frac{r_s}{r}\right)\left(\frac{l(l+1)}{r^2} - \frac{3r_s}{r^3}\right). \tag{4.24}$$

Proof. First we compute the Linearized Einstein equations for odd parity modes of the form as in Eq. 4.20. Most components of the linearized Einstein equations will vanish, but there will remain three non-trivial equations

$$\left(1 - \frac{r_s}{r}\right)^{-1} i\omega h_0 + \frac{d}{dr}\left(1 - \frac{r_s}{r}\right) h_1 = 0 \qquad (\delta R_{23} = 0), \tag{4.25}$$

$$\left(1 - \frac{r_s}{r}\right)^{-1} i\omega \left[\frac{dh_0}{dr} + i\omega h_1 - \frac{2h_0}{r}\right] + (l+2)(l-1)\frac{h_1}{r^2} = 0 \qquad (\delta R_{13} = 0), \tag{4.26}$$

$$\frac{d}{dr}\left(i\omega h_1 + \frac{dh_0}{dr}\right) + 2i\omega\frac{h_1}{r} + \left(1 - \frac{r_s}{r}\right)^{-1}\left(\frac{2r_s}{r^3} - \frac{l(l+1)}{r^2}\right) h_0 = 0 \qquad (\delta R_{03} = 0). \tag{4.27}$$

The third equation can be derived directly from the other two, so we will focus on the first two. We define the **tortoise coordinate** using the differential relation

$$\frac{dr}{dr^*} = \left(1 - \frac{r_s}{r}\right). \tag{4.28}$$

This leads to the following relation

$$r^* = r + r_s \log\left(\frac{r}{r_s} - 1\right), \qquad -\infty < r^* < \infty. \tag{4.29}$$

Furthermore, we define a new quantity

$$Q(r) = \left(1 - \frac{r_s}{r}\right)\frac{h_1(r)}{r}.$$

If we eliminate h_0 out of the equations, then we end up with a second-order Schrödinger-like equation for Q, which is the master equation in Eq. 4.23. □

Let us take a step back and look at what Eq. 4.23 can tell us about the mode stability of the Schwarzschild metric. Recall from section 2.2 that a metric has mode stability if there are no exponentially growing modes. If we now look back to the master equation for the odd parity perturbation in Eq. 4.20, we see that an imaginary ω would lead to exponential growth of the perturbation, whereas modes with real ω are oscillatory and will for that reason not grow in size over time. Therefore, what we need to prove is that the spectrum of the operator on the left hand side of Eq. 4.23 consists of positive numbers. Then any mode has real frequency ω. Consequently, we prove that the Schwarzschild metric has mode stability under odd perturbations.

In 1957, Regge & Wheeler proved this by constructing solutions to Eq. 4.23 at the ranges $r \to \infty$ and $r \to r_s$ and then argued that these solutions cannot be matched together for imaginary ω [20]. Later, in 1970, Vishveshwara not only redid this proof, but also gave a mathematically more rigorous alternative proof [21, Section 5A]. Vishveshware used spectral theory to analyse the spectrum of the frequencies. We already did most of the work in Section 2.3. The mode stability is proven by applying Theorem 2.3.1.

Lemma 4.1.12. *All odd parity modes of the Schwarzschild black hole $(\mathbb{R}^4, g_s)$ have a real frequency.*

Proof. Now that we have a master equation of Schrödinger form we can use results from section 2.3 to find the frequencies of the modes. The first step is to translate the problem to an eigenvalue problem. We define the operator

$$A = -\frac{d^2}{dr^*} + V_{\text{odd}}.$$

According to Theorem 2.3.1, we have mode stability if V_{odd} is piecewise continuous, bounded and non-negative in the range $r_s < r < \infty$. Looking at Eq. 4.24, V_{odd} is indeed bounded and continuous in this range. To observe the non-negativity note that $1 - \frac{r_s}{r} > 0$ in this range. Furthermore, if $l \geq 2$ then

$$\frac{l(l+1)}{r^2} - \frac{3r_s}{r^3} > \frac{l(l+1)}{r^2} - \frac{3}{r^2} > 0. \tag{4.30}$$

This proves the stability for $l \geq 2$.

For the case $l = 0$, note that $P_0(x) = 1$ such that the odd parity perturbations in Eq. 4.20 vanish. In the case of $l = 1$, it is shown in [21, P. 37] that the odd parity perturbations are pure gauge. Therefore, they can be removed with a gauge transformation. □

Next we derive mode stability of the even parity perturbations. In [20, P. 5] it is shown that the even $l = 0$ perturbations correspond to the difference between two Schwarzschild solutions of mass M and $M+\delta M$. Furthermore, the even $l = 1$ perturbations correspond to a displacement of the black hole by δx. These are stable transformations. Therefore, we only need to show the stability for $l \geq 2$.

Lemma 4.1.13. *The linearized Einstein equations of the Schwarzschild metric for even parity modes and $l \geq 2$ can be rewritten into a **even parity master equation** of the following form*

$$-\frac{d^2\hat{K}}{dr^{*2}} + V_{even}\,\hat{K} = \omega^2 \hat{K}, \tag{4.31}$$

with the potential

$$V_{even}(r) = \frac{(r - r_s)(8r^3\lambda(1+\lambda) + 12r_s r^2\lambda^2 + 18{r_s}^2 r\lambda + 9{r_s}^3)}{r^4(3r_s + 2r\lambda)^2}. \tag{4.32}$$

Proof. Perturbations of even parity can be written as in Eq. 4.21. The linearized Einstein equations in the even parity case for $l \geq 2$ give two algebraic relations, three first order differential equations, and three second order differential equations. From $\delta R_{22} = 0$ we derive that $H_0 = H_2 \equiv H$. Using this relation to replace H_0 and H_2, the first order differential equations are

$$\frac{dK}{dr} + \frac{l(l+1)}{2i\omega r^2} H_1 - \frac{1}{r} H + \frac{r - \frac{3}{2} r_s}{r(r - r_s)} K = 0 \qquad (\delta R_{01} = 0), \tag{4.33}$$

$$\frac{dH_1}{dr} + \frac{r_s}{r(r - r_s)} H_1 + \frac{i\omega r}{r - r_s} H + \frac{i\omega r}{r - r_s} K = 0 \qquad (\delta R_{02} = 0), \tag{4.34}$$

$$\frac{dH}{dr} + \left[\frac{i\omega r}{r - r_s} + \frac{l(l+1)}{2i\omega r^2} \right] H_1 + \frac{r - 2r_s}{r(r - r_s)} H + \frac{r - \frac{3}{2} r_s}{r(r - r_s)} K = 0 \qquad (\delta R_{12} = 0). \tag{4.35}$$

The other algebraic relation follows from $\delta R_{11} = 0$, from which we get

$$\begin{aligned} 2(r - r_s)\frac{dH}{dr} - (2r - 2r_s)\frac{dK}{dr} + 4i\omega r H_1 - \\ (l+2)(l-1)H + \left[(l+2)(l-1) - \frac{2\omega^2 r^3}{r - r_s} \right] K = 0. \end{aligned} \tag{4.36}$$

If we substitute the derivatives in Eq. 4.36 with the expressions we get from Eq. 4.33 and 4.35, then we end up with the relation

$$\begin{aligned} \left[2i\omega r + \frac{l(l+1) r_s}{2i\omega r^2} \right] H_1 - \left[(l+2)(l - 1 + \frac{3 r_s}{r} \right] H + \\ \left[(l+2)(l-1) + \frac{r_s(r - \frac{3}{2} r_s)}{r(r - r_s)} - \frac{2\omega^2 r^3}{r - r_s} \right] K = 0. \end{aligned} \tag{4.37}$$

It can be shown that the three second order equations follow directly from these relations. For the full set of equations we refer to the Regge & Wheeler paper [20, P. 5].

We would like to obtain an equation of Schrödinger type, where we can describe the system with one function. Using the algebraic relation from Eq. 4.37, we can already get rid of one function. We choose to solve it for H, and substitute this expression in the differential equations for H_1 and K. Additionally, it turns out to be convenient to define $R = \frac{H_1}{\omega}$. Using R the differential equations will be of the following form

$$\frac{dK}{dr} = \left[\alpha_0(r) + \alpha_2(r)\omega^2 \right] K + \left[\beta_0(r) + \beta_2(r)\omega^2 \right] R, \tag{4.38}$$

$$\frac{dR}{dr} = \left[\gamma_0(r) + \gamma_2(r)\omega^2 \right] K + \left[\delta_0(r) + \delta_2(r)\omega^2 \right] R, \tag{4.39}$$

where the α, β, γ and δ functions only depend on r, m^* and l and not on ω.

We now want to make a transformation [22]

$$K = f_1(r)\hat{K} + f_2(r)\hat{R}, \tag{4.40}$$

$$R = g_1(r)\hat{K} + g_2(r)\hat{R}, \tag{4.41}$$

such that these new functions $\hat{K}$ and $\hat{R}$ satisfy the differential relations

$$\frac{d\hat{K}}{dr^*} = \hat{R}, \tag{4.42}$$

$$\frac{d\hat{R}}{dr^*} = \left[V(r) - \omega^2 \right] \hat{K}, \tag{4.43}$$

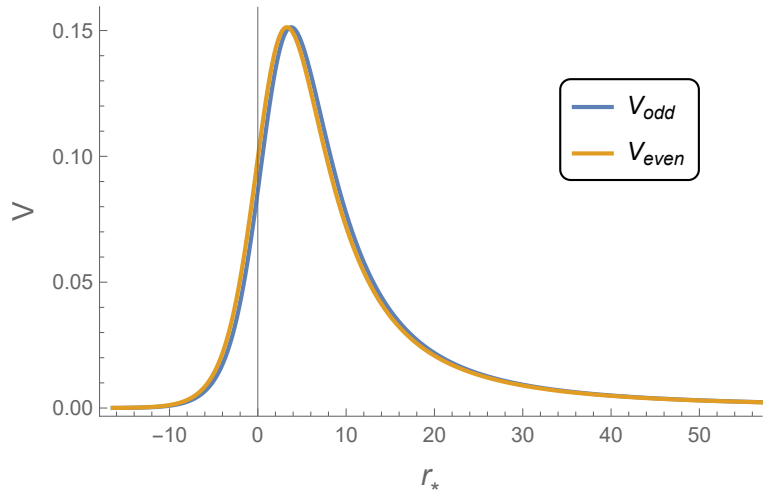

Figure 4.1: The odd and even potentials belonging to the master equations 4.23 and 4.31, respectively. The horizontal axis represents the tortoise coordinate r_*. We set $r_s = 2$ and $\lambda = l = 2$.

where r^* is the tortoise coordinate 4.29, and $V(r)$ is some potential. If such a transformation exists, then we can combine the two differential relation to find a master equation of the desired Schrödinger form 2.59.

We can substitute Eq. 4.40 and 4.41 into Eq. 4.38 and 4.39. If we combine the resulting equations with our requirements, then we have four equations to solve for the four unknown functions f_1, f_2, g_1 and g_2. This can be done to find

$$f_1(r) = \frac{\lambda(\lambda+1)r^2 + 3m^* r\lambda + 6m^{*2}}{r^2(\frac{3}{2}r_s + r\lambda)}, \qquad f_2(r) = 1 \tag{4.44}$$

$$g_1(r) = \frac{i(r^2\lambda - \frac{3}{2}r_s r\lambda - 3m^{*2})}{(r_s - r)(\frac{3}{2}r_s + r\lambda)}, \qquad g_2(r) = \frac{ir^2}{r - r_s}, \tag{4.45}$$

where $\lambda = \frac{1}{2}(l-1)(l+2)$. Finally, we find the master equation from Eq. 4.31. □

On first sight the potential in Eq. 4.32 looks very different compared to the potential in the odd case in Eq. 4.24. However, if we look at Fig. 4.1, then we see that they are actually very similar. With this fact, we conclude that there is no difference between the behaviour of odd and even perturbations. In particular, by Cor. 2.3.20 and Theorem 2.3.23 we conclude that the even perturbation modes all have real frequency and that there are no exponentially growing modes.

Lemma 4.1.14. *All even parity modes of the Schwarzschild black hole* $(\mathbb{R}^4, g_s)$ *have a real frequency.*

With Lem. 4.1.12 and 4.1.14 it follows that all modes of the Schwarzschild black hole are stable. In particular this proves Theorem 4.1.10.

4.2 Gregory-Laflamme Instability

In the previous section we have proven the stability of the Schwarzschild metric in four dimensions. In this section we analyse the stability of black holes in five-dimensional flat space. According to Gregory and Laflamme [18], there exist unstable five-dimensional black holes. We analyse this instability such that we can generalize it to the instabilities in the RS model in the next section.

In Section 4.2.1, we derive two different five-dimensional black hole solutions: the hyperspherical black hole and the black string. In Section 4.2.2, we use an entropy argument to argue that the hyperspherical black hole is preferred over the black string if the extra dimension is large. This indicates the existence of an instability of the black string. We analytically prove this mode instability in the rest of the subsections.

We prove it by first deriving the master equation of the modes of the black string in Section 4.2.3. This master equation defines the black string operator with a potential. The strategy to prove the instability is to construct proper test functions and use Theorem 2.3.16 to prove that the black string operator admits negative eigenvalues. In Section 4.2.4 we define the asymmetric finite well potential, which is a good approximation of the black string potential. We can use the eigenfunctions of the asymmetric finite well operator as test functions. The eigenfunctions are derived in Section 4.2.5. Finally, we use these eigenfunctions and apply Theorem 2.3.16 to prove the existence of negative eigenvalues in Section 4.2.6.

4.2.1 Black holes and black strings

In this section we derive two black hole solutions in five-dimensional flat space. In four dimensions, the Schwarzschild solution is derived by solving the vacuum Einstein equations 2.27. The Schwarzschild solution is the unique, static and spherically symmetric solution solving the vacuum Einstein equations for $\mu = 0$. However, in higher dimensions, there are multiple black hole solutions.

Birkhoff's theorem 2.1.17 can be generalized to five-dimensions [61, Theorem 1]. In that case we consider the five-dimensional spherical symmetry. This gives a five-dimensional generalization of the Schwarzschild solution. This leads to a hyperspherical black hole with metric in spherical coordinates given by

$$g_{\text{HS}} = -f_5(r)dt^2 + f_5(r)^{-1}dr^2 + r^2 d\Omega_3^2, \tag{4.46}$$

where $d\Omega_3^2$ is the standard metric on S^3 and f_5 is given by

$$f_5(r) = 1 - \frac{r_5^2}{r^2}, \quad r_5^2 = \frac{8G_5 M}{3\pi}. \tag{4.47}$$

Here r_5 denotes the radius of the horizon and M the mass of the five-dimensional black hole.

However, also non-spherically symmetric black holes exist in five-dimensions [62]. Namely, we can still construct solutions which are spherically symmmetric in a four-dimensional plane. Similar to RS, there exists a black string solution in five-dimensional flat space. Any metric of the form

$$g^{(4)}(x) + dy^2, \tag{4.48}$$

is Ricci flat if the four-dimensional metric $g^{(4)}$ is Ricci flat. Therefore, a solution is obtained by substituting the Schwarzschild metric for $g^{(4)}$. This is the **black string** solution given by

$$g_{\text{BS}} = -(1 - \frac{r_s}{r})dt^2 + \frac{1}{1 - \frac{r_s}{r}}dr^2 + r^2 d\Omega_2^2 + dy^2, \tag{4.49}$$

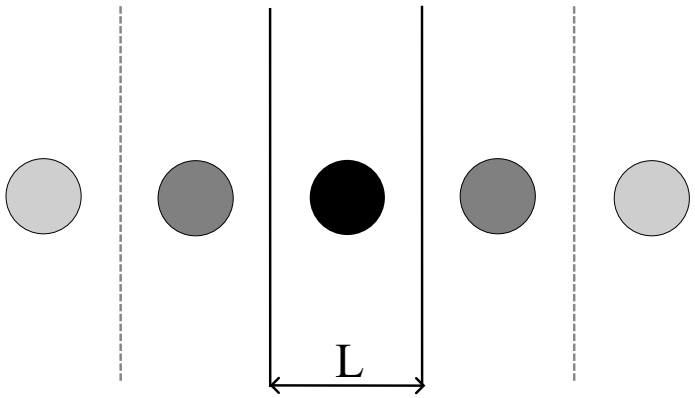

Figure 4.2: The spherical black hole in a space with compact extra dimensions of length L. It interacts with itself along the extra dimension.

with the Schwarzschild radius

$$r_s = 2G_4 M. \tag{4.50}$$

One could ask why this does not give a string-like black hole in four-dimensions using the same construction. However, in three dimensions general relativity is much simpler. In fact the Riemann tensor is fully determined by the Ricci tensor [63, Eq. 7]. Therefore, a Ricci flat space is completely flat. Therefore, there are no Ricci flat black hole solutions in three dimensions.

Now we found two different black hole solutions in five dimensions. We can ask ourselves which type of black hole is more natural, i.e. which type would form after the collapse of a star. Let us consider the five-dimensional case with one compact dimension of length L such that the manifold would become $(\mathbb{R}^4 \times S^1, g)$. Then the black string metric in Eq. 4.49 is still valid. However, the hyperspherical black hole is not an exact solution any more. As can be seen in Fig. 4.2, the hyperspherical black hole will now interact with itself along the extra dimension. This will cause a distortion in the black hole. When the size of the black hole is much smaller than L, one can use construct a solution using Weyl metrics as is explained in [64], it turns out that the metric in Eq. 4.49 is still a good approximation. When the size of the black hole becomes comparable to L an exact solution can no longer be constructed and numerical computations are necessary.

For very big masses, when the size of the black hole becomes bigger than L, a hyperspherical is no longer possible. Therefore, in this case it is clear which solution is favourable. The hyperspherical black hole no longer fits into the cage, and a black string solution is forced. The story is different for small black holes. When M is small we can still approximate the hyperspherical black hole by the solution in Eq. 4.46. Likewise, the black string is still a solution. Normally, a physical system evolves to the state with lowest energy. However, in this case both solutions have the same energy M. Instead, we have to study the entropy of the black holes. According to the second law of thermodynamics, the entropy of a system is always growing. Therefore, the state with the highest entropy will be the preferred one.

4.2.2 Entropy of black holes

In the previous section we derived that there exist two types of black holes in five-dimensional flat space. We want to determine which state is the preferred physical state after for example gravitational collapse of a star. In this section we use an entropy argument to prove the following lemma.

Lemma 4.2.1. *Let $(\mathbb{R}^4 \times S^1, g_{HS})$ and $(\mathbb{R}^4 \times S^1, g_{BS})$ be the hyperspherical black hole and black string, respectively. Suppose both spaces have mass M and size of the compact dimension L. Then the hyperspherical black hole is entropically favourable over the black string if*

$$M < \frac{8L}{27\pi} \approx 0.09L. \tag{4.51}$$

According to Bekenstein and Hawking [65], information of a black hole is stored on its boundary. Therefore, the entropy of a black hole S_{BH} is proportional to its surface area A

$$S_{BH} = \frac{A}{4G_5}. \tag{4.52}$$

We can compare the entropy of the spherical black hole to the entropy of the black string. Using Eq. 4.52 and the surface areas, the entropies are given by

$$S_{BH} = \frac{\pi^2 r_5^3}{2L}, \quad S_{BS} = \frac{\pi L G_4^2 r_s^2}{G_5}. \tag{4.53}$$

With these expressions for the entropy, we can determine which state is preferred.

Proof of Lemma 4.2.1. From Eq. 3.7 we can read off how the four-dimensional Newton's constant relates to the five-dimensional one. It is given by

$$G_5 = LG_4 = L,$$

if we set $G_4 = 1$. Using this relation and Eq. 4.47 and 4.50, we can express the entropy of the black holes in terms of the mass

$$S_{BH} = \sqrt{\frac{128\pi L M^3}{27}}, \quad S_{BS} = 4\pi M^2. \tag{4.54}$$

Clearly, by fixing M and raising L, then at some point the hyperspherical black hole becomes entropically favourable over the black string. From Eq. 4.54 we read off that the hyperspherical black hole is favourable when

$$M < \frac{8L}{27\pi}. \tag{4.55}$$

□

Therefore, we expect long wavelength instabilities for the black string in this range. We derive the existence of these instabilities in the next subsections.

4.2.3 Perturbations of the black string

According to the entropy argument that was just derived, a long wavelength instability in the black string can be expected. In this section we take the first step in finding this instability by perturbing the metric.

Let g_{BS} denote the black string metric from Eq. 4.49, and let $g = g_{\text{BS}} + h$ be the perturbed metric. We would expect this instability to already occur on the spherically symmetric level. This corresponds in terms of spherical harmonics to the $l = 0$ case. Odd parity perturbations vanish at the $l = 0$ level. Therefore, we can decompose the perturbation in one even parity component. Additionally, since the background metric is independent of both t and y we can take a Fourier-Lagrange transform over both of these coordinates. We define

$$h_{ab} = \int d\omega \int dm\, e^{\omega t} e^{imy} \tilde{h}_{ab}(\omega, m, r). \tag{4.56}$$

Since we are looking for an instability we decomposed the perturbation in a way such that the modes with $\omega \in \mathbb{R}_{\geq 0}$ correspond to an instability. It is only necessary to analyse each mode individually. Therefore, we can decompose the perturbation as

$$h_{MN} = e^{\omega t} e^{iny} \begin{pmatrix} H_0 & H_1 & 0 & 0 & H_3 \\ H_1 & H_2 & 0 & 0 & H_4 \\ 0 & 0 & K & 0 & 0 \\ 0 & 0 & 0 & K \sin^2\theta & 0 \\ H_3 & H_4 & 0 & 0 & H_5 \end{pmatrix}, \tag{4.57}$$

where the H_i and K are scalar functions that only depend on the r-coordinate. In this section we derive the following master equation for mode perturbations of the black string.

Lemma 4.2.2. *The modes of the flat black string $(\mathbb{R}^4 \times S^1, g_{BS})$ from Eq. 4.57 that have $\omega \in \mathbb{R}$ are determined by the* ***black string master equation*** *given by*

$$-\frac{d^2\hat{H}}{dx^2} + V_{\hat{m}}(\hat{r})\hat{H} = -\hat{\omega}^2\hat{H}. \tag{4.58}$$

with potential

$$V_{\hat{m}}(\hat{r}) = \frac{(-1+\hat{r})\left(1 + 3\hat{m}^2(3-4\hat{r})\hat{r}^3 + \hat{m}^6\hat{r}^9 + 3\hat{m}^4\hat{r}^6(-3+2\hat{r})\right)}{\hat{r}^4\left(1+\hat{m}^2\hat{r}^3\right)^2}. \tag{4.59}$$

By Def. 2.2.9 the modes from Eq. 4.57 need to satisfy $\Delta_L h = 0$, where Δ_L is the Lichnerowicz operator defined in Eq. 2.50. Note that so far we have assumed spherical symmetry, however we have not done any gauge fixing yet. Since we are in vacuum, we can fix h to be in the transverse traceless gauge, which simplifies the Lichnerowicz operator.

Lemma 4.2.3. *There exist a gauge transformation such that the metric $g_{BS} + h$ is in the transverse traceless gauge from Def. 2.2.11.*

Proof. Using the Regge-Wheeler harmonics from section 4.1.1 a spherically symmetric covector has components

$$X_a = e^{\omega t} e^{imy} \begin{pmatrix} f_0(r) \\ f_1(r) \\ 0 \\ 0 \\ f_2(r) \end{pmatrix}.$$

Therefore, we have three degrees of freedom. One can show for perturbations as in Eq. 4.57 we already have

$$\nabla_M h_2^M = \nabla_M h_3^M = \nabla_M h_5^M = 0.$$

Therefore, only have to fix the three quantities h_M^M, $\nabla_M h_0^M$ and $\nabla_M h_1^M$ to be zero. This we can do using the three degrees of freedom we have. □

Another simplification happens because the background metric is Ricci flat. With these facts the Lichnerowicz operator becomes

$$\Delta_L h_{MN} = \Box_{g_{\rm BS}} h_{MN} + 2R_{MPNQ}h^{PQ}. \tag{4.60}$$

Lemma 4.2.4. *The y-components of the Riemann tensor associated to the black string metric in Eq. 3.42 vanish.*

Proof. Note that a Christoffel symbol with a y-component vanishes, $\Gamma^N_{M5} = 0$ for $M, N = 0, 1, 2, 3, 5$. Therefore, also all y-components of the Riemann tensor vanish. □

From the lemma it follows that the (55)-component of Eq. 4.60 is given by

$$\Delta_L h_{55} = \Box_{g_{\rm BS}} h_{55} = H_5'' + \left(\frac{2r - r_s}{r - r_s}\right)\frac{H_5'}{r} - \left(m^2 r(r - r_s) + \omega^2 r^2\right)\frac{H_5}{(r - r_s)^2} = 0. \tag{4.61}$$

Close to the horizon of the black hole and at $r \to \infty$ solutions to Eq. 4.61 behave as

$$H_5 \sim e^{\pm\sqrt{\omega^2+m^2}\,r} \qquad \text{as } r \to \infty, \tag{4.62}$$

$$H_5 \sim (r - r_s)^{\pm\omega r_s} \qquad \text{as } r \to r_s. \tag{4.63}$$

For a proper perturbation we expect that $H_5 \in H^2(\mathbb{R})$. Then according to Lem. 2.3.6, H_5 vanishes both at the horizon $x \to -\infty$ and asymptotically $x \to \infty$. To show that h_{55} does not contribute to the instability the following lemma is useful.

Lemma 4.2.5. *Let $f \in C^2((a, b), \mathbb{R})$ non-zero such that $\lim_{x\to a} f(x) = 0$ and $\lim_{x\to b} f(x) = 0$, then there exists a turning point $x \in (a, b)$ for which $f'(x) = 0$ and*

$$\frac{f''(x)}{f(x)} < 0. \tag{4.64}$$

Therefore, there exists a $r \in (r_s, \infty)$ with $H_5'(r) = 0$ and $H_5''(r)/H_5(r) < 0$. From Eq. 4.61 at this r we have

$$\frac{H_5''}{H_5} = \frac{m^2 r(r - r_s) + \omega^2 r^2}{(r - r_s)^2}. \tag{4.65}$$

This can only become negative when ω is imaginary. In our decomposition unstable modes had real ω. Consequently, an unstable mode has $H_5 = 0$.

With the same arguments we can conclude that H_3 and H_4 are zero for unstable modes. So any unstable mode can now be reduced to the form

$$h_{ab} = e^{\omega t}e^{imy}\begin{pmatrix} H_0 & H_1 & 0 & 0 \\ H_1 & H_2 & 0 & 0 \\ 0 & 0 & K & 0 \\ 0 & 0 & 0 & K\sin^2\theta \end{pmatrix}, \tag{4.66}$$

for $a, b = 0, 1, 2, 3$ and $h_{M5} = 0$ for $M = 0, 1, 2, 3, 5$.

Lemma 4.2.6. *For an unstable mode of the black string, the Lichnerowicz operator reduces to the four-dimensional Lichnerowicz operator plus a mass term*

$$\Delta_L h_{ab} = \Delta_L^s h_{ab} - m^2 h_{ab}, \tag{4.67}$$

here Δ_L^s denotes the Lichnerowicz operator associated to the four-dimensional Schwarzschild solution.

Proof. Since both the y-components of the Riemann tensor and the perturbation vanish for unstable modes, we have $\Delta_L h_{M5} = 0$ already. For the other components of the equation we have

$$\begin{aligned}\Delta_L h_{ab} =& \Box_{g_{\mathrm{BS}}} h_{ab} + 2R_{aMbN}h^{MN} \\ =& \Box_{g^s} h_{ab} + h''_{ab} + 2R^s_{abcd}h^{ab} \\ =& \Delta^s_L h_{ab} - m^2 h_{ab}.\end{aligned}$$

Here g^s denotes the four-dimensional Schwarzschild metric and R^s the corresponding Riemann tensor. Furthermore, the second equality is a consequence of the fact that all y-components of the Christoffel symbol vanish. □

We have now simplified the linearized Einstein equations enough to be able to compute the master equation.

Proof of Lem. 4.2.2. Using this result we can compute the equations we get from the linearized Einstein equations $\Delta_L h_{MN} = 0$. This leads to two differential equations and one relation. They are given by

$$H_+ = \frac{H_-}{V}\frac{\left(2r^2\omega^2 + r^2m^2V - (1-V^2)/2\right)}{(r^2m^2+1-V)} - \frac{rH}{\omega}\frac{\left(4\omega^2 + m^2(1-3V)\right)}{(r^2m^2+1-V)}, \tag{4.68}$$

$$H' = \frac{\omega\left(H_+ + H_-\right)}{2V} - \frac{(1+V)H}{rV}, \tag{4.69}$$

$$H'_- = \frac{m^2 H}{\omega} + \frac{H_+}{r} + \frac{(1-5V)H_-}{2rV}, \tag{4.70}$$

where we defined

$$V = 1 - \frac{rs}{r}, \tag{4.71}$$

$$H_\pm = \frac{H_0}{V} \pm V H_2, \tag{4.72}$$

$$H = H_1. \tag{4.73}$$

By redefining $R = \omega H_-$ and using the relation in Eq. 4.68 to get rid of H_+, we obtain a system of two differential equations of the form

$$\frac{dR}{dr} = (\alpha_0 + \omega^2\alpha_2)R + (\beta_0 + \omega^2\beta_2)H, \tag{4.74}$$

$$\frac{dH}{dr} = (\gamma_0 + \omega^2\gamma_2)R + (\delta_0 + \omega^2\delta_2)H. \tag{4.75}$$

This is system similar to the even parity Schwarzschild case. Therefore, we again define a transformation to $\hat{R}$ and $\hat{H}$ with

$$R = f_1(r)\hat{R} + f_2(r)\hat{H}, \tag{4.76}$$

$$H = g_1(r)\hat{R} + g_2(r)\hat{H}. \tag{4.77}$$

In order to obtain a Schrödinger equation we want the derivatives of the new variables to be equal to

$$\frac{d\hat{H}}{dr^*} = \hat{R}, \quad \frac{d\hat{R}}{dr^*} = \left(\omega^2 - V_m(r)\right)\hat{H}, \tag{4.78}$$

where again r^* is the tortoise coordinate. Additionally, the potential V_m should only depend on m and not on the frequency ω. There are multiple solutions that solve this. The solution

we will use is the following:

$$f_1(r) = 1, \qquad f_2(r) = \frac{m^2r^2 + m^4r^4 - (6 + m^2r^2)V + 6V^2}{2r^2\,(r + m^2r^3 - rV)},$$
$$g_1(r) = -\frac{r}{2V}, \qquad g_2(r) = \frac{(-1+V)\left(1 + m^2r^2 + 5V\right)}{4r^2V(-1 - m^2r^2 + V)}.$$

To simplify the equation it is useful to work with the dimensionless variables, $x = r^*/r_s$, $\hat{r} = r/r_s$, $\hat{m} = r_s m$ and $\hat{\omega} = r_s\omega$. The coordinate $\hat{r}$ has domain $(1, \infty)$ and is related to x by

$$x = \hat{r} + \log(\hat{r} - 1). \tag{4.79}$$

With these new variables the potential in Eq. 4.78 for this solution is given by Eq. 4.59. We can combine the two differential relations in Eq. 4.78 to find the Schrödinger type master equation in Eq. 4.58. □

We have found a $\hat{m}$-dependent potential. To determine if modes with wavenumber $\hat{m}$ are stable we need to analyse these potentials. We can derive some properties that are independent of $\hat{m}$.

Lemma 4.2.7. *The **black string potential** $V_{\hat{m}}$ from Eq. 4.59 has the following limits*

$$\lim_{x\to-\infty} V_{\hat{m}}(x) = 0, \tag{4.80}$$
$$\lim_{x\to\infty} V_{\hat{m}}(x) = \hat{m}^2. \tag{4.81}$$

Proof. From Eq. 4.79 we see that $\hat{r}$ goes to 1 as x goes to $-\infty$, and $\hat{r}$ goes to ∞ as x goes to ∞. Using Eq. 4.59 we indeed see that

$$\lim_{x\to-\infty} V_{\hat{m}}(x) = \lim_{\hat{r}\to1} V_{\hat{m}}(\hat{r}) = 0,$$
$$\lim_{x\to\infty} V_{\hat{m}}(x) = \lim_{\hat{r}\to\infty} V_{\hat{m}}(\hat{r}) = \hat{m}^2.$$

□

Since we have written Eq. 4.58 in Schrödinger form we can turn the left hand side into an operator.

Definition 4.2.8. *The **black string operator** $A_{\hat{m}} : H^2(\mathbb{R}) \to L^2(\mathbb{R})$ of wavenumber $\hat{m}$ is the Schödinger operator*

$$A_{\hat{m}} = -\frac{d^2}{dx^2} + V_{\hat{m}}, \tag{4.82}$$

with potential $V_{\hat{m}}(\hat{r})$ as in Eq. 4.59.

Lemma 4.2.9. *The black string operator $A_{\hat{m}}$ is self-adjoint on $D(A_{\hat{m}}) = H^2(\mathbb{R})$ for any $\hat{m} \in \mathbb{R}$.*

Proof. Note that the potential $V_{\hat{m}}$ from Eq. 4.59 is bounded for any $\hat{m}$. Therefore, by Cor. 2.3.20 the black string operator is self-adjoint on $H^2(\mathbb{R})$. □

We conclude that unstable modes correspond to eigenfunctions of the black string Schrödinger operator with negative eigenvalue. The self-adjointness of $A_{\hat{m}}$ allows us to study its spectrum. In the next subsections we will try to estimate the lowest eigenvalue of the black string operator.

4.2.4 The asymmetric finite well potential

In the previous subsection we derived the master equation 4.58 for spherically symmetric perturbations on a black string spacetime. This equation is written in Schrödinger form. In this subsection we will take the first step in finding negative eigenvalues of the black string Schrödinger operator by approximating the potential by a step function.

Looking at the numerical results of Gregory and Laflamme [18, P. 11], we expect the lowest negative eigenvalue of the operator to be around $\hat{m} = 0.4$. The plot of the potential for this wavenumber can be seen in fig. 4.3. Note that by Lem. 4.2.7 the potential converges to 0 as $x \to -\infty$ and to $\hat{m}^2 = 0.16$ as $x \to \infty$. Around $x = 0$, there is a dip in the potential and it has a negative minimum. The fact that the potential takes negative values indicates that there might exist negative eigenvalues.

The strategy that we use to find these negative eigenvalues is the strategy explained in section 2.2. According to Theorem 2.3.16 a negative eigenvalue exists, if there exists a $f \in D(A_m) = H^2(\mathbb{R})$ such that $\langle f, A_m f\rangle < 0$. To find such a f we try to approximate the black string potential by a simpler potential such that we can analytically derive eigenfunctions of the new Schrödinger operator. Once we have these eigenfunctions we can estimate the negative eigenvalues of the black string operator.

Let us try to determine what such a function f should look like. We have

$$\begin{aligned}\langle f, A_{\hat{m}} f\rangle &= \int_{-\infty}^{\infty} -\frac{d^2 f}{dx^2} f(x) + V_{\hat{m}}(x) f(x)^2 \, dx \\ &= \int_{-\infty}^{\infty} \left(\frac{df}{dx}\right)^2 + V_{\hat{m}}(x) f(x)^2 \, dx.\end{aligned}$$

We want this to be negative. Therefore, we want f to be a bump function that peaks at the minimum of the potential $V_{\hat{m}}$. However, this bump function must have a very gradual slope, since a non-zero derivative will have a positive contribution to the inner product. This contribution should not cancel the negative contribution from the potential term.

To find a bump function that has this behaviour, we construct eigenfunctions of a Schrödinger operator with a potential that has similar behaviour as the black string potential. Recall the asymptotic behaviour from Lem. 4.2.7. If we combine this with the fact that there is a dip around $x = 0$, we can approximate the potential by a discontinuous step function that has precisely these three properties.

Definition 4.2.10. *Let $a, V_0, m \in \mathbb{R}_{\geq 0}$. The **asymmetric finite well potential** $V_{afw} : \mathbb{R} \to \mathbb{R}$ of width a, depth V_0 and a wall of height m^2 is defined by*

$$V_{afw}(x) = \begin{cases} 0 & \text{if } x < -a, \\ -V_0 & \text{if } -a < x < a, \\ m^2 & \text{if } a < x. \end{cases} \tag{4.83}$$

We can then approximate the black string potential of wavenumber $\hat{m}$ by an asymmetric finite well potential that has V_0 equal to the absolute value of the minimum of the black string potential, a equal to the distance from the minimum to the first zero of the potential, and $m = \hat{m}$. In Fig. 4.3 we can see how the asymmetric finite well approximates the black string potential.

Note that the asymmetric finite well potential is bounded for any choice of parameters. Let A be a Schrödinger operator with an asymmetric finite well potential. According to Cor.

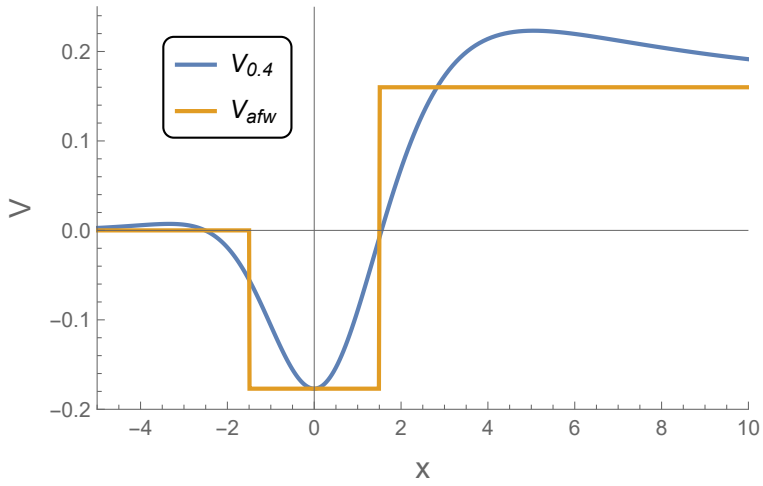

Figure 4.3: The black string potential for $\hat{m} = 0.4$ compared to the asymmetric finite well potential with $a = 1.5$, $V_0 = 1.7$ and $m = 0.4$.

2.3.20 A is self-adjoint on $H^2(\mathbb{R})$. By constructing eigenfunctions with negative eigenvalues of this operator, we generate a set of test functions that we can use to prove the existence of negative eigenvalues of the black string operator. Therefore, we are interested in finding negative eigenvalues of A. These eigenfunctions will be constructed in the next section.

4.2.5 Eigenfunctions of the asymmetric finite well operator

In the previous section we derived a simple potential that is a good approximation the black string potential. This potential is called the asymmetric finite well potential. In this section we construct the eigenfunctions with negative eigenvalues of the Schrödinger operator with asymmetric finite well potential 4.83. It turns out that not for every set of parameters (a, V_0, m) a negative eigenvalue exists. In particular, as one might expect the existence of a negative eigenvalue is less likely if m is really large, or when the well is shallow. In this section we prove the following relation.

Theorem 4.2.11. *The Schrödinger operator A with asymmetric finite well potential V_{afw} of width a, depth V_0 and height m^2, has at least one negative eigenvalue if and only if*

$$2\sqrt{V_0}a > arctan\left(\frac{m}{\sqrt{V_0}}\right). \tag{4.84}$$

If this inequality is satisfied, then every $E \in \sigma(A)$ with $-V_0 < E < 0$, has a corresponding eigenfunction $\psi \in H^2(\mathbb{R})$ given by

$$\psi(x) = \begin{cases} Ce^{\sqrt{-E}(x+a)}\sqrt{1+\frac{E}{V_0}} & \text{if } x < -a, \\ C\cos\left(\sqrt{V_0+E}(x+a) - arctan(\frac{\sqrt{-E}}{\sqrt{V_0+E}})\right) & \text{if } -a < x < a, \\ Ce^{-\sqrt{m^2-E}(x-a)}\sqrt{\frac{V_0+E}{V_0+m^2}} & \text{if } a < x, \end{cases} \tag{4.85}$$

where $C \in \mathbb{R}$ is a normalization constant.

Let us construct a solution $\psi \in H^2(\mathbb{R})$ such that $A\psi = E\psi$ for $E \in \mathbb{R}$ with $-V_0 < E < 0$. To achieve this we analyse what ψ should look like in each region of the potential and try to glue these solutions together.

First of all, if $x < -a$, then it holds that $\frac{d^2\psi}{dx^2} = -E\psi$. This is solved by

$$\psi(x) = Ae^{\sqrt{-E}x} + Be^{-\sqrt{-E}x}, \tag{4.86}$$

with constants $A, B \in \mathbb{R}$. Since ψ should decay when $x \to -\infty$, we can discard the $e^{-\sqrt{-E}x}$ solution and we are left with $\psi(x) = Ae^{\sqrt{-E}x}$.

Secondly, in the region where $-a < x < a$ the equation becomes $\frac{d^2\psi}{dx^2} = -(V_0 + E)\psi$. Now there is a negative value on the right hand side, therefore it is solved by

$$\psi(x) = C\cos\Big(\sqrt{V_0 + E}x + \delta\Big), \tag{4.87}$$

with coefficient $C \in \mathbb{R}$ and phase shift $\delta \in (-\pi, \pi]$.

Thirdly, for $x > a$ the equation becomes $\frac{d^2\psi}{dx^2} = (m^2 - E)\psi$. Now the factor on the right hand side is positive again, so this is solved by

$$\psi(x) = Fe^{\sqrt{m^2-E}x} + Ge^{-\sqrt{m^2-E}x}, \tag{4.88}$$

with constants $F, G \in \mathbb{R}$. Since we want $\psi(x)$ to vanish as $x \to \infty$, we have to set $F = 0$. Combining Eq. 4.86, 4.87 and 4.88 a solution of $A\psi = E\psi$ is given by

$$\psi(x) = \begin{cases} Ae^{\sqrt{-E}x} & \text{if } x < -a, \\ C\cos\big(\sqrt{V_0 + E}x + \delta\big) & \text{if } -a < x < a, \\ Ge^{-\sqrt{m^2-E}x} & \text{if } a < x. \end{cases} \tag{4.89}$$

We want $\psi \in H^2(\mathbb{R})$, to achieve this we have to fix the constants A, C, D and G such that both ψ and ψ' are continuous. This gives us the following conditions

$$Ae^{-\sqrt{-E}\,a} = C\cos\Big(-\sqrt{V_0 + E}\,a + \delta\Big), \qquad (\psi(-a)) \tag{4.90}$$

$$Ge^{-\sqrt{m^2-E}\,a} = C\cos\Big(\sqrt{V_0 + E}\,a + \delta\Big), \qquad (\psi(a)) \tag{4.91}$$

$$A\sqrt{-E}e^{-\sqrt{-E}\,a} = -C\sqrt{V_0 + E}\sin\Big(-\sqrt{V_0 + E}\,a + \delta\Big), \qquad (\psi'(-a)) \tag{4.92}$$

$$G\sqrt{m^2 - E}e^{-\sqrt{m^2-E}\,a} = C\sqrt{V_0 + E}\sin\Big(\sqrt{V_0 + E}\,a + \delta\Big), \qquad (\psi'(a)). \tag{4.93}$$

As we will see shortly, these conditions put relations on the coefficients A, C, G and the phase shift δ, but also restrict the possible eigenvalues E.

Let us first focus on the terms that come from the continuity conditions at $x = -a$. From Eq. 4.90 we can find an expression for A, namely

$$A = Ce^{\sqrt{-E}a}\cos\Big(-\sqrt{V_0 + E}a + \delta\Big). \tag{4.94}$$

If we substitute this into Eq. 4.92, we end up with

$$C\sqrt{-E}\cos\Big(-\sqrt{V_0 + E}a + \delta\Big) = -C\sqrt{V_0 + E}\sin\Big(-\sqrt{V_0 + E}a + \delta\Big). \tag{4.95}$$

Therefore, we either have $C = 0$ or

$$\tan\Big(-\sqrt{V_0 + E}a + \delta\Big) = -\frac{\sqrt{-E}}{\sqrt{V_0 + E}}. \tag{4.96}$$

Setting $C = 0$ would lead to the trivial solution, so we discard this possibility.

Similarly, using the conditions that we got from demanding continuity at $x = a$, we can use Eq. 4.92 to derive an expression for G. It is given by

$$G = Ce^{\sqrt{m^2-E}a}\cos\Big(\sqrt{V_0+E}a+\delta\Big). \tag{4.97}$$

Then this can be substituted into Eq. 4.93 to find

$$\tan\Big(\sqrt{V_0+E}a+\delta\Big) = \frac{\sqrt{m^2-E}}{\sqrt{V_0+E}}. \tag{4.98}$$

Now we have two equations for δ that should both hold. By eliminating δ from the equations we get restrictions on the allowed values of E.

To simplify the resulting equation we define new variables $z_0 = \sqrt{V_0}$ and $z = \sqrt{V_0+E}$. Using this new variable and combining Eq. 4.96 and 4.98 we find an equation for z, which is given by

$$\arctan\left(\sqrt{\frac{z_0^2}{z^2}-1}\right) + \arctan\left(\sqrt{\frac{z_0^2+m^2}{z^2}-1}\right) = 2za - k\pi, \tag{4.99}$$

where $k \in \mathbb{Z}$. We define the functions $f_m(z) : (0, z_0) \to \mathbb{R}$ and $l_k(z) : \mathbb{R} \to \mathbb{R}$, as the left and right hand side of Eq. 4.99, respectively. Now each point of intersection between f_m and l_k for some $k \in \mathbb{Z}$ corresponds to a negative eigenvalue of the Schrödinger operator A. Even though the left hand side of Eq. 4.99 is well defined in the point $z = z_0$, we excluded it from the domain of f_m since an intersection in the point $z = z_0$ would correspond to an eigenvalue $E = 0$, whereas we are interested in strictly negative eigenvalues. In Fig. 4.4 we see a plot of both side of Eq. 4.99. In this figure we see that when the height of the wall m increases, the function f_m moves up. As a consequence, it is possible that f_0 has a point of intersection with l_k, but f_m does not.

Lemma 4.2.12. *If f_m and l_k have a point of intersection, then $k \geq 0$.*

Proof. The function f_m monotonically decreases on the domain $(0, z_0]$ and has a range $(\pi, \arctan\left(\frac{m}{z}\right)]$. If $k < 0$ then on this domain l_k monotonically and has range $(-k\pi, 2z_0a - k\pi]$. There is no overlap between these ranges, so there cannot be a point of intersection. □

Lemma 4.2.13. *If f_m has a point of intersection with l_k for $k \in \mathbb{N}$ and $k \neq 0$, then f_m has a point of intersection with l_{k-1}.*

Proof. Suppose that $f_m(\hat{z}) = l_k(\hat{z})$. Note that $l_{k-1}(z) = l_k(z) + \pi$. Furthermore, f_m is a positive function and monotonically decreases on the domain $(0, \hat{z})$ from π to $l_k(\hat{z})$. On the same domain l_{k-1} monotonically increases from $(1-k)\pi$ to $l_k(\hat{z}) + \pi$. Now we have

$$\begin{aligned} l_{k-1}(0) &= (1-k)\pi < \pi \\ l_{k-1}(\hat{z}) &= l_k(\hat{z}) + \pi > l_k(\hat{z}). \end{aligned}$$

Therefore, there must be a point of intersection between f_m and l_{k-1} on the domain $(0, \hat{z})$. □

Combining these two lemma's, we get a improved requirement for the existence of a negative eigenvalue.

Corollary 4.2.14. *The Schrödinger operator A with asymmetric finite well potential has a negative eigenvalue if and only if f_m and l_0 have a point of intersection.*

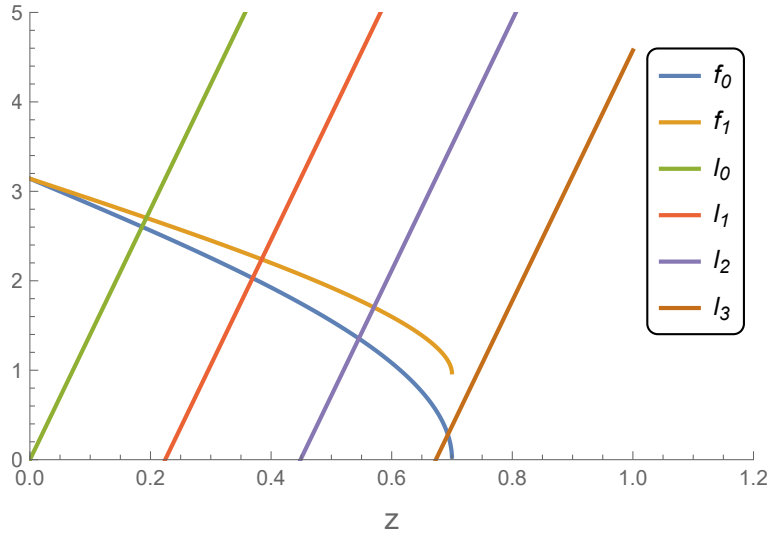

Figure 4.4: The functions on both sides of Eq. 4.99 for different m and k. In these plots we set $a = 7$, $V_0 = 0.49$ and compare the cases $m = 0$ and $m = 1$. Each intersection corresponds to a negative eigenvalue of the Schrödinger operator.

Proof. If f_m and l_0 have a point of intersection, then this corresponds to a negative eigenvalue of A.

If A has a negative eigenvalue, then we derived that f_m has a point of intersection with a l_k, with $k \in \mathbb{Z}$. From Lem. 4.2.12 it follows that $k \geq 0$. Additionally, by applying Lem. 4.2.13 repetitively, it follows that f_m has a point of intersection with l_0. □

We now have all the ingredients we need to prove Theorem 4.2.11.

Proof of Theorem 4.2.11. By Cor. 4.2.14 we know that A has a negative eigenvalue if and only if f_m and l_0 have a point of intersection. Since f_m monotonically decreases on its domain $(0, z_0]$ from π to $\arctan\left(\frac{m}{z}\right)$ and l_0 monotonically increases on this domain from 0 to $2z_0a$, there is a point of intersection if and only if

$$2z_0a > \arctan\left(\frac{m}{z_0}\right). \tag{4.100}$$

Using that $z_0 = \sqrt{V_0}$, we find the inequality from Eq. 4.84.

The corresponding eigenfunctions can be computed from the previous derivation. An eigenfunction of the asymmetric finite well operator is of the form as in Eq. 4.89. We can substitute the coefficients A and G by the expressions in Eq. 4.94 and 4.97, respectively. Furthermore, from Eq. 4.96 we get an expression for δ

$$\delta = \sqrt{V_0 + E}a - \arctan\left(\frac{\sqrt{-E}}{\sqrt{V_0 + E}}\right).$$

This gives the eigenfunction in Eq. 4.85.

Finally, if $f_m(\hat{z}) = l_k(\hat{z})$ then a negative eigenvalue is given by

$$E = z^2 - z_0^2. \tag{4.101}$$

□

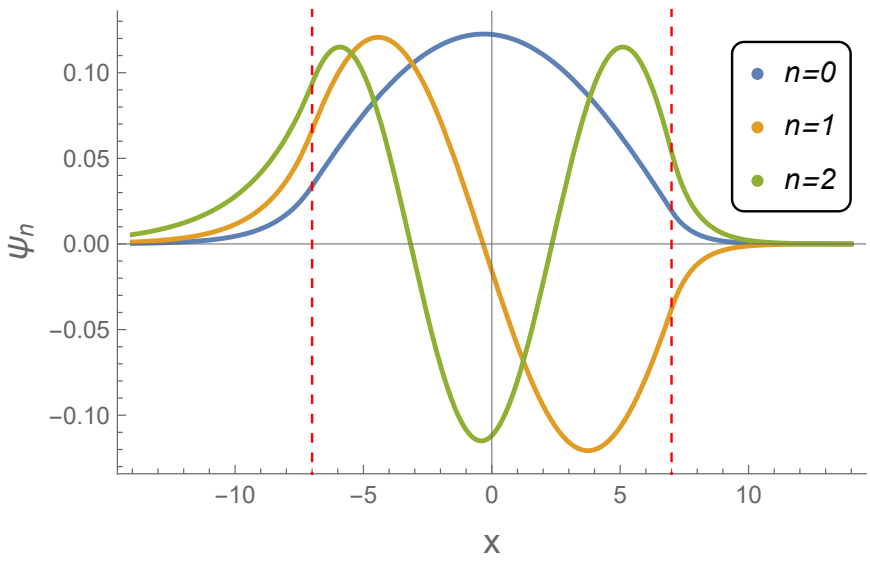

Figure 4.5: The eigenfunctions of the Schrödinger operator with parameters $a = 7$, $z_0 = 0.7$ and $m = 1$. The eigenfunctions correspond to the three intersections in Fig. 4.4 from left to right. the red dashed lines are the lines $x = \pm 7$, indicating the different regions of the potential.

Note that in the limit $m = 0$, the potential is no longer asymmetric. This case is called the finite well potential and it is a well-studied problem in quantum mechanics. As a sanity check, we can see if our results agree with the literature on the finite well in the case that $m = 0$. From Eq. 4.84 it follows that for $a, V_0 > 0$ and $m = 0$, a negative eigenvalue always exists. From Eq. 4.99 it follows that an eigenvalue solves the equation

$$\tan(za) = \sqrt{\frac{z_0^2}{z^2} - 1}. \tag{4.102}$$

This corresponds with the results from any quantum mechanics textbook [24].

The story changes once $m \neq 0$. In Fig. 4.4 the end point of the function is moved slightly up compared to the end point in the $m = 0$ case in Fig. 4.4. When $m \neq 0$, the left hand side of Eq. 4.99 still has a domain $(0, z_0)$ but now a range between $\arctan\left(\sqrt{\frac{m^2}{z_0^2}}\right)$ and π. Therefore, f_m can have less points of intersection compared to f_0. In Fig. 4.4 we see that f_0 intersects l_3, whereas f_1 does not. In Fig. 4.5 the eigenfunction are plotted corresponding to the case $m = 1$.

When the inequality 4.84 is not satisfied, there is no negative eigenvalue. This happens for a very shallow well as can be seen in Fig. 4.6. For a wide and deep well a negative eigenvalue always exists. Namely, note that the right hand side of Eq. 4.84 is always smaller than $\pi/2$. Therefore, as long as $\sqrt{V_0}a > \pi/4$ there always exists a negative eigenvalue.

If we look at the $n = 0$ eigenfunction in Fig. 4.5, we see that this function meets the requirements we set for a suitable bump function in Sec. 4.2.4. Namely, this function peaks at the minimum of the potential, and it decays very gradually at the asymptotes. Furthermore, note that the peak is slightly moved towards the side where potential equals 0. In the next section we use these eigenfunctions to prove the existence of negative eigenvalues of the black string operator.

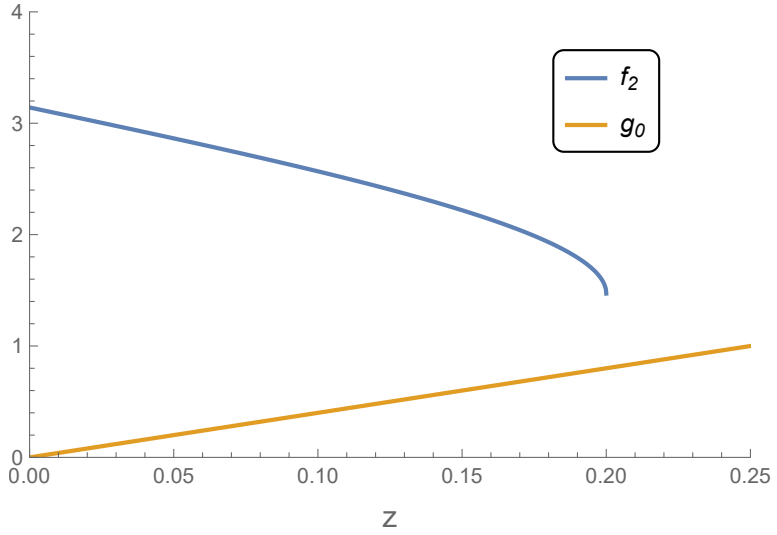

Figure 4.6: The two functions in Eq. 4.99 for $a = 2$, $z_0 = 0.16$ and $m = 2$. In this case there is no intersection.

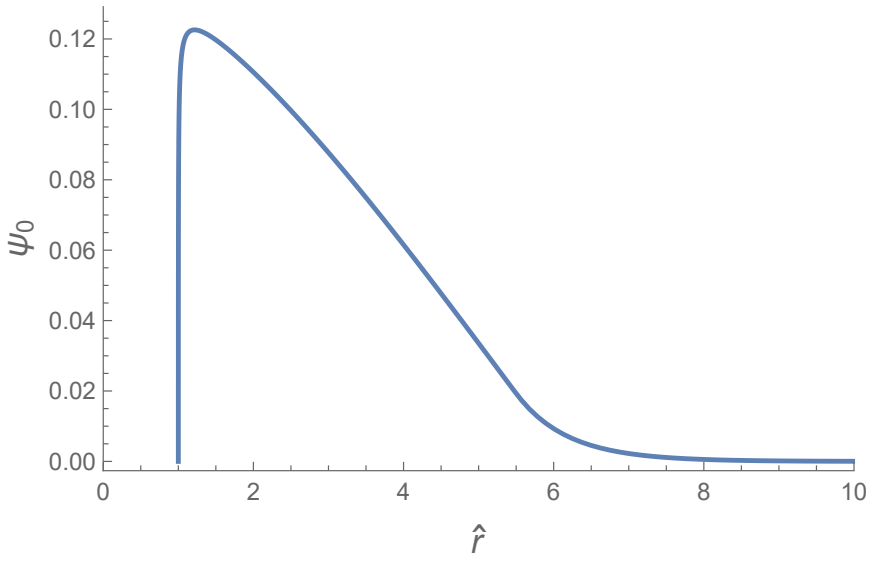

Figure 4.7: The eigenfunction in the original $\hat{r}$-coordinate for the asymmetric finite well potential with $a = 7$, $V_0 = 0.49$, $m = 1$.

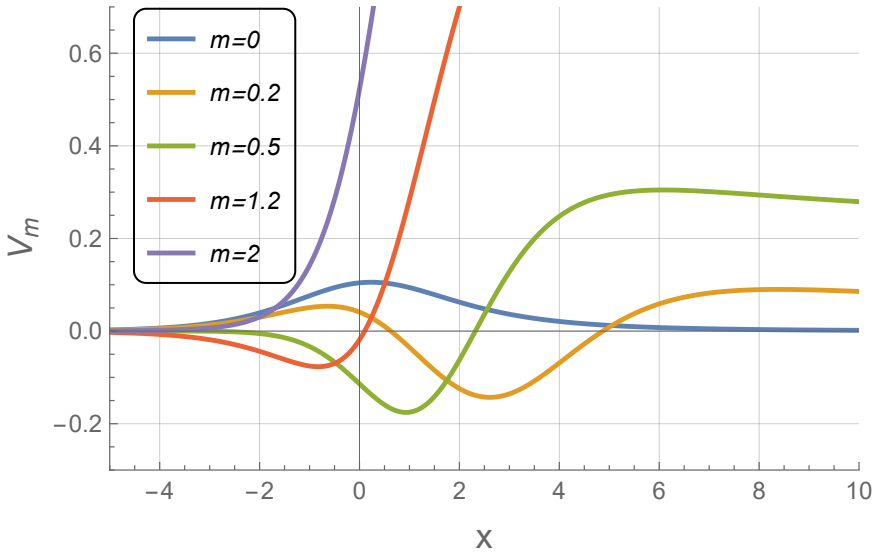

Figure 4.8: The black string potential for different wavenumbers.

4.2.6 Unstable modes of the flat black string

In the previous subsection the eigenfunctions of the asymmetric finite well operator were constructed. The eigenfunctions corresponding to the lowest negative eigenvalue have the behaviour that is required for bump functions with $\langle f, Af\rangle < 0$. Therefore, these eigenfunctions form a set of suitable test functions. In this subsection we use these test functions to prove the existence of a negative eigenvalue of the black string operator. We use Theorem 2.3.16 for this. We compute $\langle f, A_{\hat{m}} f\rangle$ for different test functions. If there is a test function for which this becomes negative, then the black string operator admits a negative eigenvalue. With this we can determine at which mass black strings become unstable.

Theorem 4.2.15. *The Einstein manifold $(\mathbb{R}^4 \times S^1, g_{BS})$ with compact extra dimension of length L, and g_{BS} the black string metric 3.42 with mass M admits unstable modes when*

$$M \in \left[\frac{0.1L}{4\pi}, \frac{0.85L}{4\pi}\right]. \tag{4.103}$$

The asymmetric finite well potential is not a good approximation of $V_{\hat{m}}$ for all $\hat{m} \geq 0$. The black string potential has the same asymptotic behaviour for every $\hat{m}$, which we derived in Lem. 4.2.7. However, not for every $\hat{m}$ there is a minimum around $x = 0$. In Fig. 4.8 the black string potential 4.59 is plotted for different $\hat{m}$. At $\hat{m} = 0$ there is no minimum. For small $\hat{m} \neq 0$ the dip appears. For $m = 1.2$ there is still a dip, however it seems negligible compared to the high wall. Around $\hat{m} = 2$ the dip completely disappears again. According to Theorem 2.3.23 if the potential is non-negative, then there cannot exist a negative eigenvalue. Therefore, to find the unstable modes we only need study the operators where the potential becomes negative somewhere.

As discussed in section 4.2.4, for the $\hat{m}$ for which the potential does become negative somewhere we need to find a $f \in D(A_{\hat{m}})$ such that $\langle f, A_{\hat{m}} f\rangle < 0$. We use the eigenfunctions with negative eigenvalue of the asymmetric finite well operator as test functions.

It is important that we make smart choices for the parameters of the asymmetric finite well, such that it approaches the black string potential as good as possible. For V_0 and m it seems clear what good choices would be. Namely, for $\hat{m}$ we can set V_0 to be equal to the absolute

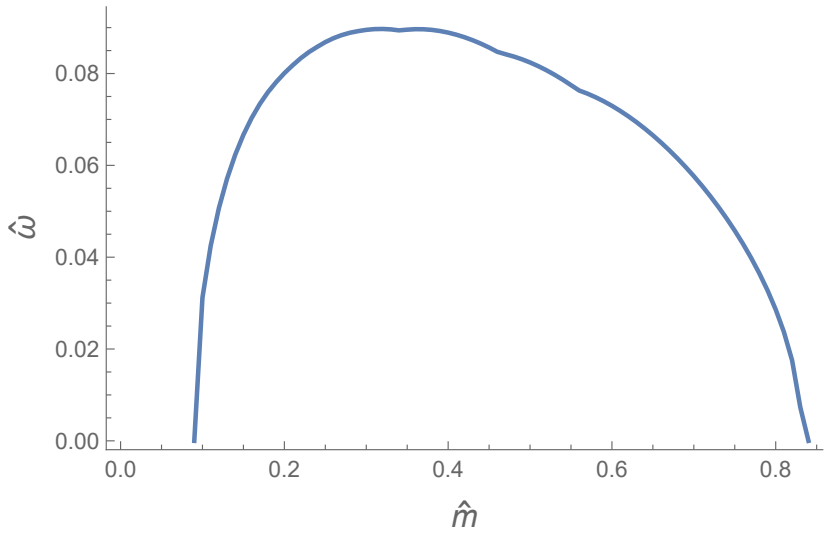

Figure 4.9: A lower bound for the negative eigenvalues of the black string operator using eigenfunctions of the asymmetric finite well operator. The black string operator admits negative eigenvalues for $0.1 < \hat{m} < 0.85$.

value of the minimum of the potential $V_{\hat{m}}$, and m to be equal to $\hat{m}$. For a the choice is less trivial, with some trial and error we found that the best choice is around $a = 1.2 + \hat{m}^2$.

We compute $\langle \psi, A_{\hat{m}} \psi \rangle$ for different normalized eigenfunctions of the asymmetric finite well operator in Eq. 4.85, where the parameters are close to the best approximation described above. In Fig. 4.9 the estimated eigenvalues are shown which are found using this procedure. From this plot we conclude that the black string operator admits a negative eigenvalue when $0.1 < \hat{m} < 0.85$. Comparing this plot with the negative eigenvalues Gregory and Laflamme found by numerically integrating the equations, we see that the estimates are quite good. Another way to estimate the eigenvalues is by approximating the black string potential by the asymmetric finite well potential and determine the negative eigenvalues for this operator. In Fig. 4.10 these eigenvalues are plotted. The plot has very similar shape as the plot in Fig. 4.9, however it seems like it overestimates the eigenvalues.

Proof of Theorem 4.2.15. Recall the decomposition of the perturbation h in Eq. 4.66. We require that $h(y) = h(y + L)$. This limits the amount of possible values for m. This requires $m = \frac{2\pi k}{L}$ for $k \in \mathbb{N}$. The smallest $m > 0$ then has $k = 1$. According to our calculations, an unstable mode has $0.1 < \hat{m} < 0.85$, where $\hat{m} = m r_s$. This can be rewritten to

$$\frac{0.1L}{4\pi} < M < \frac{0.85L}{4\pi}. \tag{4.104}$$

□

Comparing this result with Lem. 4.2.1, we see that the range when the black string becomes unstable according to the analysis agrees very well with what is expected from the entropy argument. However, we expect that there also should be unstable modes in the range $M < \frac{0.1L}{4\pi}$.

To fully prove the instability it is important to show that these modes are physical. Therefore, we have to show that they cannot be removed by a gauge transformation.

Lemma 4.2.16. *The unstable modes in Eq. 4.66 with $\omega > 0$ are not pure gauge.*

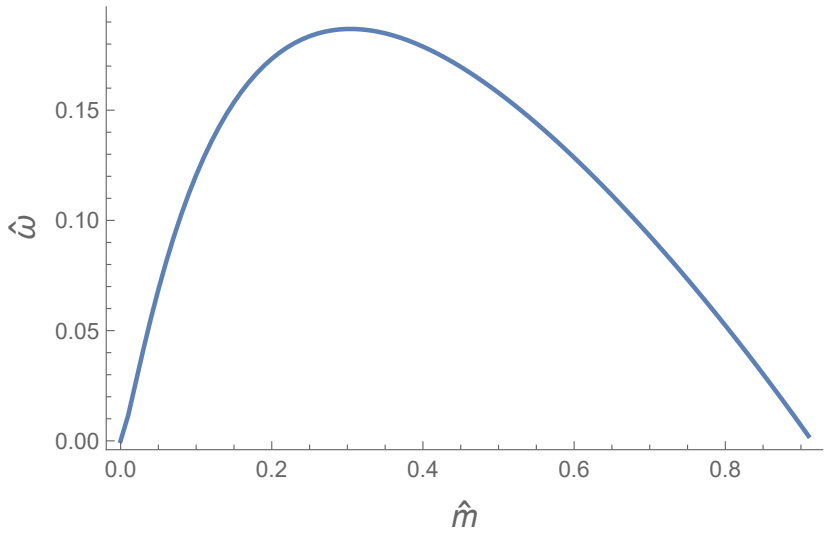

Figure 4.10: An estimate of the negative eigenvalues of the black string operator for different $\hat{m}$. The eigenvalues are obtained by approximating the black string potential by the asymmetric finite well potential. For the asymmetric finite well potential we fixed $a = 1.7$ and set V_0 to match with the minimum of the black string potential.

Proof. If these modes were pure gauge then there should be a small vector field $X \in \Gamma(T\mathbb{R}^4 \times S^1)$ such that

$$h_{MN} = \nabla_M X_N + \nabla_N X_M. \tag{4.105}$$

Suppose that h_{MN} is of this form. Then X should be of the form $X = e^{\omega t} e^{imy} v(r)$ for some $v \in \Gamma(T\mathbb{R}^4 \times S^1)$, similar to the modes. However, if $m \neq 0$, then either $X = 0$ or $h_{5M} \neq 0$ for some $M = 0, 1, 2, 3, 5$. However, for unstable modes we showed that $h_{5M} = 0$. □

We conclude that there are unstable modes that cannot be removed by a gauge transformation. Therefore, the black string is modally unstable. An intuitive picture of what this perturbation looks like is shown in Fig. 4.11. For unstable modes, the notches grow until the black string 'snaps'. What remains is an array of hyperspherical black holes. This procedure is explained in more detail in [66]

4.3 Unstable modes of the Randall-Sundrum black string

In the previous section we have seen that the black string in five-dimensional flat space is unstable under long wavelength perturbations. It turns out that we can generalize these instabilities to curved five-dimensional space, such as RS. Recall the black string solution which we derived in Section 3.2.6. In this section we will derive the instabilities of the RS black string.

Theorem 4.3.1. *The RS1 black string with curvature scale κ, size of the extra dimension y_c and mass M has unstable modes if*

$$M < \frac{0.12}{\kappa y_c} e^{\kappa y_c}. \tag{4.106}$$

This section is dedicated to prove this theorem. However, let us first analyse some of the consequences of this theorem. If RS1 would represent our universe, then for sure the black

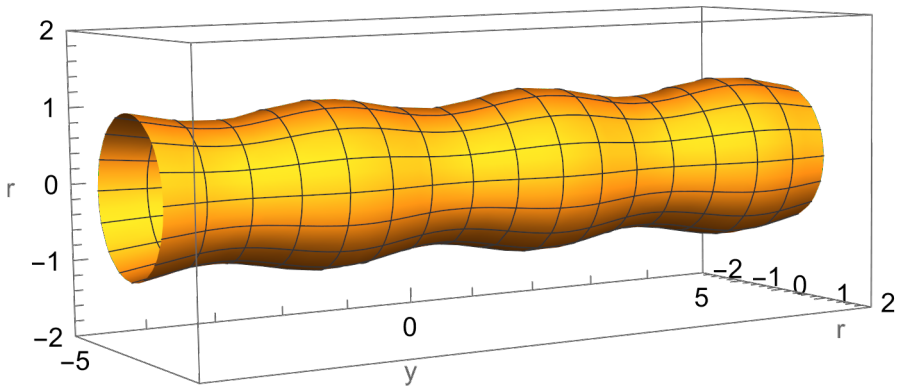

Figure 4.11: The shape of the perturbed black string.

holes we observe should be stable. If a black hole has mass M in the RS1 model, then recall Lem. 3.2.19 where it was shown that on the visible brane we would observe a black hole of mass $M_{\text{vis}} = Me^{-\kappa y_c}$. Black holes that form through stellar collapse have a mass of at least three solar masses. Therefore, we would expect black strings with $M_{\text{vis}} > M_\odot$, where $M_\odot$ denotes one solar mass, to be stable. In the RS1 model a solar mass black hole on the visible brane would correspond to a black hole of mass

$$M = M_\odot e^{\kappa y_c}. \tag{4.107}$$

Assuming Theorem 4.3.1 is valid we can already deduce the main result of the thesis.

Corollary 4.3.2. *The RS1 black string with $\kappa y_c \sim 35$ and $M < M_\odot e^{\kappa y_c}$ is modally unstable.*

Proof. From Theorem 4.3.1 it follows that a RS1 black string is stable if the inequality in Eq. 4.106 holds. Converting this to the effective masses on the visible brane, we have to multiply both sides of Eq. 4.106 by $e^{-\kappa y_c}$. For $\kappa y_c \sim 35$, This becomes

$$M_{\text{vis}} = Me^{-\kappa y_c} < \frac{0.12}{\kappa y_c} \approx 2 \times 10^{-6} M_\odot. \tag{4.108}$$

In particular we conclude that solar mass black holes are stable. □

Let us now prove Theorem 4.3.1. We perturb the RS black string metric $\hat{g}$ from Eq. 3.42

$$g = \hat{g} + h.$$

We need to determine the linearized Einstein equations 2.51. For this we need the following lemmas.

Lemma 4.3.3. *Let $(M = \mathbb{R}^4 \times I, \hat{g})$ with $\hat{g}$ a warped metric of the form*

$$\hat{g} = A^2(y) g^{(4)}(x) + dy^2. \tag{4.109}$$

Let $g = \hat{g} + h$ be a metric tensor, with $h_{a5} = h_{55} = 0$, and $\Box_{\hat{g}}$ the wave operator associated to $\hat{g}$. Then

$$\Box_{\hat{g}} h = \frac{1}{A^2} \Box_{g^{(4)}} h + \frac{\partial^2 h}{\partial y^2} - \left(4 \left(\frac{A'}{A} \right)^2 + 2 \frac{A''}{A} \right) h.$$

Proof. The non-trivial Christoffel symbols associated to $\hat{g}$ are given by

$$\begin{aligned}\Gamma^c_{ab} &= \Gamma^{(4)}{}^c_{ab},\\ \Gamma^5_{ab} &= -A'Ag^{(4)}_{ab},\\ \Gamma^b_{a5} &= \frac{A'}{A}\delta^b_a,\end{aligned}$$

where $a,b,c = 0,1,2,3$ and $\Gamma^{(4)}$ denotes the Christoffel symbol associated to $g^{(4)}$. Keeping this in mind we can compute the wave operator acting on h. We have

$$\begin{aligned}\Box_{\hat{g}}h_{ab} =& g^{MN}\nabla_M\nabla_N h_{ab}\\ =&\frac{1}{A^2}g^{(4)cd}\nabla_c\nabla_d + \nabla_5\nabla_5 h_{ab}\\ =&\frac{1}{A^2}g^{(4)cd}\left(\partial_c\nabla_d h_{ab} - \Gamma^M_{cd}\nabla_M h_{ab} - \Gamma^M_{ca}\nabla_d h_{Mb} - \Gamma^M_{cb}\nabla_d h_{aM}\right)\\ &+\nabla_5\left(\partial_5 h_{ab} - \Gamma^M_{5a}h_{Mb} - \Gamma^M_{5b}h_{aM}\right)\\ =&\frac{1}{A^2}g^{(4)cd}(\partial_c\nabla_d h_{ab} - \Gamma^e_{cd}\nabla_e h_{ab} - \Gamma^e_{ca}\nabla_d h_{eb} - \Gamma^e_{cb}\nabla_d h_{ae}\\ &-\Gamma^5_{cd}\nabla_5 h_{ab} - \Gamma^5_{ca}\nabla_d h_{5b} - \Gamma^5_{cb}\nabla_d h_{a5}) + \nabla_5\left(\partial_5 h_{ab} - \Gamma^M_{5a}h_{Mb} - \Gamma^M_{5b}h_{aM}\right)\end{aligned}$$

Now we can substitute the expression for the Christoffel symbols that we found

$$\begin{aligned}\Box_{\hat{g}}h_{ab} =&\frac{1}{A^2}g^{(4)cd}(\partial_c\nabla_d h_{ab} - \Gamma^{(4)}{}^e_{cd}\nabla_e h_{ab} - \Gamma^{(4)}{}^e_{ca}\nabla_d h_{eb} - \Gamma^{(4)}{}^e_{cb}\nabla_d h_{ae}\\ &+AA'\left(g^{(4)}_{cd}\nabla_5 h_{ab} + g^{(4)}_{ca}\nabla_d h_{5b} + g^{(4)}_{cb}\nabla_d h_{a5}\right)) + \nabla_5\left(\partial_5 h_{ab} - 2\frac{a'}{a}h_{ab}\right).\end{aligned}$$

Note that even though we assumed $h_{a5} = 0$, we still have that

$$\nabla_c h_{a5} = -\Gamma^d_{c5}h_{ad} = -\frac{a'}{a}h_{ac}.$$

Additionally, note that

$$\begin{aligned}\nabla_c h_{ab} &= \partial_c h_{ab} - \Gamma^M_{ca}h_{Mb} - \Gamma^M_{cb}h_{aM}\\ &= \partial_c h_{ab} - \Gamma^{(4)}{}^\gamma_{ca}h_{\gamma b} - \Gamma^{(4)}{}^\gamma_{cb}h_{a\gamma} + 0\\ &= \nabla^{(4)}_c h_{ab}.\end{aligned}$$

Where $\nabla^{(4)}$ denotes the covariant derivative induced by $g^{(4)}$. We use this to find

$$\begin{aligned}\Box_{\hat{g}}h_{ab} =&\frac{1}{A^2}\Box_{g^{(4)}}h_{ab} + \frac{A'}{A}\left(4(\partial_5 h_{ab} - \Gamma^M_{5a}h_{Mb} - \Gamma^M_{5b}h_{aM}) - \frac{A'}{A}\delta^d_a h_{db} - \frac{A'}{A}\delta^d_b h_{ad})\right)\\ &+\partial_5^2 h_{ab} - \Gamma^M_{55}\partial_M h_{ab} - \Gamma^M_{5a}\partial_5 h_{Mb} - \Gamma^M_{5b}\partial_5 h_{a5} - 2\left(\frac{A''}{A} - \left(\frac{A'}{A}\right)^2\right)h_{ab}\\ &-2\frac{A'}{A}\left(\partial_5 h_{ab} - \Gamma^M_{5a}h_{Mb} - \Gamma^M_{5b}h_{aM}\right)\\ =&\frac{1}{A^2}\Box_{g^{(4)}}h_{ab} + \frac{A'}{A}\left(4\partial_5 h_{ab} - 10\frac{A'}{A}h_{ab}\right) + \partial_5^2 h_{ab} - 2\frac{A'}{A}\partial_5 h_{ab} - 2\frac{A''}{A}h_{ab} + 2\left(\frac{A'}{A}\right)^2 h_{ab}\\ &-2\frac{A'}{A}\left(\partial_5 h_{ab} - 2\frac{A'}{A}h_{ab}\right)\\ =&\frac{1}{A^2}\Box_{g^{(4)}}h_{ab} + \partial_5^2 h_{ab} - 4\left(\frac{A'}{A}\right)^2 h_{ab} - 2\frac{A''}{A}h_{ab}.\end{aligned}$$

□

Lemma 4.3.4. *Let $(M = \mathbb{R}^4 \times I, \hat{g})$ with $\hat{g}$ a warped metric of the form*

$$\hat{g} = A^2(y) g^{(4)}(x) + dy^2.$$

Let $g = \hat{g} + h$ be a metric tensor, with $h_{a5} = h_{55} = 0$,. Then

$$R^{c\,d}_{a\,b} h_{cd} = \frac{1}{A^2} R^{(4)}_{acbd} h^{cd} + \left(\frac{A'}{A}\right)^2 h_{ab},$$

where we used $g^{(4)}$ to raise the indices of h, and $R^{(4)}_{acbd}$ is the Riemann tensor associated to $g^{(4)}$.

Proof. Note that

$$\begin{aligned} R_{acbd} =& g_{ac} R^{c}{}_{cbd} \\ =& g_{ac} \left(\partial_b \Gamma^c_{cd} - \partial_d \Gamma^c_{cb} + \Gamma^c_{bM} \Gamma^M_{cd} - \Gamma^c_{dM} \Gamma^M_{cb}\right) \\ =& g_{ac} \left(R^{(4)\,c}{}_{cbd} + \Gamma^c_{b5} \Gamma^5_{cd} - \Gamma^c_{d5} \Gamma^5_{cb}\right) \\ =& A^2 R^{(4)}_{acbd} - A'^2 A^2 g^{(4)}_{ab} g^{(4)}_{cd} + A'^2 A^2 g^{(4)}_{ad} g^{(4)}_{cb}. \end{aligned}$$

Using this we find

$$\begin{aligned} R^{d\,c}_{a\,b} h_{dc} =& g^{dc} g^{cd} R_{acbd} h_{dc} \\ =& \frac{1}{A^4} \left(A^2 R^{(4)}_{acbd} - A'^2 A^2 g^{(4)}_{ab} g^{(4)}_{cd} + A'^2 A^2 g^{(4)}_{ad} g^{(4)}_{cb}\right) h^{cd} \\ =& \frac{1}{A^2} R^{(4)}_{acbd} h^{cd} + \left(\frac{A'}{A}\right)^2 h_{ab}. \end{aligned}$$

□

We want to find unstable modes. Therefore, we can fix our modes into any form we want, as long as they are unstable. We gauge fix our metric in the RS gauge from Def. 3.3.6. The linearized Einstein equations are given by

$$\Delta_L h_{MN} = \Box_{\hat{g}} h_{MN} + 2 R^{P\,Q}_{M\,N} h_{PQ} = 0 \tag{4.110}$$

The RS black string metric $\hat{g}$ is of the form of Eq. 4.109, with $A = e^{-\kappa y_c |y|}$ and $g^{(4)} = g_s$ the Schwarzschild metric. Using Lem. 4.3.3 and 4.3.4 together with the fact that the y-component of both the Riemann tensor and the perturbation h vanish in the RS gauge, the equations for the metric reduce to

$$\frac{1}{A^2}\left(\Box_{g_s} h_{ab} + 2 R^s_{acbd} h^{cd}\right) + h''_{ab} - 2\left(\frac{A''}{A} + \left(\frac{A'}{A}\right)^2\right) h_{ab} = 0. \tag{4.111}$$

Here $\Box_{g_s}$ and R^s_{abcd} denote the wave operator and Riemann tensor associated to the Schwarzschild metric, respectively. If we can somehow rewrite this equation into the form of Eq. 4.67, then the modes of the flat black string can be related to the modes of the RS black string. In particular, we can use the results from the previous sections to find unstable modes of RS black string. This requires

$$h''_{ab} - 2\left(\frac{A''}{A} + \left(\frac{A'}{A}\right)^2\right) h_{ab} = -\frac{m^2}{A^2} h_{ab}. \tag{4.112}$$

To find a suitable h for this, we make an ansatz

$$h_{ab} = u_m(y) \chi_{ab}(x). \tag{4.113}$$

We want to find suitable functions u_m, such that h solves Eq. 4.112. Substituting the ansatz and the expression for A, Eq. 4.112 becomes

$$u_m'' - 4\kappa^2 y_c^2 u_m - 4\kappa y_c \left(\delta(y) - \delta(y-1)\right) u_m = -m^2 e^{2\kappa y_c |y|} u_m. \tag{4.114}$$

This can be solved with Bessel functions.

Definition 4.3.5. *The **Bessel functions** of the first kind J_α and second kind Y_α are two linearly independent solutions of the differential equation*

$$z^2 \frac{d^2 u}{dz^2} + z\frac{du}{dz} + (z^2 - \alpha^2)u = 0. \tag{4.115}$$

According to [32, P. 361], the Bessel functions have the following useful differential relation.

Lemma 4.3.6. *Let f_α be a Bessel function and $n \in \mathbb{N}$ then*

$$\left(\frac{1}{z}\frac{d}{dz}\right)^n (z^\alpha f_\alpha(z)) = z^{\alpha-n} f_{\alpha-n}(z). \tag{4.116}$$

With these Bessel functions we can construct the following solution to Eq. 4.114.

Lemma 4.3.7. *The functions*

$$u_m(y) = BJ_2\left(\frac{m}{\kappa y_c} e^{\kappa y_c |y|}\right) + CY_2\left(\frac{m}{\kappa y_c} e^{\kappa y_c |y|}\right) \tag{4.117}$$

with coefficients $B, C \in \mathbb{R}$ such that

$$BJ_1\left(\frac{m}{\kappa y_c}\right) = -CY_1\left(\frac{m}{\kappa y_c}\right) \tag{4.118}$$

and m such that

$$J_1\left(\frac{m}{\kappa y_c}\right) Y_1\left(\frac{m}{\kappa y_c} e^{\kappa y_c}\right) = J_1\left(\frac{m}{\kappa y_c} e^{\kappa y_c}\right) Y_1\left(\frac{m}{\kappa y_c}\right) \tag{4.119}$$

are solutions to Eq. 4.114.

Proof. To solve Eq. 4.114, we define $z = \frac{m}{\kappa y_c} e^{\kappa y_c y}$. Then away from the branes, the equation in terms of this new variable becomes

$$z^2 \frac{d^2 u_m}{dz^2} + z\frac{du_m}{dz} + (z^2 - 4)u_m = 0. \tag{4.120}$$

Comparing this to the differential equation defining the Bessel functions in Eq. 4.115, we see that this is solved by Eq. 4.117. The coefficients B and C are determined by the boundary conditions at the branes. The boundary conditions are obtained by integrating over a small area around the branes. By integrating around $y = 0$ we obtain the condition

$$2u_m'(0) - 4\kappa y_c u_m(0) = 0. \tag{4.121}$$

Using the differential relation of the Bessel functions from Eq. 4.116 in the case $n = 1$, $\alpha = 2$, we get the relation

$$\frac{m}{\kappa y_c} J_2'\left(\frac{m}{\kappa y_c}\right) + 2J_2\left(\frac{m}{\kappa y_c}\right) = \frac{m}{\kappa y_c} J_1\left(\frac{m}{\kappa y_c}\right). \tag{4.122}$$

The same can be done for the Y_2 term. By using the solution in Eq. 4.117 and these differential relations of the Bessel functions, we can rewrite the boundary condition in Eq. 4.121 to the relation

$$BJ_1\left(\frac{m}{\kappa y_c}\right) = -CY_1\left(\frac{m}{\kappa y_c}\right). \tag{4.123}$$

This applies to both the RS1 and RS2 model.

In the RS1 model, we obtain an additional boundary condition due to the presence of a second brane at $y = 1$. In a similar fashion this boundary condition is given by

$$BJ_1\left(\frac{m}{\kappa y_c}e^{\kappa y_c}\right) = -CY_1\left(\frac{m}{\kappa y_c}e^{\kappa y_c}\right). \tag{4.124}$$

This puts a restriction on the allowed values of m, since the two boundary conditions in Eq. 4.123 and 4.124 can be combined into the requirement in Eq. 4.119. □

We conclude that with the ansatz from Eq. 4.113 and u_m of the form as in Eq. 4.117, the linearized Einstein equations of the RS black string reduce to the linearized Einstein equations of the flat black string. Therefore, for $0.1 < 2Mm < 0.85$ we can find unstable modes of the RS black string using our results from the previous sections. Nevertheless, there are boundary conditions caused by the branes such that the wavenumbers m have to satisfy Eq. 4.119. Therefore, fixing a value for the curvature scale κ and the size of the extra dimension y_c, limits the amount of allowed values for the wavenumber m in the RS1 model. We are interested in the smallest $m > 0$ that solves Eq. 4.119, because this will give an upper bound to the mass of unstable black holes. Recall that RS1 solves the hierarchy problem if $\kappa y_c \sim 35$, in which case $e^{\kappa y_c} \gg 1$. Therefore, $J_1(\frac{m}{\kappa y_c}e^{\kappa y_c})$ and $Y_1(\frac{m}{\kappa y_c}e^{\kappa y_c})$ oscillate very quickly, so we expect the first m to be very small.

Lemma 4.3.8. *The smallest wavenumber $m > 0$ of the RS1 black string modes with $\kappa y_c \gg 1$ is equal to the smallest $m > 0$ for which*

$$J_1(\frac{m}{\kappa y_c}e^{\kappa y_c}) = 0. \tag{4.125}$$

Proof. We know that the wavenumbers satisfy Eq. 4.119. We want to prove that for $\kappa y_c \gg 1$, we can approximate the first $m > 0$ solution to this equation by solutions of Eq. 4.125. For $z \ll 1$ the Bessel functions have the following asymptotic form

$$J_1(z) = \frac{z}{2} + \mathcal{O}(z^2), \quad Y_1(z) = -\frac{2}{\pi z} + \mathcal{O}(1). \tag{4.126}$$

For $z \gg 1$ the Bessel functions behave as

$$J_1(z) = \sqrt{\frac{2}{\pi z}}\cos\left(z - \frac{3\pi}{4}\right) + \mathcal{O}(z^{-1}), \quad Y_1(z) = \sqrt{\frac{2}{\pi z}}\sin\left(z - \frac{3\pi}{4}\right) + \mathcal{O}(z^{-1}). \tag{4.127}$$

For big κy_c, we expect for this m that $\frac{m}{\kappa y_c} < 1$, but $\frac{m}{\kappa y_c}e^{\kappa y_c} \gg 1$. Using the asymptotics from Eq. 4.126 and 4.127 we see that in this range the functions $J_1\left(\frac{m}{\kappa y_c}\right) \sim \frac{m}{2\kappa y_c} \ll 1$ and $Y_1\left(\frac{m}{\kappa y_c}e^{\kappa y_c}\right)$ is oscillatory in m. Therefore, the left hand side of Eq. 4.119 will be an oscillatory function of m with a small amplitude.

On the right hand side of Eq. 4.119, in this range it holds that $Y_1\left(\frac{m}{\kappa y_c}\right) \sim -\frac{2\kappa y_c}{\pi m} \gg 1$ and $J_1\left(\frac{m}{\kappa y_c}e^{\kappa y_c}\right)$ is oscillatory as a function of m. Therefore, the right hand side of Eq. 4.119 will be an oscillatory function of m with a big amplitude. We want to determine the first point of intersection between the left and right hand side. According to our observations this would approximately correspond to the point where $J_1\left(\frac{m}{\kappa y_c}e^{\kappa y_c}\right) = 0$. □

In [32] we find that the first zero of $J_1(z)$ is at $z = 3.8317$. Therefore, the smallest $m > 0$ for which the eigenfunctions u_m exist is

$$m \approx 4\kappa y_c e^{-\kappa y_c}. \tag{4.128}$$

With this we can prove Theorem 4.3.1.

Proof of Theorem 4.3.1. In section 4.2.6 we saw that unstable modes of the flat black string exist when $0 < 2mM < 0.9$. In Lem. 4.3.7, we constructed functions such that the RS black string linearized Einstein equations reduce to the black string linearized Einstein equations. Therefore, also for the RS black string, unstable modes exist when $0 < 2mM < 0.9$. In the RS1 model, due to the boundary conditions, the spectrum of allowed values of m is discrete. In Lem. 4.3.8 we derived that the smallest allowed $m > 0$ is equal to the first zero of Eq. 4.125. Using the zeroes of the Bessel function this is given by Eq. 4.128. By combining the results we indeed find that the RS1 black string is unstable if

$$8M\kappa y_c e^{-\kappa y_c} < 0.9.$$

This can be rewritten to the inequality from the theorem in Eq. 4.106. □

On the other hand, since in the RS2 model there is only one brane which is located at $y = 0$, the only boundary condition is the condition in Eq. 4.123. Consequently, there is a continuous spectrum for allowed values of m. Therefore, there exist unstable modes for the RS black string of any mass. This agrees with Hawking's expectation that the black string cannot reach the AdS horizon, which was discussed in section 3.2.6. However, instead of resulting in the black cigar that Hawking postulated, it seems that this instability causes the black string to split apart into an array of disc shaped black holes, which become smaller and smaller as the y-coordinate increases. Therefore, towards the AdS horizon this would lead to Planck mass black holes stacked together as can be seen in Fig. 4.12.

Lemma 4.3.9. *Let m be the wavenumber of an unstable mode of the RS black string. Then in the y-direction, consecutive zeroes of the mode are separated by*

$$\delta y = \frac{\pi}{m} e^{-\kappa y_c |y|}. \tag{4.129}$$

Proof. The distance between black holes corresponds with the consecutive zeroes of the function u_m. According to the asymptotic behaviour of the Bessel functions from Eq. 4.127, the consecutive zeroes are separated by a distance of π. Therefore, suppose $u_m(y_0) = 0$ and let $u_m(y_0 + \delta y)$ be the next zero. Then we can approximate δy using the fact that

$$\frac{m}{\kappa y_c} e^{\kappa y_c (y_0 + \delta y)} - \frac{m}{\kappa y_c} e^{\kappa y_c y_0} = \pi.$$

We can rewrite this to

$$\kappa y_c \delta y = \log\left(1 + \frac{\kappa y_c \pi}{m} e^{-\kappa y_c y_0}\right).$$

Recall that $\frac{m}{\kappa y_c} e^{-\kappa y_c} \gg 1$, such that we can approximate this by

$$\delta y = \frac{\pi}{m} e^{-\kappa y_c y_0}.$$

□

So indeed the distance between black holes decreases as y increases. As the mass of the black holes also decreases in the positive y-direction, the instability results into an accumulation of mini-black holes stacked together towards the AdS horizon. This might be a consequence of the singularity at $y = \infty$. Note that this array of black holes can always be prevented or stopped by adding another brane in front of the AdS horizon.

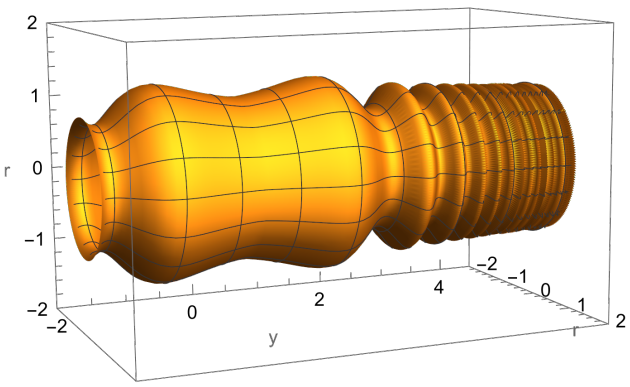

Figure 4.12: The shape of the perturbed RS black string. Notice that the distance between consecutitive peaks decreases quickly as y increases.

Chapter 5

Conclusion and outlook

5.1 Discussion and conclusion

In this thesis we analysed the mode stability of black strings in the warped spacetime called the Randall-Sundrum model. In particular, we derived the range of masses for which Randall-Sundrum black strings are unstable for both the finite and infinite model.

In Chapter 2 we defined the stability problem in general relativity in accordance with the literature. Furthermore, we stated some results from spectral theory there were powerful tools for solving stability problems. We saw that once we can rewrite a stability problem in a Schrödinger type of equation, the problem analysis comes down to studying the potential. We proved that bounded and piecewise continuous potentials induce self-adjoint Schrödinger operators. We followed the ideas of Visheswara to show that if the potential is non-negative as well, then mode stability follows immediately.

We wanted to apply this to the Randall-Sundrum model. We considered both the finite RS1 model and infinite RS2 model. We showed how Randall and Sundrum constructed this model and came up with a unique solution to the hierarchy problem. The hierarchy problem was solved due to the warping factor. Additionally, we saw that four-dimensional gravity was retained on the brane where the standard model is located. We were also able to construct black hole solutions in the form of RS black strings. However, Hawking derived that the Riemann tensor has a singularity at the AdS horizon for the RS2 model. This indicated the existence of an instability.

To understand this instability we first analysed the stability of other black holes. By combining the results from Regge and Wheeler [20], Vishveshwara [21] and Zerilli [22], we were able to show the mode stability of the Schwarzschild black hole in four-dimensions for both even and odd parity perturbations. We saw that both type of perturbations have similar potentials in the final Schrödinger equation, showing that these have similar behaviour.

One of the main results of the thesis was the analytical prove of the Gregory-Laflamme instability for the black string in flat space. This long wavelength instability was expected because in large extra dimensions the hyperspherical black hole has a higher entropy compared to the black string. We analytically showed that there is an instability for

$$mr_s \in [0.1, 0.8]. \tag{5.1}$$

This is in agreement with the numerical results in [23]. These unstable modes were derived using

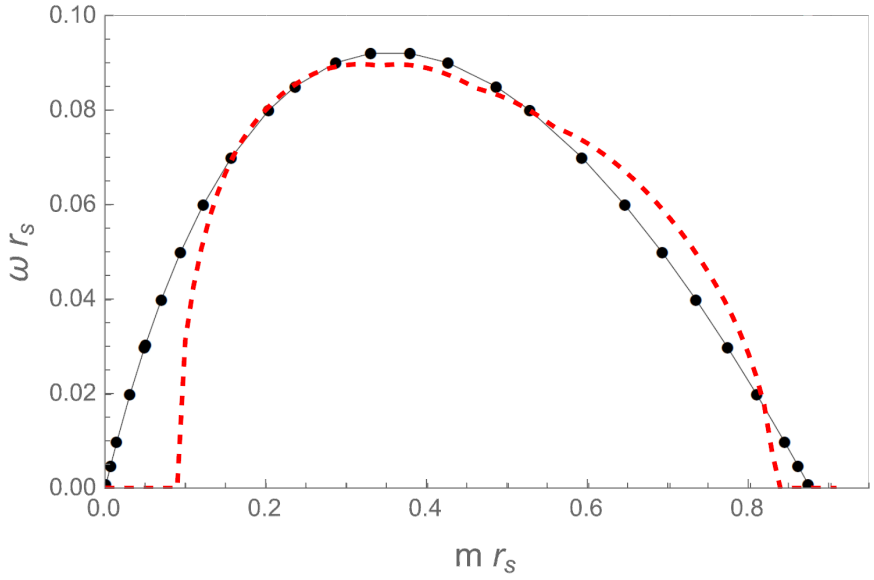

Figure 5.1: The comparison between the approximation of negative eigenvalues using test functions from Section 4.2.6 (red dotted line) and the numerical frequencies Gregory & Laflamme found (black line) [23]. For consistent results one would expect the red graph to be below the black graph.

the self-adjoint Schrödinger operator and using eigenfunctions of a similar potential, which is the asymmetric finite well potential. We saw that these eigenfunctions have negative energies also for the black string operator which meant that this operator admits negative eigenvalues. This shows that functions of the simplified potential have the same type of behaviour as for the black string potential. This improves the understanding of the black string.

However, some of the negative values we found disagree with the results of Gregory and Laflamme. According to Theorem 2.3.16 the test functions should always find a value higher than the lowest eigenvalue. In Fig. 5.1 it can be seen that for $mr_s \sim 0.7$ we found higher frequency values, which means that these modes have an energy lower than the lowest eigenvalue found by Gregory and Laflamme. Therefore, either our calculations are not precise enough and the value we found is incorrect, or the numerical values found by Gregory and Laflamme are incorrect. The error on our calculations is estimated to be 10^{-4}.

The other method we tried was to approximate the black string potential with the asymmetric finite well potential. One would expect that this overestimates the negative eigenvalues, since now the potential takes its minimal value over an entire range instead of just at one point. This is indeed the case as can be seen in Fig. 5.2. We can combine our two methods to find a region where we would expect the negative eigenvalue to be located. This is shown in Fig. 5.3. As we just discussed, the values found by Gregory & Laflamme fall out of this region around $mr_s = 0.7$.

Furthermore, in 2021, Collingbourne [25, Prop. 4.5] analytically proved the Gregory Laflamme instability in the range $mr_s \in [0.3, 0.8]$. His proof used test functions that were constructed by hand. The advantage of this was that he could compute the integrals analytically. In this thesis we have improved this result to the range in Eq. 5.1. Furthermore, in Fig. 5.1, we see that the test functions approach the eigenfunctions really well at some points. Therefore, we can improve our understanding of the black string perturbations by studying the quantum physics problem of the asymmetric finite well. This observation improves our understanding of the mode instability.

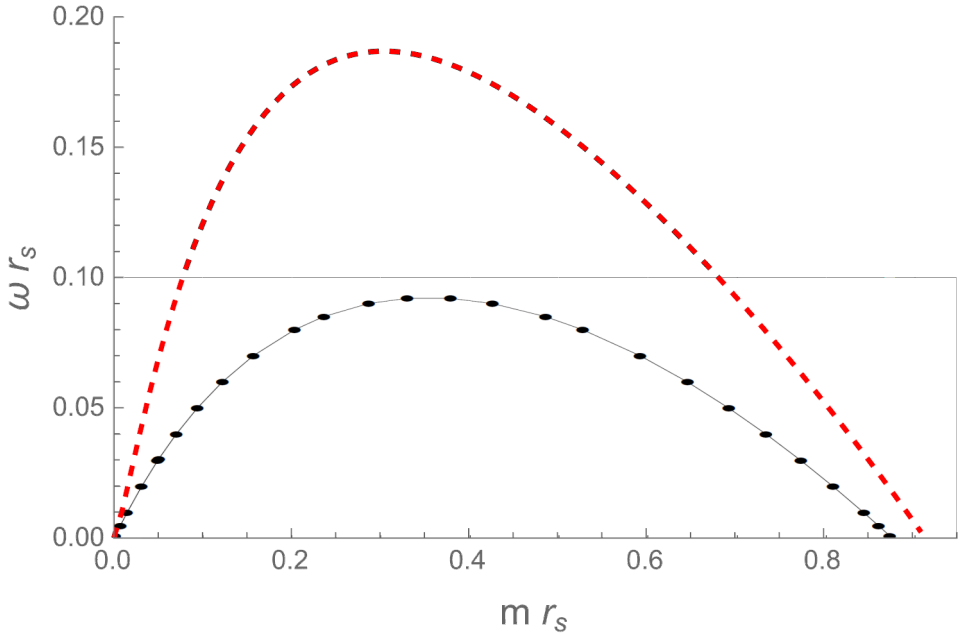

Figure 5.2: The comparison between the estimation of the eigenvalues by approximating the potential by the asymmetric finite well potential and the negative eigenvalues Gregory & Laflamme found through numerical results [23] These estimates overshoot the negative eigenvalues of Gregory & Laflamme.

Finally, we could generalize the Gregory Laflamme instability to the RS black string. We concluded that in the RS1 model with $\kappa y_c \sim 35$, black holes with a mass below the mass of the Earth, are unstable on the visible brane. Moreover, in RS2 black strings of any mass are unstable. This prevents the formation of the singularity at the AdS horizon. Nevertheless, as a consequence there appears to arise an array of Planck mass black holes closely packed together at the AdS horizon. This can be prevented by adding an additional brane as in the RS1 model. We conclude that Hawkings intuition was right and that the RS2 black string is modally unstable. Nevertheless, we note that, at least on this mode level, this instability does not form the black cigar shape as postulated by Hawking.

5.2 Outlook

Of course the story does not end here, and there are many topics that are interesting to study further. First of all, the analyses in this thesis does not yet prove the mode stability of solar mass black holes. The construction in Section 4.3 only considers perturbations of a suitable form, such that the linearized Einstein equations of the RS black string reduce to the same form as in the flat case. In order to prove mode stability one needs to consider the full set of perturbations of a particular mode. Nevertheless, observe that the bound for the mass under which black holes become unstable that we found is equal to $M_{\text{vis}} < 2 \times 10^{-6} M_{\odot}$. This is six orders of magnitude lower than the mass of the sun. Therefore, we conjecture that solar mass black holes are indeed stable.

Conjecture 5.2.1. *The RS1 black string with $\kappa y_c \sim 35$ and $M > M_{\odot} e^{\kappa y_c}$ has mode stability.*

The first motivation to study this topic was to derive the waveform of gravitational wave signals originating from binary black hole mergers in Randall-Sundrum. This study has already been

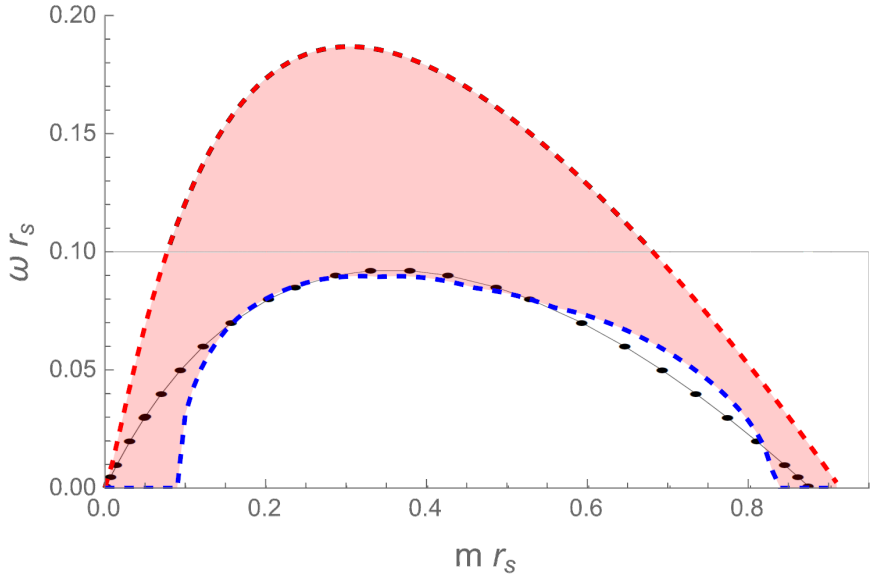

Figure 5.3: Combining the overestimation and the underestimation we would expect the true frequencies to be in the red-zone. However, around $m/r_s = 0.7$ the numerical values found by Gregory & Laflamme lay outside of this zone.

done for small compact flat extra-dimensions [9], but is interesting to study for warped spaces. Especially now that we believe that solar mass black holes are stable in RS1 it makes sense to study gravitational waves from binary black holes in this model. Comparing the waveforms with gravitational wave observations, could be a new way of restricting the parameters of the Randall-Sundrum model.

Conjecture 5.2.2. *Gravitational waveforms in the RS1 model agree with gravitational wave observations.*

Another gravitational wave related topic is the study the $l > 0$ perturbation modes of the black string. To derive the Gregory-Laflamme instability we assumed that the perturbations are spherically symmetric. For the non-spherically symmetric modes one can derive a Schrödinger operator with bounded positive potential. Therefore, these modes are stable. This potential only slightly differs from the four-dimensional potential we obtained from the Schwarzschild solution. In particular, in the case $m \to 0$, the two potentials agree. This extra m-dependent terms would effect the quasi-normal modes emitted during the ringdown of a black hole. Using an Eikonal approximation [67], it is possible to derive differences between waveforms from a black string and a four-dimensional black hole. This is another nice way to probe extra dimensions using gravitational waves.

Question 5.2.3. *What is the m-dependence of the quasi-normal modes of the black string?*

Additionally, it is interesting to improve the analyses of the Gregory-Laflamme instability. We analytically proved the instability in the range in Eq. 5.1, but according to the numerical simulations there should exist unstable modes in the range $mr_s \in (0, 0.9)$. Other hints for the existence of unstable modes in a wider range are that the potential already becomes negative for any small $\hat{m} > 0$. It would be a great achievement to prove the stability in this whole range. This could be done by improving the approximation. For example, extra steps could be included in the step potential. As can be seen in Fig. 4.3, there are still maxima of $V_{0.4}$ around $x = -3$ and $x = 5$. By adding two extra steps in the potential, these properties could also be taken into account and the resulting eigenfunctions might even be a better approximation.

One could also try the method of Coulingbourne, who computed the test functions by hand. Possibly different functions are required at the edges of the range, but one can analyse the required behaviour and try to construct suitable functions.

Conjecture 5.2.4. *The black string is modally unstable in the range* $0 < mr_s < 0.9$.

Another way to increase our understanding of the black string is to analyse the linear instability. A possible way would be similar to the proof of Price's law [68]. The equation describing the linear problem is obtained by replacing each ω term by a time-derivative. Then the equation becomes

$$\frac{d^2}{dt^2}\psi(t) + A\psi(t) = 0$$

where $\psi : \mathbb{R} \to L^2(\mathbb{R})$, and A is the self-adjoint Schrödinger operator. Then by using results the spectral theorem 2.3.25, the solution with initial conditions $\psi(0) = f$ and $\psi'(0) = g$ is given by

$$\psi(t) = \cos\left(t\sqrt{A}\right)f + \frac{\sin\left(t\sqrt{A}\right)}{\sqrt{A}}g, \tag{5.2}$$

where operators such as $\sqrt{A}$ are defined by the spectral mapping. Studying the linear stability then comes down to understanding the operators $\cos\left(t\sqrt{A}\right)$ and $\frac{\sin\left(t\sqrt{A}\right)}{\sqrt{A}}$. The black string would be linearly unstable if there exist arbitrarily small f and g such that $\psi(t)$ diverges as $t \to \infty$.

Conjecture 5.2.5. *The black string* $(\mathbb{R}^4 \times S^1, g_{BS})$ *is linearly unstable.*

Finally, the main reason to study the RS black string instability was because of Hawking's discovery that the RS2 black string is singular at the AdS horizon. He postulated that instead a black cigar would form. Since then black cigar are interesting objects, and there are many studies on them [69]. By studying the mode instability, we saw that this instability could be visualised as in Fig. 4.12. Instead of forming a black cigar, it seems that an array of mini-black holes is formed. It is interesting to study whether there is a relation or a possible transformation from this mode instability to a black cigar solution.

Conjecture 5.2.6. *The RS2 black string unstable modes can be combined to form a black cigar.*

Bibliography

[1] B. P. e. a. Abbott. "Observation of Gravitational Waves from a Binary Black Hole Merger". In: *Phys. Rev. Lett.* 116 (6 Feb. 2016), p. 061102.

[2] A. Joyce et al. "Beyond the cosmological standard model". In: *Physics Reports* 568 (Mar. 2015), pp. 1–98.

[3] T. Clifton et al. "Modified gravity and cosmology". In: *Physics Reports* 513.1-3 (Mar. 2012), pp. 1–189.

[4] D. Tong. *Lectures on String Theory*. 2012. arXiv: `0908.0333 [hep-th]`.

[5] A. Tomasiello. *Geometry of String Theory Compactifications*. Cambridge University Press, 2022.

[6] I. Antoniadis and K. Benakli. "LIMITS ON THE SIZE OF EXTRA-DIMENSIONS". In: *Particles, Strings and Cosmology (PASCOS 99)*. WORLD SCIENTIFIC, Aug. 2000.

[7] L. Randall and R. Sundrum. "Large Mass Hierarchy from a Small Extra Dimension". In: *Physical Review Letters* 83.17 (Oct. 1999), pp. 3370–3373.

[8] L. Randall and R. Sundrum. "An Alternative to Compactification". In: *Physical Review Letters* 83.23 (Dec. 1999), pp. 4690–4693.

[9] Y. Du et al. "Probing compactified extra dimensions with gravitational waves". In: *Phys. Rev. D* 103 (4 Feb. 2021), p. 044031.

[10] K. Pardo et al. "Limits on the number of spacetime dimensions from GW170817". In: *Journal of Cosmology and Astroparticle Physics* 2018.07 (July 2018), p. 048.

[11] C. Palenzuela et al. "Electromagnetic and Gravitational Outputs from Binary-Neutron-Star Coalescence". In: *Physical review letters* 111 (Aug. 2013), p. 061105.

[12] B. A. et al. "GW170817: Observation of Gravitational Waves from a Binary Neutron Star Inspiral". In: *Physical Review Letters* 119.16 (Oct. 2017).

[13] B. P. A. et al. "Gravitational Waves and Gamma-Rays from a Binary Neutron Star Merger: GW170817 and GRB 170817A". In: *The Astrophysical Journal Letters* 848.2 (Oct. 2017), p. L13.

[14] Singh, Neha et al. "Exploring compact binary populations with the Einstein Telescope". In: *AA* 667 (2022), A2.

[15] B. e. a. Abbott. "GWTC-1: A Gravitational-Wave Transient Catalog of Compact Binary Mergers Observed by LIGO and Virgo during the First and Second Observing Runs". In: *Physical Review X* 9.3 (Sept. 2019).

[16] A. H. Nitz et al. "1-OGC: The First Open Gravitational-wave Catalog of Binary Mergers from Analysis of Public Advanced LIGO Data". In: *The Astrophysical Journal* 872.2 (Feb. 2019), p. 195.

[17] A. Chamblin, S. W. Hawking, and H. S. Reall. "Brane-world black holes". In: *Physical Review D* 61.6 (Feb. 2000).

[18] R. Gregory. *The Gregory-Laflamme instability.* 2011. arXiv: 1107.5821 [gr-qc].

[19] R. Narayan and J. E. McClintock. *Observational Evidence for Black Holes.* 2014. arXiv: 1312.6698 [astro-ph.HE].

[20] T. Regge and J. A. Wheeler. "Stability of a Schwarzschild singularity". In: *Phys. Rev.* 108 (1957), pp. 1063–1069.

[21] C. V. Vishveshwara. "Stability of the Schwarzschild Metric". In: *Phys. Rev. D* 1 (10 May 1970), pp. 2870–2879.

[22] F. J. Zerilli. "Gravitational Field of a Particle Falling in a Schwarzschild Geometry Analyzed in Tensor Harmonics". In: *Phys. Rev. D* 2 (10 Nov. 1970), pp. 2141–2160.

[23] R. Gregory and R. Laflamme. "Black strings and p-branes are unstable". In: *Physical Review Letters* 70.19 (May 1993), pp. 2837–2840.

[24] D. J. Griffiths and D. F. Schroeter. *Introduction to Quantum Mechanics.* 3rd ed. Cambridge University Press, 2018.

[25] S. C. Collingbourne. "The Gregory–Laflamme instability of the Schwarzschild black string exterior". In: *Journal of Mathematical Physics* 62.3 (Mar. 2021), p. 032502. eprint: https://pubs.aip.org/aip/jmp/article-pdf/doi/10.1063/5.0043059/19746399/032502_1_online.pdf.

[26] S. M. Carroll. *An Introduction to General Relativity: Spacetime and Geometry.* Cambridge University Press, 2019.

[27] S. Weinberg. *Gravitation and Cosmology: Principles and Applications of the General Theory of Relativity.* New York: John Wiley and Sons, 1972.

[28] J. M. Lee. *Introduction to Smooth Manifolds.* Springer, 2002.

[29] S. W. Hawking and G. F. R. Ellis. *The Large Scale Structure of Space-Time.* Cambridge Monographs on Mathematical Physics. Cambridge University Press, 1973.

[30] S. K. D. Christodoulou. "The global nonlinear stability of the Minkowski space". In: *Princeton University Press* (1994).

[31] S. Klainerman and J. Szeftel. *Brief introduction to the nonlinear stability of Kerr.* 2022. arXiv: 2210.14400 [math.AP].

[32] Abramowitz and Stegun. *Handbook of Mathematical Functions.* United States Department of Commerce, 1964.

[33] B. S. Michael Reed. *Methods of Modern Mathematical Physics I: Functional Analysis.* Academic Press, Inc., 1972.

[34] H. Brezis. *Functional Analysis, Sobolev Spaces and Partial Differential Equations.* Springer, 2010.

[35] G. Teschl and A. M. Society. *Mathematical Methods in Quantum Mechanics: With Applications to Schrödinger Operators.* Graduate studies in mathematics. American Mathematical Society, 2009.

[36] T. Rothman and S. Boughn. "Can Gravitons be Detected?" In: *Foundations of Physics* 36.12 (Nov. 2006), pp. 1801–1825.

[37] J. F. Donoghue. "General relativity as an effective field theory: The leading quantum corrections". In: *Physical Review D* 50.6 (Sept. 1994), pp. 3874–3888.

[38] G. e. a. Aad. "Observation of a new particle in the search for the Standard Model Higgs boson with the ATLAS detector at the LHC". In: *Physics Letters B* 716.1 (Sept. 2012), pp. 1–29.

[39] A. Zee. *Quantum Field Theory in a Nutshell: Second Edition.* Princeton University Press, Feb. 2010.

[40] N. Arkani–Hamed, S. Dimopoulos, and G. Dvali. "The hierarchy problem and new dimensions at a millimeter". In: *Physics Letters B* 429.3–4 (June 1998), pp. 263–272.

[41] J. R. Taylor. *Classical Mechanics*. University Science Books, 2005.

[42] C. D. Hoyle et al. "Submillimeter tests of the gravitational inverse-square law". In: *Physical Review D* 70.4 (Aug. 2004).

[43] R. M. Calvo. "Geometry of (Anti-)De Sitter space-time". In: 2018.

[44] J. Maldacena. In: *International Journal of Theoretical Physics* 38.4 (1999), pp. 1113–1133.

[45] S. D. Haro and J. Butterfield. *A Schema for Duality, Illustrated by Bosonization*. 2018. arXiv: `1707.06681 [physics.hist-ph]`.

[46] L. Susskind. "The world as a hologram". In: *Journal of Mathematical Physics* 36.11 (Nov. 1995), pp. 6377–6396.

[47] S. Chakraborty and K. Lochan. "Black Holes: Eliminating Information or Illuminating New Physics?" In: *Universe* 3.3 (2017), p. 55. arXiv: `1702.07487 [gr-qc]`.

[48] S. W. Hawking. "Particle Creation by Black Holes". In: *Commun. Math. Phys.* 43 (1975). Ed. by G. W. Gibbons and S. W. Hawking. [Erratum: Commun.Math.Phys. 46, 206 (1976)], pp. 199–220.

[49] W. D. Goldberger and M. B. Wise. "Modulus Stabilization with Bulk Fields". In: *Physical Review Letters* 83.24 (Dec. 1999), pp. 4922–4925.

[50] A. G. Riess et al. "Observational Evidence from Supernovae for an Accelerating Universe and a Cosmological Constant". In: *The Astronomical Journal* 116.3 (Sept. 1998), pp. 1009–1038.

[51] S. W. Hawking, T. Hertog, and H. S. Reall. "Brane new world". In: *Physical Review D* 62.4 (June 2000).

[52] F. Abu-Ajamieh. "The radion as a dark matter candidate". In: *International Journal of Modern Physics A* 33.24 (Aug. 2018), p. 1850144.

[53] M. Gabella. "The Randall-Sundrum Model". In: 2006.

[54] B. Zwiebach. *A First Course in String Theory*. 2nd ed. Cambridge University Press, 2009.

[55] R. Bellman. *Stability Theory of Differential Equations*. McGraw-Hill, 1953.

[56] T. Tanaka. "Classical Black Hole Evaporation in Randall-Sundrum Infinite Braneworld". In: *Progress of Theoretical Physics Supplement* 148 (2002), pp. 307–316.

[57] P. Figueras and T. Wiseman. "Gravity and Large Black Holes in Randall-Sundrum II Braneworlds". In: *Physical Review Letters* 107.8 (Aug. 2011).

[58] W. D. Biggs and J. E. Santos. "Rotating Black Holes in Randall-Sundrum II Braneworlds". In: *Physical Review Letters* 128.2 (Jan. 2022).

[59] N. Wheeler. *Algebraic Theory of Spherical Harmonics*. Reed College Physics Department, 1996.

[60] K. S. Thorne. "Multipole expansions of gravitational radiation". In: *Rev. Mod. Phys.* 52 (2 Apr. 1980), pp. 299–339.

[61] K. A. Bronnikov and V. N. Melnikov. "The Birkhoff theorem in multidimensional gravity". In: *General Relativity and Gravitation* 27.5 (May 1995), pp. 465–474.

[62] R. Emparan and H. S. Reall. "Black Holes in Higher Dimensions". In: *Living Reviews in Relativity* 11.1 (Sept. 2008).

[63] Y. Ali-Haïmoud. "Lecture 11: The Riemann tensor". In: *Lecture Notes* (2019).

[64] A. V. Frolov and V. P. Frolov. "Black holes in a compactified spacetime". In: *Physical Review D* 67.12 (June 2003).

[65] J. D. Bekenstein. "Black-hole thermodynamics". In: *Physics Today* 33.1 (Jan. 1980), pp. 24–31. eprint: `https://pubs.aip.org/physicstoday/article-pdf/33/1/24/7413775/24\_1\_online.pdf`.

[66] P. Figueras et al. "Endpoint of the Gregory-Laflamme instability of black strings revisited". In: *Physical Review D* 107.4 (Feb. 2023).

[67] K. Glampedakis and H. O. Silva. "Eikonal quasinormal modes of black holes beyond general relativity". In: *Physical Review D* 100.4 (Aug. 2019).

[68] R. Donninger, W. Schlag, and A. Soffer. "A proof of Price's Law on Schwarzschild black hole manifolds for all angular momenta". In: *Advances in Mathematics* 226.1 (Jan. 2011), pp. 484–540.

[69] S. Aoki, T. Onogi, and S. Yokoyama. "What does a quantum black hole look like?" In: *Physics Letters B* 814 (2021), p. 136104.